EXAMINATION OF THE ROLE OF PTEN IN IONOTROPIC GLUTAMATE RECEPTOR EXPRESSION

By

TATIANA MARIA KAZDOBA-LEACH

A Dissertation submitted to the

Graduate School-New Brunswick

Rutgers, The State University of New Jersey

And

The Graduate School of Biomedical Sciences

University of Medicine and Dentistry of New Jersey

In partial fulfillment of the requirements

For the degree of

Doctor of Philosophy

Graduate Program in Neuroscience

Written under the direction of

Gabriella D'Arcangelo, Ph.D.

And approved by

_____

_____

_____

_____

New Brunswick, New Jersey

January 2014

ABSTRACT OF THE DISSERTATION

EXAMINATION OF THE ROLE OF PTEN IN IONOTROPIC GLUTAMATE RECEPTOR EXPRESSION

By TATIANA MARIA KAZDOBA-LEACH

Dissertation Director:

Gabriella D'Arcangelo, Ph.D.

The phosphatase Pten negatively regulates PI3K/Akt/mTOR signaling, a pathway critical for cell growth and protein synthesis. Germline *PTEN* mutations are implicated in seizure and autism, suggesting that alterations in PTEN affect neuronal function and development. Several brain-specific conditional Pten knockout (KO) mice exhibit enlarged brains, neuronal hypertrophy and increased seizure susceptibility, which may be indicative of altered glutamate receptor function. mTOR inhibition can suppress seizure activity observed in these *Pten* mutant models, revealing the importance of mTOR signaling in Pten-dependent phenotypes. To better understand how Pten may regulate neuronal excitability, ionotropic glutamate receptor expression was examined in NEX-*Pten* homozygous KO mice, which lack Pten in nearly all forebrain excitatory neurons. Biochemical analyses revealed alterations in select NMDA and AMPA receptor subunit protein levels in the forebrains of newly born NEX-*Pten* KO mice, suggesting developmental loss of Pten can affect synaptic proteins important for neurotransmission. Similarly, initial analysis of

CaMKIIα-*Pten* KO mice indicated postnatal loss of Pten in excitatory neurons may also alter NMDA receptor subunits in the cortex, but not the hippocampus, underscoring the importance of Pten for proper synaptic protein expression. To further characterize the effects of *Pten* deletion on glutamate receptor subunit expression, dissociated cortical neuronal cultures were used to evaluate how chronic Pten deficiency alters glutamate receptors over time. NMDA receptor abnormalities were modest and transient, indicating that alterations in glutamate receptor subunits may normalize due to homeostatic mechanisms. Further, pharmacological inhibition of PI3K reduced select NMDA receptor subunits in dissociated cortical cultures. Together, these data suggest that *in vivo* activation of PI3K through loss of Pten leads to selective increases in NMDA receptor subunits in cortical neurons, but not hippocampal neurons, since no alterations were detected in this region. Additional studies with rapamycin and second generation mTOR inhibitors are required to determine how mTOR function contributes to the glutamate receptor phenotype. The NEX-*Pten* model demonstrates that Pten may be crucial in controlling neuronal excitability at the synapse. Dysregulation of these functions may underlie some of the phenotypes associated with *PTEN* mutations in the human population.

Dedication

This dissertation is dedicated to my family, in particular my husband, Prescott Tarn Leach, my son, William Barrie Leach, and my parents, William and Maria Kazdoba.

Throughout my scientific career, Prescott has been my sounding board for ideas, ramblings and brainstorming. Although it was challenging living apart from him while we both tackled graduate school in separate cities, I cannot imagine going through this experience without Prescott and his constant encouragement by my side. His kindness and strength of character are the type I strive to have, and I can only hope our son inherits these traits from his Tato. The next several months bring more change for our family as we move across the country to California, but I look forward to this next chapter and the possibilities it holds, particularly as we experience them together.

I would be incredibly remiss if I did not acknowledge what an extraordinary support system my parents have been for me, Prescott and Will. Their work ethic and unconditional love have influenced me in more ways than I probably realize. Words cannot describe how lucky I am to have parents who are unrelentingly supportive of my decisions, and just so helpful with small and large gestures, particularly throughout the last five years. From feeding my cats during weekends when I was away in Philly to bringing me flowers for celebrations of all kinds to being the best daycare we could hope to have for Will … the list goes on and would be as long as this dissertation.

Prescott and my parents have allowed me to accomplish so much more than if I was on my own. I cannot thank them enough.

Acknowledgements

The most beautiful thing we can experience is the mysterious.

It is the source of all true art and all science.

~Albert Einstein

I would like to thank my dissertation advisor, Dr. Gabriella D'Arcangelo, for her guidance and support during my graduate studies. Dr. D'Arcangelo accepted me into her lab when my only experience with cell cultures and biochemistry was reading about these techniques in the literature. Whenever I would go to Dr. D'Arcangelo's office to discuss data or research, I would leave it brimming with new ideas. Her mentorship and enthusiasm has allowed me to greatly expand my scientific breadth and skills, and I am very thankful that I spent my time in graduate school in the research environment she created.

I would like to thank the following faculty for being members of my dissertation committee: Dr. Bonnie Firestein, Dr. John McGann and Dr. Steven Zheng. Their commentary and suggestions strengthened this body of work, and I thank them for their time, guidance and thoughtful discussions.

I would like to thank all the members of the D'Arcangelo lab, past and present, for their interesting discussions (scientific and otherwise) and their friendships. Graduate school is difficult in its own right, but is made so much easier when you are surrounded by people who can tell a great story and share a laugh with you. It's a bonus when they also listen as you talk through your study design and lend a helping a hand when needed. I would like to especially thank Beth Crowell and Gum Hwa Lee, who were in the D'Arcangelo lab when I joined and have seen me to the finish line. They have helped me through my studies in a multitude of ways, and are always there for a good conversation. Although it saddens me to leave, I am very thankful for the huge collection of experiences that were created during my time in this lab, and when I think of these stories, they bring a smile to my face.

I would like to thank Dr. Lynn Hyde, who was my first scientific mentor, for all her encouraging words and support in the years prior to and during graduate school. Lynn hired me to work in the Behavioral Pharmacology research group at the Schering-Plough Research Institute shortly after I graduated college. Lynn's love of science and meticulous approach to research design helped foster my own love of neuroscience and put me on the path towards my doctorate. Lynn has been integral to so many aspects of my life, and I am grateful to call her my mentor, colleague and friend.

I would like to thank my friends and family for all their support during my graduate studies. To my friends…thank you for your understanding when my time was limited, talking me through my struggles, and your encouragement. To my husband, Prescott… thank you for all the wonderful things you did for me and us as we adventured through grad school together. Thank you for critically reading through countless manuscripts and posters, and sending me papers you thought would be helpful or interesting. You are the best, and I couldn't ask for a better partner and best friend. To my son, Will… know that seeing your face (and that smile) every morning before I headed into lab made my day. To my parents….thank you for everything! I can't say it enough.

I would also like to acknowledge the funding sources that provided support during my dissertation research: the Foundation of UMDNJ Society of Research Scholars, Rutgers' Graduate School-New Brunswick, the Department of Cell Biology and Neuroscience, the New Jersey Commission on Brain Injury Research, the New Jersey Governor's Council for Medical Research and Treatment of Autism, Citizens United for Research in Epilepsy, and Executive Women of New Jersey.

Last, but certainly not least, I would like to acknowledge the research mice that were used for these studies. These animals made it possible to further our scientific understanding of the brain, which will hopefully lead to better clinical treatments in the future.

Table of Contents

List of Tables

List of Figures

Chapter 1. Introduction

1. Pten and the mTOR Pathway

1-1. Pten – Function and Structure

Phosphatase and tensin homolog on chromosome ten (*PTEN*; also known as *MMAC1*) is a tumor suppressor gene located at chromosome 10q23, a locus with a high frequency of mutations in many human cancers (Li et al., 1997; Steck et al., 1997; Ali et al., 1999; Saal et al., 2008). *PTEN* is expressed in all eukaryotic cells and encodes a non-redundant protein and lipid phosphatase that negatively regulates the phosphoinositide-3-kinase (PI3K)/AKT/mammalian target of rapamycin (mTOR) signaling pathway (Figure 1). PTEN contains a tyrosine phosphatase domain that has dual specificity for protein and lipid phosphatase activity (Maehama and Dixon, 1998), the latter of which has been extensively characterized. The primary target of PTEN's lipid phosphatase activity is phosphatidylinositol (3, 4, 5)-triphosphate (PIP_3), which is converted to phosphatidylinositol (4,5)-biphosphate (PIP_2) by PTEN (Cantley and Neel, 1999). PTEN's canonical role as a lipid phosphatase is thought to be highly specific and its predominant function, although there is evidence that PTEN can also dephosphorylate the focal adhesion kinase (FAK) protein, which is involved in cellular adhesion (Tamura et al., 1998). The interaction between PTEN and FAK may be limited, as other studies using *Pten* null cells and PTEN overexpression have not found direct interactions between these two proteins (Maier et al., 1999; Sun et al., 1999).

Analysis of the crystal structure of human PTEN revealed key features of its enzymatic activity. There are two adjacent phosphatase and C2-domain lobes as well as several transmembrane domains near the N-terminal (Lee et al., 1999). The interface between the phosphatase and C2-domains is critical for PTEN phosphatase activity as mutations in this region resulted in impaired function and have been found in many human cancers (Lee et al., 1999). The C2-domain is necessary for PTEN's interaction with the plasma membrane and is calcium independent. Numerous mutations have been observed in human PTEN and are associated with a

wide range of disruptions in PTEN function, particularly for PTEN's lipid phosphatase activity. PTEN mutations identified in cases of Cowden Syndrome, an autosomal dominant disorder characterized by benign growths and increased risk of cancer, suggest that C2-domain mutations that truncate this region affect PTEN localization, phosphorylation, stability and protein-protein interactions but can maintain PTEN's phosphatase activity (Han et al., 2000; Waite and Eng, 2002; Trotman et al., 2007). N-terminal mutations also preserve PTEN catalytic activity, but affect PTEN stability (Han et al., 2000). These mutations have been informative in indicating the function of specific regions (i.e., C2-domain, N-terminal) and their importance for normal PTEN function.

PTEN stability can be influenced by protein-protein interactions and post-translational modifications including phosphorylation. PTEN's C-terminal contains several residues, which when phosphorylated, increase PTEN stability (i.e., serine 370 and 385) (Georgescu et al., 1999; Torres and Pulido, 2001). Conversely, PTEN can be destabilized by phosphorylation at other sites (i.e., threonine 366) (Maccario et al., 2007). Further, catalytic activity can also be altered by phosphorylation depending on the location of this modification. For example, mutation studies focusing on a cluster of PTEN phosphorylation sites (i.e., serine 380, threonine 382, and threonine 383) demonstrated that phosphorylation at these sites promoted a closed protein conformation (Salmena et al., 2008). When these sites remained unphosphorylated, PTEN phosphatase activity increased, likely due to an open protein conformation which enhances protein-protein interactions (Vazquez et al., 2000; Vazquez et al., 2001; Leslie and Downes, 2004).

PTEN function is highly dependent on its cellular localization. Initially, PTEN was thought to be localized primarily to the cytosol, allowing PTEN to be in close proximity to the plasma membrane for its lipid phosphatase activity. PTEN has a lipid binding domain, and several nuclear localization signal (NLS)-like sequences (Chung et al., 2005). Despite lacking a traditional NLS sequence, studies have demonstrated that there is a pool of PTEN located in the

nucleus in differentiated cells, including neurons (Lachyankar et al., 2000). PTEN's substrate, PIP_3, is also found in the nucleus, but does not seem to be sensitive to PTEN's lipid phosphatase activity at this location (Lindsay et al., 2006). Rather, nuclear PTEN is implicated in cell cycle regulation via cyclin D1 suppression (Radu et al., 2003; Chung et al., 2006). PTEN localizes to the nucleus during the G_0-G_1 cell cycle phases, which are the resting phase and the intermediate phase prior to DNA replication, respectively. During this part of the cell cycle, *in vitro* studies demonstrated nuclear PTEN reduced cyclin D1 activity either by transcriptional downregulation or decreasing the nuclear localization of cyclin D1 (Radu et al., 2003; Chung et al., 2006). The mechanism responsible for the trafficking of PTEN into the nucleus is largely unknown but is thought to be dependent on the PI3K/AKT/mTOR pathway (Liu et al., 2007). Bassi and colleagues (2013) demonstrated that PTEN is retained in the nucleus when it is modified by SUMO, a small ubiquitin-like modifier. DNA damage reduced the amount of SUMOylated PTEN, and reduced PTEN's nuclear accumulation as well. PTEN's catalytic activity and SUMOylation were required for DNA repair, suggesting that nuclear PTEN and its SUMO modification are protective against DNA damage.

Recently, a novel variant of PTEN, PTEN-Long, was identified in several cell types, including mouse embryonic stem cells and human breast tissue (Hopkins et al., 2013). PTEN-Long is translated using an alternative start sequence and is secreted by cells. This membrane permeable variant of PTEN possesses a polyalanine sequence near the N-terminal that is required for its movement into and out of cells. When exogenous PTEN-Long was applied to cultured cells, it inhibited PI3K/Akt signaling and activated cell death in PTEN-deficient brain and breast tumor cell lines. The discovery of a new mechanism of PTEN activity underscores the diversity of this phosphatase and the importance of further investigation of its functions.

1-2. The PI3K/Akt/mTOR Pathway

The PI3K/Akt/mTOR signaling pathway is a critical modulator of cell proliferation and growth. Signaling through mTOR, an evolutionarily conserved serine/threonine kinase, is critical for cellular growth and survival as well as protein synthesis (Sato et al., 2008). By working in opposition to PI3K activity, Pten suppresses mTOR signaling, acting as a cellular growth regulator. Pten converts PIP_3 into PIP_2 by hydrolyzing the D3 phosphate of PIP_3's inositol ring (Stambolic et al., 1998) (Figure 1). By shifting the balance from PIP_3 to PIP_2, Pten works in opposition to the function of PI3K, which converts PIP_2 to PIP_3. PIP_3 recruits several proteins containing pleckstrin homology (PH) domains to the cellular membrane, including the Akt family and 3-phosphoinositide-dependent protein kinase 1 (PDK1) (Varnai et al., 2005). Subsequently, Akt is activated near the plasma membrane via phosphorylation of threonine 308 (Thr308) by PDK1 and phosphorylation of serine 473 (Ser473) by mTOR complex 2 (mTORC2) (Maehama and Dixon, 1998; Sarbassov et al., 2005; Manning and Cantley, 2007). Akt is involved in cell proliferation, survival, growth and metabolism through downstream effectors, such as TSC2, GSK3β, MDM2, BAD and p27 (Manning and Cantley, 2007). Activated Akt inhibits a complex composed of TSC1 (hamartin) and TSC2 (tuberin), which normally suppress Rheb, a small GTPase (Sato et al., 2008). Inhibition of TSC1/TSC2, therefore, increases Rheb activity, which leads to mTOR complex 1 (mTORC1) activation.

mTOR participates in two complexes with differing functions, mTORC1 and mTORC2. Some components in these complexes are shared, such as G-protein β-subunit like protein/mammalian LST8 (GβL/mLst8) (Yang and Guan, 2007), whereas other components of mTORC1 and mTORC2 are not shared. For example, mTORC1 contains regulatory-associated protein of mTOR (Raptor) and PRAS40 (Yang and Guan, 2007). In contrast, mTORC2 is composed of rapamycin-insensitive companion of mTOR (Rictor) and mammalian stress-activated protein kinase interacting protein 1 (mSIN1) (Kim et al., 2002; Kim et al., 2003; Wang et al., 2007; Cybulski and Hall, 2009). mTORC1 is involved in protein translation and cellular

growth via phosphorylation of p70 S6 kinase (S6K1) and eukaryotic initiation factor 4E (eIF4E) binding protein (4EBP1), while mTORC2 participates in a positive feedback loop by phosphorylating Akt at a second site distinct from the PDK1 phosphorylation site (Ser473) (Sarbassov et al., 2005). mTORC2 regulates cell survival in response to hormones and growth factors (Zhou and Huang, 2010) and is involved in long-term memory and the late phase of hippocampal long term potentiation via regulation of the actin cytoskeleton (Huang et al., 2013).

mTORC1 is regulated by a complex of TSC1 and TSC2, which when mutated, lead to increased mTOR activity and seizure liability (Crino et al., 2002; Holmes and Stafstrom, 2007; Meikle et al., 2007; Zeng et al., 2008). Cap-dependent protein translation via mTORC1 is a key step in translation initiation (Richter and Sonenberg, 2005). eIF4E recognizes the 5' mRNA cap on the coding sequence and recruits eIF4G as well as the small ribosomal subunit, 40S. 4EBP1, part of a family of eIF4E-binding proteins, can bind to eIF4E to inhibit its function. mTORC1 phosphorylates 4EBP1 and relieves its inhibition of eIF4E, thereby promoting cap-dependent initiation of protein synthesis. Because loss of function of the TSC1/TSC2 complex increases mTORC1 activity, inactivation of TSC1/TSC2 can promote protein translation (Tavazoie et al., 2005). Several new mTOR targets, including Grb10, were identified using proteomic screens (Hsu et al., 2011; Yu et al., 2011). These new downstream proteins may yield insight into how mTOR is involved in a multitude of functions, including seizure activity and synaptic plasticity.

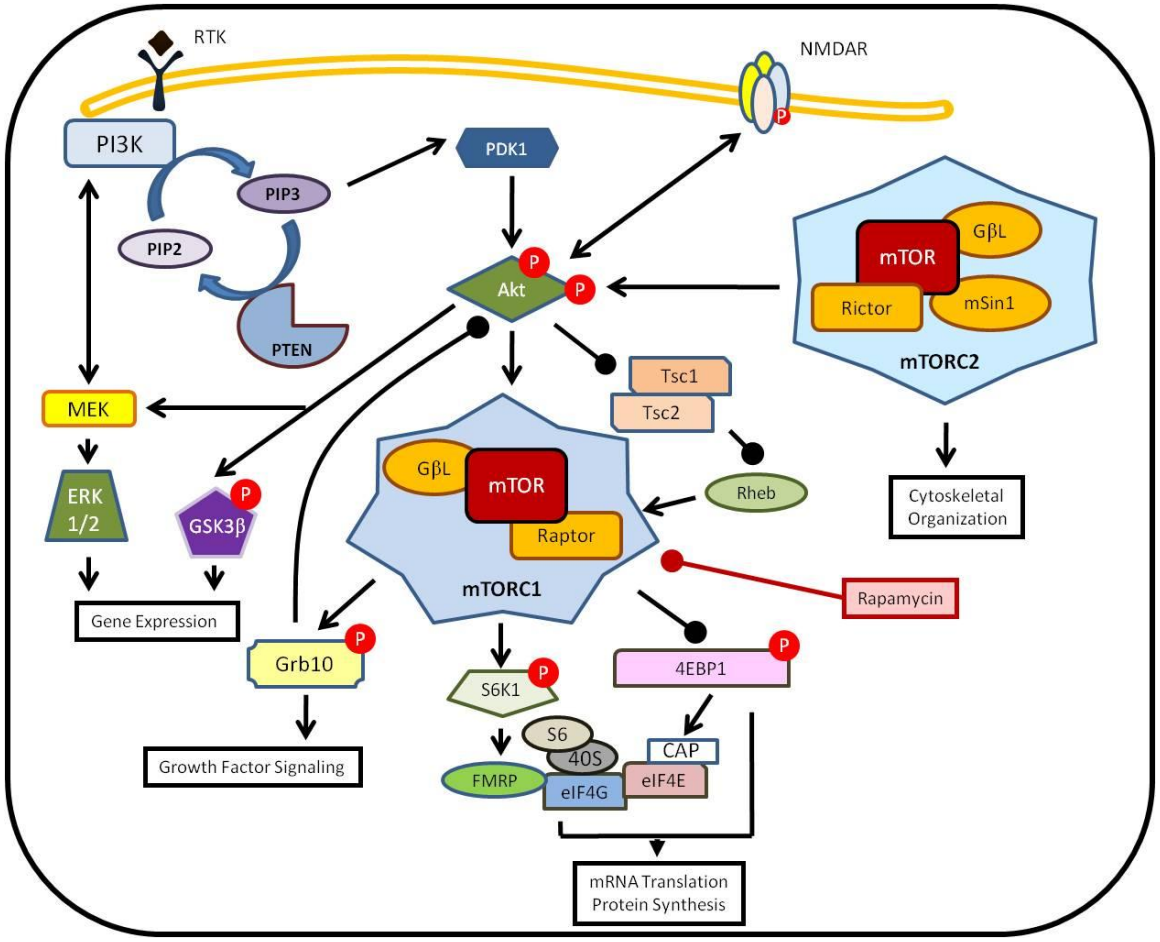

Figure 1. The mTOR Pathway.

The PI3K/Akt/mTOR pathway is critical for cellular growth and protein synthesis. RTK = Receptor Tyrosine Kinase. NMDA = NMDA Receptor. Arrows (⟶) indicate activation, while closed circles (●) indicate inhibition. (P) indicates a phosphorylation event.

1-3. Clinical symptomology and manifestations of *PTEN* mutations

In humans, germline *PTEN* mutations are associated with a group of autosomal dominant syndromes termed PTEN hamartoma tumor syndromes (PHTS). PHTS includes Bannayan-Riley-Ruvalcaba syndrome, Cowden syndrome, Lhermitte-Duclose disease, Proteus syndrome and Proteus-like syndrome. These syndromes are characterized by neurodevelopmental deficits,

multiple hamartomas (benign, tumor-like malformations) and increased cancer risk (Pilarski, 2009; Pilarski et al., 2011; Angurana et al., 2013; Chippagiri et al., 2013; Nieuwenhuis et al., 2013), highlighting PTEN's role in cellular growth and tumor suppression.

PTEN mutations are also implicated in epilepsy and autism (Zhou and Parada, 2012), indicating that alterations in PTEN may affect neuronal function and development. Several PHTS case studies have identified autism-relevant symptoms in affected individuals (Zori et al., 1998; Goffin et al., 2001; Parisi et al., 2001), such as impaired social communication. Approximately 10-20% of autistic children develop macrocephaly (Lainhart et al., 1997; Fidler et al., 2000; Lainhart et al., 2006), suggesting that excessive growth, in particular brain growth, may contribute to aspects of this disorder (Courchesne et al., 2003; Courchesne, 2004). In a clinical study of individuals with autism and macrocephaly, 17% of individuals had germline *PTEN* mutations (Butler et al., 2005), strengthening a connection between PTEN and a subset of cases with autism. It is estimated that 1-5% of the total autism population carries *PTEN* germline mutations (Butler et al., 2005; Buxbaum et al., 2007; Herman et al., 2007; McBride et al., 2010).

Although PTEN has been linked to a small portion of autism cases, the mechanism by which PTEN contributes to autism phenotypes is not well understood. Redfern and colleagues (2010) characterized the structural properties and subcellular location of a *PTEN* mutation identified in autism, H93R PTEN, which is located at the phosphatase active site. This mutation increased PTEN's association with the plasma membrane, but did not increase its phosphatase activity. Rather, it interfered with the structural changes that PTEN undergoes upon interaction of its N-terminal with PIP_2. These data suggest that in the case of this specific autism-related mutation, the conformational change that normally induces PTEN's phosphatase activity is unable to occur as efficiently. Given the range in autism symptomology, it is likely that other *PTEN* mutations identified in autistic individuals may also impact PTEN function, albeit to varying degrees.

1-4. Pten conditional mouse models

In order to model how human PTEN affects the central nervous system, several conditional *Pten* knockout (KO) mouse models have been generated to address how Pten may alter neuronal excitability and function. Conditional knockout models are necessary, since constitutive *Pten* inactivation causes tumors and leads to embryonic lethality (Di Cristofano et al., 1998; Stambolic et al., 1998; Podsypanina et al., 1999). Using Cre/loxP site-specific recombination technology (Sauer and Henderson, 1988; van Diepen and Eickholt, 2008), the Pten gene is flanked by two *loxP* sites, which allows Cre recombinase to catalyze DNA recombination at these sites. Because *Cre* is driven by a temporal and tissue specific promoter, *Pten* loss can be selectively induced in these conditional knockout models.

Brain specific homozygous conditional deletions of *Pten* produce neuronal hypertrophy and seizures (Backman et al., 2001; Kwon et al., 2001). The increased cell size seen in Pten mutants is thought to be mediated through translational control via S6K1- and eIF4E-mediated processes, since individual overexpression of either of these two proteins increases cell size, while co-overexpression increases cell size even further (Backman et al., 2002; Fingar et al., 2002). Mutant chimera mice with a mosaic *Pten* deletion in a subset of neuronal progenitor cells (NS-*Pten* mice) have abnormally large cell bodies only in those neurons lacking *Pten* (Backman et al., 2001; Kwon et al., 2001). Further, NS-*Pten* homozygous mutant mice developed spontaneous seizure activity, as measured by electroencephalography (EEG), which was suppressed by the mTORC1 inhibitor, rapamycin (Ljungberg et al., 2009). Conditional deletion of *Pten* in mutant mice can result in premature lethality and brain enlargement, along with neuronal hypertrophy (Kwon et al., 2006; Ljungberg et al., 2009; Sperow et al., 2011; Kazdoba et al., 2012). These data reinforce Pten's importance in regulating cellular growth and neuronal development.

Behavioral characterization of conditional *Pten* mutant mice has yielded some insight into how loss of Pten may contribute to autism-relevant behaviors. Neuron-specific enolase (*Nse*)

promoter driven Cre selectively deletes *Pten* in discrete populations of mature neurons in the cerebral cortex and hippocampus, resulting in hypertrophic and ectopic dendrites and axonal tracts with increased synapses (Kwon et al., 2006). *Pten* homozygous mutant mice from this line displayed several abnormal behaviors in social interaction and social learning. For example, *Pten* homozygous mutant mice showed increased responses to sensory stimuli and decreased interaction with a novel juvenile upon repeated presentations compared to WT controls. In another series of studies, Nse-*Pten* heterozygous (Het) mice were analyzed to determine the effect of only one mutated *Pten* allele on brain structure and social behavior (Napoli et al., 2012). *Pten* haplo-insufficiency led to cortical and hippocampal hypertrophy and a preference for social avoidance, such that Nse-*Pten* Het mice spent more time with an inanimate object than another mouse. In addition, analysis of energy metabolism in these mice revealed that partial loss of *Pten* increased oxidative stress and impaired mitochondrial function via a downregulation of the p53 signaling pathway. p53 is a tumor suppressor protein that plays a role in DNA repair, cell cycle arrest and apoptosis (Wang and Gu, 2013). Defects in p53 signaling have been associated with autism (Kemper and Bauman, 1993; Araghi-Niknam and Fatemi, 2003), suggesting that mutations in *Pten* and/or this signaling pathway may contribute to the autistic phenotype.

A postnatal deletion of *Pten* driven by the CamKIIα-*Cre* promoter results in loss of Pten in hippocampal and cortical excitatory neurons around postnatal day 16 (Sperow et al., 2011). Hippocampal structure and pyramidal neuron morphology were not affected by postnatal *Pten* deletion. However, long term potentiation (LTP) and long term depression (LTD), two types of synaptic plasticity thought to represent cellular correlates of learning and memory, were impaired in CaMKIIα-*Pten* KO mice. In addition, CaMKIIα-*Pten* KO mice were impaired in the probe trial of the Morris water maze, a hippocampal-dependent spatial memory task. These data suggest that Pten modulates synaptic plasticity independent of its role in cellular growth and neuronal development.

2. Ionotropic glutamate receptors

2-1. NMDA Receptors

N-Methyl-D-aspartate (NMDA) receptors are ionotropic, ligand- and voltage-gated transmembrane receptors that open in response to glutamate binding, allowing cations into (e.g., sodium and calcium) and out of (e.g., potassium) the neuron (Yu et al., 1999; Liu and Zhang, 2000). NMDA receptors are heterotetramers that can be composed of 7 different subunits, including at least one copy of an NR1 subunit, along with varying expression of NR2 (NR2A-D) and NR3 (NR3A or NR3B) subunits (Ghasemi and Schachter, 2011). NR1 and NR2 subunits combine to form the ion pore of the NMDA receptor. The NR2 subunits contain the glutamate binding site, while NR1 subunits contain glycine and D-serine binding sites, which must be occupied with glycine or D-serine before glutamate can activate the receptor. A magnesium ion blocks the NMDA receptor pore under basal conditions and is alleviated through cellular depolarization. Once the magnesium blockade is removed, the NMDA channel can conduct ions into and out of the cell. Importantly, because calcium plays a vital role in neuronal development and synaptic plasticity, such as learning and memory (Maren and Baudry, 1995), optimal levels of NMDA receptors are critical for these processes (Tsien et al., 1996a; Chen and Tonegawa, 1997; Nakazawa et al., 2004).

Since NMDA receptors are integral for neuronal excitation and calcium signaling, alterations in levels of this glutamate receptor type can have significant repercussions on synaptic plasticity and neuronal activity. Glutamate, the principal excitatory neurotransmitter in the brain, is also implicated in excessive neural activity, including seizure (Meldrum, 1994). Rodent models of seizure, such as kindling, depend on NMDA receptor function, which is enhanced in these models, as well in the cerebral cortex of human focal epilepsy cases. These studies suggest that increases in glutamate or NMDA receptors can contribute to epileptiform activity. Additionally, glutamate abnormalities have been implicated in autism. Adults with autism have

higher serum levels of glutamate (Shinohe et al., 2006), and glutamate antagonists have shown some efficacy for the treatment of autism in humans (Niederhofer, 2007) and animal models (Silverman et al., 2010; Mehta et al., 2011). Further, prenatal exposure to valproic acid, an anti-epileptic drug and mood stabilizer, led to selective overexpression of NR2A and NR2B NMDA receptor subunits in a rodent model of autism (Rinaldi et al., 2007). Together, these data suggest that glutamatergic neurotransmission and NMDA receptors should be investigated further to determine their contribution to neurodevelopmental disorders.

NMDA receptors subunits have unique spatio-temporal expression patterns, which suggests that NMDA receptor subtypes have distinct roles depending on where and when they are present during development. Several NMDA receptor subunits have been cloned from the rodent brain, including NR1 and NR2A-D (McBain and Mayer, 1994; Zukin and Bennett, 1995). NR1 is required for NMDA function (i.e., it is an obligatory subunit), and is expressed ubiquitously throughout embryonic and postnatal periods (McBain and Mayer, 1994). The NR2 subunits have varying electrophysiological and pharmacological properties, and exhibit distinct expression patterns. Given this, it is unsurprising that the expression of NR2A- and NR2B-containing NMDA receptors is differential regulated during development and in adulthood. Of the NR2 family of subunits, NR2A and NR2B subunit-containing receptors have been characterized most extensively. Throughout embryonic development and during the early postnatal period, NMDA receptors are primarily composed of NR2B/NR1 subunits (Monyer et al., 1994; Sheng et al., 1994; Kirson and Yaari, 1996). NR2B expression peaks in the cortex and hippocampus around postnatal day 21 (P21), and then declines to moderately low levels in the adult (Ewald RC, 2009). Similar to NR2B, NR2A levels peak around P21 before declining to adult levels. As synapses mature and cortical circuits are refined, there is an increase in NMDA receptors containing NR2A subunits, which have a significantly greater peak channel open probability compared to NR2B/NR1 receptors (Chen et al., 1999). NR2A and NR2B differ in their sensitivity to glutamate and deactivation kinetics, with NR2A receptors possessing a faster decay time (Monyer

et al., 1994; Vicini et al., 1998). Generally speaking, more NR2A/NR1 receptors are present as neurons and synapses mature, outnumbering NR2B/NR1 receptors, which are predominant in immature neurons (Cline et al., 1996; Kew et al., 1998; Stocca and Vicini, 1998; Tovar and Westbrook, 1999; Aizenman and Cline, 2007). NR2C is primarily limited to the cerebellum, peaking in granule cells around P21 (Monyer et al., 1994; Vicini et al., 1998). NR2C remains the predominant subunit in the cerebellum where it is expressed at high levels throughout adulthood. In contrast, NR2D mRNA has very low expression in the forebrain at P0, but is expressed at higher levels in the diencephalon, mesencephalon and spinal cord (Monyer et al., 1994).

Two additional NMDA subunits, NR3A and NR3B, were identified as the final members of the mammalian NMDA receptor family (Pachernegg et al., 2012). Physiologically, their role remains elusive. Similar to the NR1 subunit, NR3 subunits possess glycine and D-serine binding sites instead of a glutamate binding site. Early in postnatal development, NR3A mRNA is expressed in various brain regions, including the entorhinal cortex and layer V of the neocortex, but declines in the adult brain (Sucher et al., 1995; Sun et al., 1998). In contrast, NR3B is only weakly expressed until late postnatal stages, but is widely expressed in adulthood (P40) in the rat forebrain, including the hippocampus and cerebral cortex (Wee et al., 2008). *In vivo* and *in vitro* studies have suggested that NR3 subunits act as dominant negative regulators of NMDA receptors. NR3 co-immunoprecipitates with the obligatory NR1 subunit as well as NR2, and evidence suggests they change the electrophysiological properties of NMDA receptors from that of the classic NR2/NR1 receptors (Das et al., 1998; Al-Hallaq et al., 2002). For example, NR3 expression can reduce cellular current (Das et al., 1998; Nishi et al., 2001). Additionally, presynaptic NR3A-containing receptors are thought to participate in the regulation of glutamate release (Larsen et al., 2011). Because the presence of NR3 subunits lowers calcium permeability of NMDA receptors, it is possible that NR3 may be neuroprotective and lower glutamate-induced excitotoxicity due to excess calcium.

Several studies suggest that reduction of NR3A-containing receptors is involved in synapse maturation and memory consolidation during development, including long-term memory formation (Roberts et al., 2009). Cerebrocortical neurons from NR3A knockout mice exhibited increased NMDA responses in whole cell recordings, as well as increased dendritic spines, as assessed by Golgi stain at P19 (Das et al., 1998). Glutamatergic receptors concentrated at the synapse earlier in young (P8) NR3A KO mice, accelerating the expression of NR1, NR2A and the AMPA subunit GluR1 in the postsynaptic density (Henson et al., 2012). Behaviorally, NR3A KO mice had reduced locomotor activity, but enhanced performance on spatial learning and memory tasks (Mohamad et al., 2013). The latter correlated with increased LTP in NR3A KO hippocampal slices, as well as increased forebrain expression of CaMKII, an important mediator of learning and memory (Yamauchi, 2005). These data suggest that NR3A is not only a negative regulator of spine growth and synaptogenesis but also a modulator of learning and memory.

Increasingly, the mTOR pathway is being implicated as having a role in memory formation due to its importance in protein synthesis (Hoeffer and Klann, 2010). Genetic and pharmacological studies have demonstrated that long-term memory is protein synthesis-dependent (Abel et al., 1997). In addition, several proteins in the mTOR signaling cascade have been associated with key components involved in synaptic plasticity and neural activity. In co-immunoprecipitation studies, Pten associates with NR1, NR2A and NR2B subunits (Ning et al., 2004; Jurado et al., 2010; Ventruti et al., 2011). Further, Ning and colleagues (2004) demonstrated that Pten downregulation inhibited extrasynaptic NMDA receptors and suppressed their activity; this reduction in Pten protected against delayed neuronal death in the hippocampus in a transient global ischemic model. Additionally, Rheb, an activator of mTORC1, associated with the NR3A subunit, providing another link between synaptic NMDA receptors and the mTOR pathway (Sucher et al., 2010). Pten was found to associate with the scaffolding protein PSD-95 at the synapse and was recruited to the postsynaptic terminal during LTD, an activity dependent reduction in neural activity (Jurado et al., 2010). Luikart and colleagues (2011)

demonstrated that Pten knockdown increased the excitatory drive (i.e., frequency of excitatory miniature and spontaneous postsynaptic currents) of dentate granule cells in acute slice cultures without affecting inhibitory synaptic activity. This suggests that lack of Pten may shift the balance between excitatory and inhibitory activity towards excitation. In CamKIIα-*Pten* KO mice, both LTP and LTD were disrupted, although this did not seem to be due to abnormal expression of postsynaptic NMDA or AMPA receptors (Sperow et al., 2011). These data demonstrate that Pten may be involved in the modulation of synaptic plasticity, although the exact mechanism remains elusive.

2-2. AMPA Receptors

A second class of ionotropic glutamate receptors are the 2-amino-3-(5-methyl-3-oxo-1,2-oxazol-4-yl) propanoic acid (AMPA) receptors (Honore et al., 1982). AMPA receptors, which mediate fast glutamatergic transmission, are transmembrane heterotetramers composed of four possible subunits (GluR1-4; also known as GluRA-D). Each of the four AMPA subunits has two major splice variants, flip and flop, which have different pharmacokinetic properties in response to glutamate evoked currents (Sommer et al., 1990; Hollmann and Heinemann, 1994). Antibodies directed at GluR1 and GluR2/3 detect a high level of these subunits in young rat cortex, with populations of neurons primarily expressing GluR1 (Petralia and Wenthold, 1992). Of the four AMPA subunits, GluR4 expression is mostly expressed in the hippocampus during the first postnatal week, while the other AMPA subunits increase their levels of expression in this brain region, stabilizing at P20 (Zhu et al., 2000). Spontaneous neuronal activity in the early postnatal hippocampus triggers the insertion of AMPA receptors into synapses (Zhu et al., 2000; Malinow and Malenka, 2002). This is mediated by the GluR4 subunit, which complexes with GluR2 to become a functional receptor. In contrast, in the adult hippocampus, the majority of AMPA receptors are composed of GluR1 and GluR2, or GluR3 and GluR2 (Wenthold et al., 1996). GluR1 subunits bind to scaffolding proteins and can be phosphorylated during different

synaptic plasticity events (e.g., LTP and LTD) (Hayashi et al., 2000; Boehm et al., 2006). These data suggest that the differential expression of AMPA subunits is due to the unique roles for each of the subunits and their different receptor complexes, depending on where and when they are expressed.

While initially it was thought that calcium influx primarily occurred through the NMDA glutamate receptor, it is now known that certain AMPA receptor subtypes can also conduct calcium. Calcium permeability of AMPA receptors is regulated by the inclusion of the GluR2 subunit, such that GluR2-containing AMPA receptors are calcium impermeable (Jonas et al., 1994; Jonas and Burnashev, 1995). Therefore, AMPA receptors lacking GluR2 are calcium permeable; they have large single channel currents and are enriched in the dendrites of hippocampal neurons (Lerma et al., 1994; Dingledine et al., 1999). Neurons can contain multiple AMPA receptor complexes (e.g., receptors with and without calcium permeability), underscoring the diverse electrophysiological properties provided by AMPA subunit composition.

A recent study demonstrated that Pten inhibition via the hormone leptin increased AMPA GluR1 trafficking, which required NMDA receptor activation, in adult hippocampal slice cultures (Moult et al., 2010). In addition, in an *in vitro* stretch injury model using hippocampal neurons, Pten mRNA and protein levels were increased after stretch injury, while GluR2 subunit expression decreased in the neuronal membrane surface (Liu et al., 2013), suggesting Pten inhibition may reduce cell death after injury by preventing surface GluR2 reductions. These data indicate that in addition to NMDAR regulation, Pten may modulate AMPA receptor activity, and therefore have an effect on synaptic transmission as well as calcium signaling.

3. mTOR Inhibitors

3-1. Rapamycin

Much of the information about mTOR signaling has been studied using rapamycin, a macrolide (compound that contains a macrocyclic lactone ring) that is secreted by the bacterial

strain *Streptomyces hygroscopicus* found on Easter Island (Rapa Nui in the native language) (Yang and Guan, 2007). Rapamycin, as well as rapamycin analogs (rapalogs), bind to FK506-binding protein 12 kDa (FKBP12), a cytosolic protein receptor, to form a complex (Harding et al., 1989; Siekierka et al., 1989). The rapamycin/FKBP12 complex associates with mTOR near its ATP binding pocket located by the kinase domain. By binding at the FKBP12/rapamycin binding (FRB) domain near the active kinase domain, rapamycin inhibits some of the physiological functions of mTOR, primarily those of mTORC1 (Zheng et al., 1995; Yang and Guan, 2007). However, long term treatment with rapamycin can partially inhibit assembly of mTORC2 and its subsequent activity, such as Akt phosphorylation (Edinger et al., 2003; Sarbassov et al., 2005)

Rapamycin has been used as a therapeutic agent in preclinical models of Pten and mTOR signaling. Subclinical epileptiform activity exhibited by NS-*Pten* KO mice was ameliorated by rapamycin (Ljungberg et al., 2009). In another conditional Pten model, rapamycin treatment significantly extended the lifespan of NEX-*Pten* homozygous KO mice (Kazdoba et al., 2012). Further, using a combination of prenatal and postnatal rapamycin treatment, rapamycin rescued the lethality of Nse-*Cre* driven Tsc1 (Nse-*Tsc1*) mutant mouse model (Anderl et al., 2011). Other laboratories have had similar success in reducing seizure activity and premature morbidity with rapamycin and other mTOR inhibitors (e.g., CCI-779, curcumin) in several rodent models, including acute drug-induced seizure models, and conditional *Pten* and *Tsc1* KO mouse lines (Kwon et al., 2003; Zeng et al., 2008; Jyoti et al., 2009; Zeng et al., 2009; Zhou et al., 2009; Huang et al., 2010). Although *in vivo* treatment of rapamycin can have negative consequences such as weight loss (unpublished data - N.C. Sunnen and G. D'Arcangelo), the benefits of mTORC1 suppression are clearly evident in animal models of mTOR hyperactivity.

3-2. New generation mTOR inhibitors

While rapamycin and rapalogs have proven to be valuable tools and therapeutic compounds, they are not without disadvantages. As discussed in the previous section, rapamycin can only inhibit aspects of mTOR signaling via mTORC1 suppression. In addition, rapamycin has been found to increase levels of Akt and eIF4E phosphorylation (Sun et al., 2005; Wan et al., 2007). This activity can be reduced by PI3K inhibitors, indicating there is a negative feedback loop via PI3K that may compensate for rapamycin's effects on growth inhibition. Therefore, in order to completely block PI3K, Akt and mTORC2 mediated activity, other pharmacological inhibitors of this signaling cascade are necessary.

One approach has been to develop small molecule ATP-competitive mTOR kinase inhibitors (Zhang et al., 2011). Since this class of inhibitors (mTORC1/mTORC2 inhibitors) binds to the ATP-binding site in the kinase domain, essentially all mTORC1 and mTORC2 activity is reduced, shutting down both parts of the signaling cascade. mTOR's kinase domain shares certain consensus sequences similar to the PI3K kinase domain. Therefore, subsets of the ATP-competitive mTOR kinase inhibitors are also able to inhibit PI3K catalytic activity (mTOR/PI3K dual inhibitors). This additional inhibition of PI3K kinase activity has the added benefit of reducing the feedback loop to Akt, since both PI3K and mTORC2 are implicated in Akt phosphorylation. Several compounds from these classes have advanced into clinical trials for a diverse range of cancers, while additional compounds are currently being developed.

Since the PI3K/Akt/mTOR signaling cascade has numerous roles in cellular growth, synaptic plasticity and cell survival, it is likely that these second generation compounds will require careful evaluation in order to minimize mechanism-related adverse events. While promising, it is likely that both dual mTORC1/mTORC2 inhibitors and mTOR/PI3K inhibitors will need to be carefully optimized in order to identify reasonable therapeutic index.

4. Significance

PTEN's suppression of the PI3K/Akt/mTOR pathway may be crucial in controlling neuronal excitability and protein synthesis, specifically at the synapse. When left unregulated, this may lead to abnormal synaptic function, including epileptiform activity. In addition, suppression of mTOR signaling may provide a novel target for the development of more effective therapeutic treatments for disorders such as epilepsy and autism. The canonical mTOR inhibitor, rapamycin, does not completely suppress mTOR activity and possesses unwanted side effects, such as hypercholesterolaemia (high cholesterol) and thrombocytopenia (low platelet levels) (Kahan, 1998; MacDonald, 1998). In addition, there are mTOR functions that are rapamycin insensitive, due to mTOR's participation in mTORC2 (Zheng et al., 1995).

Given that mutations in Pten are associated with increased seizure activity, as well as neurodevelopmental disorders such as autism, these studies will help elucidate how Pten is affecting neuronal development and synaptic function. They will further our understanding of how this phosphatase contributes to cellular function outside its role as a growth regulator and yield insight into Pten's involvement at the synapse.

Chapter 2. Loss of Pten upregulates the mTOR pathway and alters ionotropic glutamate receptor protein levels in NEX-*Pten* knockout mice

1. Introduction

The PI3K/Akt/mTOR signaling pathway is implicated in several aspects of neuronal development, including cell body size, neuronal polarity, axon formation, dendrite arborization and synapse formation (Backman et al., 2001; Kwon et al., 2001; Kwon et al., 2006; van Diepen and Eickholt, 2008; Ljungberg et al., 2009). Given that Pten is a negative regulator of this pathway, mutations in this lipid and protein phosphatase would be expected to increase neuronal size, axon formation, dendrite arborization and synapse number. Several conditional *Pten* mutant mouse models have been developed, and display neuronal hypertrophy, macrocephaly, abnormal dendrite and axon patterning, autism-relevant altered social interaction and increased seizure activity (Backman et al., 2001; Kwon et al., 2001; Kwon et al., 2006; Ljungberg et al., 2009). In addition, *PTEN* mutations in humans have been implicated in autism and increased seizure liability, further demonstrating that PTEN plays a crucial role in neuronal development and synaptic activity. While conditional *Pten* mutant mice can model aspects of *PTEN* mutations, such as autism-relevant behaviors and seizure susceptibility, the molecular mechanism underlying these abnormalities is still unknown.

I hypothesized that loss of Pten during brain development increases the expression of glutamate receptor subunits, and thus, profoundly affects neuronal excitability, contributing to the increased seizure susceptibility associated with *Pten* mutations. There is evidence to support a relationship between Pten and ionotropic glutamate receptors, particularly NMDA receptors. Pten has been shown to co-immunoprecipitate with several NMDA receptor subunits (Ning et al., 2004; Jurado et al., 2010; Ventruti et al., 2011). Although several groups have measured abnormal synaptic activity due to genetic deletion of *Pten* (Fraser et al., 2008; Ljungberg et al., 2009; Sperow et al., 2011) or lentiviral Pten knockdown (Luikart et al., 2011), no biochemical

analyses have examined how Pten deficiency may alter ionotropic glutamate receptor expression. The present set of studies sought to further characterize how deficits in Pten function may result in abnormalities related to synaptic function.

In order to study the neuronal effects of Pten loss, the D'Arcangelo lab generated the NEX-*Pten* conditional knockout mouse. In this model, the NEX promoter begins to drive Cre expression around E11.5 in the majority of excitatory neurons in the forebrain (i.e., cortex and hippocampus), thereby deleting *Pten* in these principal neurons during embryonic development (Goebbels et al., 2006). Thus, NEX-*Pten* homozygous mutant (KO) mice provide an opportunity to study how loss of Pten function in a major class of neurons affects neuronal development and synaptic function, particularly ionotropic glutamate receptors.

One of the most striking characteristics of NEX-*Pten* KO mice is their shortened life span (Kazdoba et al., 2012). Therefore, NEX-*Pten* KO mice were characterized at postnatal day 0 (P0) in the first set of studies in this chapter. NEX-*Pten* brains were analyzed for structural anatomy, neuronal size and cortical layer formation using histology and immunofluorescence techniques. Biochemical analyses of embryonic and newly born NEX-*Pten* mice revealed how NMDA and AMPA glutamate receptor subunits were affected by loss of *Pten* and subsequent upregulation of the PI3K/Akt/mTOR pathway. Analyses of mRNA levels determined if a transcriptional mechanism was responsible for any alterations in glutamate receptor protein levels. Since NEX-*Pten* KO mice die shortly after birth, but heterozygous (Het) mice have a normal life span, these Het mice were also used to determine if glutamate receptor subunit abnormalities are present in adulthood as a consequence of long-term partial loss of Pten function.

Pten conditional mouse models can exhibit increased seizure susceptibility, which may be indicative of altered glutamate receptor functionality. Treatment with mTOR inhibitors, such as rapamycin, can suppress seizure activity and ameliorate abnormal *Pten* mutant phenotypes. For example, NS-*Pten* KO mice exhibit subclinical epileptiform activity that is mainly detectable by EEG; these seizures were ameliorated by rapamycin (Ljungberg et al., 2009). In addition, the

shortened lifespan of NEX-*Pten* KO mice can be extended by rapamycin treatment (Kazdoba et al., 2012). Rapamycin binds to FKBP12, part of mTORC1, demonstrating the importance of mTORC1 in some Pten-dependent phenotypes. Here, prenatal rapamycin treatment was employed to determine if any detected glutamate receptor subunit alterations were due to excessive mTOR complex 1 (mTORC1) activity.

2. Materials and Methods

Mice

NEX-*Pten* mice were generated by crossing NEX-*Cre* knockin mice (Goebbels et al., 2006) and Cre negative conditional neuron subset-specific *Pten* (NS-*Pten*) knockout mice (Pten $^{loxP/loxP}$). NEX-*Cre* mice on the C57Bl/6 isogenic background were provided by Dr. Klaus Nave (Max Planck Institute, Germany). NEX-*Cre* (+/+);Pten $^{(+/loxP)}$ (heterozygous; Het) mice were bred to generate NEX-*Cre* (+/+);Pten $^{(+/+)}$ (wildtype; WT), Het and NEX-*Cre* (+/+);Pten $^{(loxP/loxP)}$ (homozygous knockout; KO) mice. For embryonic and early postnatal experimental time points, NEX-*Pten* Het female mice were mated with NEX-*Pten* Het males and checked for seminal plugs on a daily basis during breeding to determine time of planned pregnancy. Animals were housed in a temperature and humidity controlled vivarium with *ad libitum* access to water and standard rodent chow and kept on a standard 12 hr light/dark cycle. All experiments and rodent housing were in accordance with protocols approved by the Animal Protocol and Use Committee at Rutgers University, according to the National and Institutional Guidelines for Animal Care established by the National Institute of Health.

Western Blot Analyses of Total Lysate and Crude Synaptosome Preparations

Brains of NEX-*Pten* pups were isolated immediately after birth at postnatal day 0 (P0) and weighed. For embryonic tissue samples, embryonic day 17.5 (E17.5) embryos were quickly harvested from pregnant NEX-*Pten* female mice. Forebrain tissue was dissected on ice and

homogenized together in RIPA lysis buffer (50 mM Tris (pH 7.4), 1% NP40, 0.25% sodium deoxycholate, 150 mM NaCl, 1nM EDTA) with protease and phosphatase inhibitors. Total lysate was cleared by centrifugation (3000xg for 5 min at 4°C) and measured by the Bradford method for protein concentration.

For older postnatal time points and crude synaptosome preparation, brains were isolated and placed in ice cold PBS for 5 minutes. NEX-*Pten* Wt and Het brains from male littermate pairs were collected at 6 months of age. Cortex and hippocampus were isolated, placed in cold Buffer A solution (5 mM HEPES) (pH 7), 1mM $MgCl_2$, 0.5 mM $CaCl_2$ with phosphatase and protease inhibitors) and homogenized. Samples were centrifuged at 1400xg for 10 min. The pellet from this step (P1) was resuspended with additional Buffer A, and centrifuged at 700xg for 10 min. Supernatant was collected from both steps (S1 and S1', respectively), combined and then centrifuged for an additional 10 min at 13,800xg. All centrifugation steps were performed at 4°C. The pellet that formed (P2) containing the crude synaptosomes was re-suspended in Buffer A, and measured for protein concentration using the Bradford method.

For Western blot analysis, protein samples were supplemented with Laemmli sample buffer, boiled for 3 minutes and then subjected to SDS-PAGE. Proteins were electro-transferred to a 0.2 µm nitrocellulose membrane using either iBlot (Invitrogen) or a standard wet tank system. The membranes were washed with TBS-T solution (0.05% Tween-20, 0.8% NaCl, 20 mM Tris (pH 7.5)), and blocked in a 3% nonfat dry milk (NFDM) solution or bovine serum albumin (BSA) (in TBS-T) for 1 hr, followed by additional washing with TBS-T. Membranes were incubated in 0.3% NFDM or BSA/TBS-T with the appropriate primary antibodies overnight at 4° C (Table 1). After primary antibody incubation, membranes were washed with TBS-T and incubated with horseradish peroxidase (HRP)-conjugated secondary antibodies for 1 hr at room temperature (Table 2). Membranes were incubated with ECL-Plus Western Blotting Detection System (Pierce/Thermo Fisher, Rockland, IL) for 5 min to develop antibody signal, and then exposed to autoradiographic films.

Antibody	Vendor	Catalogue #	Host Species	Dilution	Application
4EBP1	Cell Signaling	9452	R	1:1000	WB
Phospho-4EBP1 (Thr37/46)	Cell Signaling	2855	R	1:1000	WB
Actin	Millipore	MAB1501	M	1:10,000	WB
Total Akt	Cell Signaling	4691	R	1:1000 – 1:5000	WB
Phospho-Akt (Ser473)(D9)EXP	Cell Signaling	4060	R	1:1000 – 1:5000	WB
Phospho-Akt (Thr 308)	Cell Signaling	2965	R	1:1000 – 1:5000	WB
BrdU	Abcam	ab6326	Rat	1:100	IF
Cre	Covance	MMS-106R	M	1:100	IF
Cux1 (CDP)	Santa Cruz	sc-13024	R	1:100	IF
Dab1 (D4 Clone)	Provided by A. Goffinet**	__	M	1:1000	WB
Dab1	Rockland	100-401-225	R	1:1000	WB
GluR1	Abcam	ab31232	R	1:1000	WB
GluR2/3	Abcam	ab37174 ab53086	R R	1:1000 1:1000	WB WB
Phospho-eIF4e (Ser209)	Cell Signaling	2441	R	1:1000	WB
Erk1/2 (p42/44)	Cell Signaling	9102	R	1:2000	WB
Phospho-Erk1/2 (Phospho-p42/44) (Thr202/204)	Cell Signaling	9101S	R	1:2000	WB
Grb10 (K-20)	Santa Cruz	sc-1026	R	1:200	WB
GSK3β	Cell Signaling	9315	R	1:1000	WB
Phospho-GSK3β (Ser9)	Cell Signaling	9323	R	1:1000	WB
MAP2	Millipore	AB5622	R	1:1000 1:250	WB IF
MAP2	Leinco	M119	M	1:250	IF
MAP2	Covance	SMI-52R	M	1:250	IF
mTOR	Cell Signaling	2983	R	1:1000	WB
Phospho-mTOR (Ser2448)	Cell Signaling	2971	R	1:1000	WB
NeuN (Clone A60)	Millipore	MAB377	M	1:1000 1:200	WB IF
Neurofilament (Heavy) (NFH)	Millipore	AB8135	R	1:200	IF
Neuroligin1 (Nlg1)	Synaptic Systems	129-111	M	1:100	WB

Neuroligin3 (Nlg3)	Synaptic Systems	129-103	R	1:100	WB
NR1	Cell Signaling	5704	M	1:1000	WB
NR1	Millipore	05-432	M	1:1000	WB
NR2A	Millipore	07-632	R	1:1000	WB
NR2B	Millipore	06-600	R	1:1000	WB
NR3A	Santa Cruz	SC-98986	R	1:1000	WB
NR3B	Santa Cruz	SC-50474	R	1:1000	WB
p70 S6 Kinase (S6K1)	Cell Signaling	9202	R	1:1000	WB
Phospho-p70 S6 Kinase (S6K1) (Thr389) (108D2)	Cell Signaling	9234	R	1:1000	WB
Phalloidin (Rhodamine Conjugated)	Invitrogen	R415	--	2 units	IF
Pten (138G6)	Cell Signaling	9559	R	1:1000 – 1:2000	WB
Reelin (CR-50)	In House*	--	M	1:200	IF
Phospho-ribosomal protein S6 (Ser235/236)	Cell Signaling	4858	R	1:1000	WB
Phospho-ribosomal protein S6 (D68F8) (Ser240/244)	Cell Signaling	5364	R	1:1000	WB
Tbr1	Abcam	ab31940	R	1:100	IF
TSC2 (D93F12) XP	Cell Signaling	4308	R	1:1000	WB

Table 1: Primary antibodies for Western blot and immunofluorescence studies. Phospho = phosphorylated. Thr = Threonine. Ser = Serine. Host species: M = mouse, R = rabbit. WB = Western blot. IF = Immunofluorescence. **Dab1 (D4 clone) antibody was kindly provided by Dr. Andre Goffinet (University of Louvain, Brussels, Belgium. *CR-50 was purified from hybridoma cell culture supernatants using Hi-Trap protein G columns (Amersham Biosciences).

For quantification analysis, all protein levels were normalized to intensity values of actin or total protein of interest (e.g., total Akt for phosho-Akt) (loading control). At least three different samples of each genotype were analyzed for statistical analysis. Samples are represented as fold-change of WT intensity levels.

Conjugant	Vendor	Catalogue #	Specificity	Dilution	Application
Horseradish peroxidase (HRP)	Sigma	A2304	Mouse IgG	1:10,000	WB
HRP	Sigma	A0545	Rabbit IgG	1:10,000	WB
Alexa Fluor 488	Invitrogen	A11001	Mouse IgG	1:500	IF
Alexa Fluor 488	Invitrogen	A11008	Rabbit IgG	1:500	IF
Alexa Fluor 647	Invitrogen	A21235	Mouse IgG	1:500	IF
Alexa Fluor 647	Invitrogen	A21247	Rat IgG	1:500	IF
Alexa Fluor Cy5	Invitrogen	A10523	Rabbit IgG	1:500	IF

Table 2: Secondary antibodies for Western blot and immunofluorescence studies.

WB = Western blot. IF= Immunofluorescence.

Quantitative Real Time PCR (qRT-PCR)

To determine if alterations in glutamate receptor protein expression were due to changes in gene transcription, cortical samples were analyzed by quantitative real time PCR (qRT-PCR) to measure receptor subunit messenger RNA (mRNA) levels between NEX-*Pten* genotypes. Cortex from P0 pups were quickly harvested, dissected and frozen at -80°C until further use. Total RNA was purified from collected tissue samples using Qiagen RNeasy kit protocols. RNA was then reverse transcribed into cDNA using a reverse transcriptase. The resulting cDNA was used as a template for subsequent PCR amplification using primers that are specific for genes of interest. Appropriate primer sequences were selected using PrimerBank (http://pga.mgh.harvard.edu/primerbank/) and are listed in Table 3. qRT-PCR was run using Power SybrGreen master mix (Applied Biosystems) as a reporter on an Applied Biosystems Real-Time PCR machine. The expression of specific genes was quantified by normalizing to levels of glyceraldehyde-3-phosphate dehydrogenase (Gapdh), a standard housekeeping gene, to calculate relative levels of transcripts (Pfaffl, 2001).

Gene	Gene Product	Sequence	PrimerBank ID
Dab1	Dab1	F 5'-AAACCAGCGCCAAGAAAGACT-3' R 5'-CGGACACTTCATCAATCCCAA-3'	70909360b1
Gapdh	Gapdh	F 5'- AGGTCGGTGTGAACGGATTTG-3' R 5'- TGTAGACCATGTAGTTGAGGTCA-3'	6679937a1
Gria1	GluR1	F 5'- TCCCCAACAATATCCAGATAGGG-3' R 5'- AAGCCGCATGTTCCTGTGATT-3'	51080a1
Gria2	GluR2	F 5'- GCCGAGGCGAAACGAATGA-3' R 5'- CACTCTCGATGCCATATACGTTG-3'	7305115a1
Gria3	GluR3	F 5'- ACCATCAGCATAGGTGGACTT-3' R 5'- ACGTGGTAGTTCAAATGGAAGG-3'	8393313a1
Grin1	NR1	F 5'-ATGCACCTGCTGACATTCG-3' R 5'-TATTGGCCTGGTTTACTGCCT-3'	26331234a1
Grin2A	NR2A	F 5'- GCGCCTCGGGAAAGGTTATAG-3' R 5'- TCAGTGCGGTTCATCAATAACG-3'	6680097a1
Grin2B	NR2B	F 5'- GCCATGAACGAGACTGACCC-3' R 5'- GCTTCCTGGTCCGTGTCATC-3'	6680099a1
Grin3A	NR3A	F 5'- AGAGCCAGGGCGAAATGATG-3' R 5'- GGAAACTCGTGGCGCACTA-3'	166158133c1
Grin3B	NR3B	F 5'- TCTGGAGCTAGTGGCCGTC-3' R 5'- GCGCCTCGGGAAAGGTTATAG-3'	20127397a1

Table 3: Primer sequences for quantitative real time PCR (qRT-PCR) analyses.
Primer sequences were selected from PrimerBank (http://pga.mgh.harvard.edu/primerbank/). F = Forward. R= Reverse.

Tissue Immunofluorescence

NEX-*Pten* brains were isolated at P0 immediately after birth, fixed in 4% formaldehyde in phosphate buffered saline (PBS) for 24 hrs and then transferred to a 30% sucrose solution (in PBS) for cryoprotection. After sinking in the sucrose solution, brains were frozen in a 30% sucrose/Cryo-OCT compound solution (30:70 mixture ratio; Fisher) and serially sectioned at 30 µm on a cryostat. To determine if Pten deficiency during development affected neuronal migration, pregnant dams were treated with 100 mg of 5-bromo-2'-deoxyuridine (BrdU; Sigma-Aldrich) per kg of body weight by intraperitoneal (IP) injection at E15.5 to label proliferating cells. For immunofluorescence of BrdU and cortical layer markers, sections were incubated in

2N hydrochloric acid for 30 min at 37°C, followed by neutralization with 100 mM sodium borate (pH 8.5) for 10 min at room temperature. Sections were permeabilized with 0.1% Triton-X (in PBS) for 10 min and blocked with 10% normal goat serum in 0.1% Triton-X (in PBS; blocking solution) for 1 hr at room temperature. Sections were incubated with primary antibodies in blocking solution overnight at 4°C (Table 1). Sections were then washed and incubated with the appropriate secondary antibodies in 0.1% Triton-X in PBS (Table 2) for 1 hr at room temperature. After additional washing of PBS, sections were mounted with Vectashield Mounting Medium with DAPI (Vector Laboratories). Multiple sections from 2 to 3 mice per genotype were examined. Representative images were acquired using a Yokogawa CSU-10 spinning disk confocal head attached to an inverted fluorescence microscope (Olympus IX50).

Golgi Impregnation and Analysis

Brains from P0 NEX-*Pten* pups were isolated and processed for Golgi impregnation using the EZ Golgi Kit (Drs. Deqiang Jing and Francis Lee, Weill Cornell Medical College, Cornell University, New York, NY). Whole brains were immersed in Golgi stain for 10 days at room temperature in a dark location. Brains were then transferred to 30% sucrose (in distilled water) for 3 days at 4°C, with the sucrose solution changed after the first 12 hrs. Brains were then imbedded in 3% agarose and cut sagittally at 150 μm on a vibratome in 30% sucrose (in distilled water) at room temperature. Brain slices were mounted onto 2% gelatin covered slides and brushed with 50% sucrose (in distilled water) and allowed to dry for at least 48 hours in a dark location before stain processing. Slides were then immersed in distilled water 3 times for 10 min each with gentle shaking, and then transferred into a Blackening Solution for 5 min to develop the Golgi stain. Slides were then rinsed in distilled water 3 times for 10 min and dehydrated through graded ethanol (50%, 75%, 95% and 100% ethanol) for 10 min per step. Slides were then cleared with Histo-Clear (National Diagnostics) for 3 x 5 min washes and coverslipped with DPX mounting solution (Sigma-Aldrich). Representative images of Golgi-

impregnated brain slices were acquired using brightfield microscopy on an inverted Olympus IX50 microscope. Cell bodies were measured in the upper one third of the cortex and traced using the Freehand Selection tool in ImageJ (NIH, Bethesda, MD) to measure their size.

Tissue Histochemistry

Thionin staining (FD Neurotechnologies) was performed on 30 µm NEX-*Pten* P0 brain slices fixed in formaldehyde as described above. Sections were first immersed in xylene (3 min) and then incubated twice in 100% ethanol (3 min each). Slices were then placed in 95% and 75% ethanol (3 min each), followed by distilled water 3 times (3 min each). Brain sections were stained with thionin solution for 10 min, rinsed with distilled water and immersed in 95% ethanol with 0.1% glacial acetic acid (2 min). Sections were then dehydrated in 100% ethanol with 4 changes (2 min each), cleared in xylene for 3 changes (3 min each) and mounted with Permount (Fisher).

Drug Preparation and Administration

Pharmaceutical grade rapamycin (>99% purity; LC Laboratories) was dissolved in sterile buffer solution of 4% ethanol, 5% polyethylene glycol (PEG400; Sigma) and 5% Tween 80 (Sigma) in distilled water at a 1 mg per ml concentration. Ethanol was added to rapamycin first to dissolve it, followed by PEG400, Tween 80 and distilled water, with the solution vortexed at each step. Rapamycin (1 month shelf life) was stored at -20°C. Pregnant NEX-*Pten* Het female mice were dosed either IP or subcutaneously (SC) with rapamycin during pregnancy at E13.5 and E16.5. Dosing regimens that dosed rapamycin 3 times during gestation resulted in pregnancies that were not carried to term. Body weights of dosed females were recorded on a semi-daily basis to determine if rapamycin had any effect on body weight during gestation (data not shown). Brains of pups were collected immediately after birth at P0. Pup body and brain weights were recorded prior to tissue dissection.

Statistical Analyses

For studies using NEX-*Pten* WT, Het and KO mice, a planned comparison Student's t-test evaluated if loss of Pten in NEX-*Pten* KO mice resulted in abnormalities compared to NEX-*Pten* WT mice ($p<0.05$). Subsequently, to determine if there was an effect of gene dosage, a one-way ANOVA was run with Dunnett's post hoc tests to compare all genotypes (i.e., Het and KO) to WT. Normalized protein values in Western blot analyses and the ratio for the gene of interest in qRT-PCR studies were analyzed first by Student's t-test and then by one-way ANOVA with post hoc Dunnett's tests. For Golgi impregnated cortical neurons, soma size of individual neurons within genotype were averaged and compared between genotypes using a Student's t-test ($p<0.05$). Effect size was calculated for NMDA and AMPA receptor subunit results, along with a power analysis (Appendix).

3. Results

Characterization of NEX-Pten Cortical Layers and Neuronal Morphology

NEX-*Pten* conditional knockout mice were generated to evaluate the effects of Pten loss on brain development and ionotropic glutamate receptor expression. In NEX-*Cre* mice, Cre expression is driven by the NEX promoter in the majority of forebrain excitatory neurons soon after they become postmitotic (Goebbels et al., 2006). NEX-*Cre* mice were crossed with Pten $^{(loxP/loxP)}$ to establish the NEX-*Pten* colony. For these studies, NEX-*Cre* (+/+);*Pten*$^{(wt/loxP)}$ mice were intercrossed to generate mice that were all NEX-*Cre* (+/+) but either wildtype (WT), heterozygous (Het) and homozygous (KO) for *Pten*. NEX-*Pten* KO mice were born at the expected ratio but died shortly after birth, whereas Het littermates did not exhibit premature death (Kazdoba et al., 2012). In addition to a reduced lifespan, NEX-*Pten* KO mice did not differ in weight compared to WT mice at birth, but did fail to thrive, weighing significantly less than WT

mice by postnatal day 3 (P3). Due to the severity of the phenotype and the early postnatal lethality, the current studies focused on the analysis of newborn NEX-*Pten* KO mice (P0).

Cre immunofluorescence confirmed the predominant expression of Cre in the forebrain (i.e., cortex and hippocampus), but not the midbrain or hindbrain (i.e., cerebellum), of Cre (+/+) NEX-*Pten* WT mice (Figure 2a). Accordingly, there was a progressive loss of Pten protein expression in NEX-*Pten* Het and KO forebrain, but not the cerebellum, compared to WT, as measured by semi-quantitative Western blot analysis (Figure 2b). Further, Golgi impregnation of NEX-*Pten* brains demonstrated that the somas of cortical neurons in NEX-*Pten* KO mice (n=55) were significantly larger than those of WT neurons (n=42) [$t(95)=6.421$, $p<0.0001$] (Figure 2c, d). In addition to having larger neurons, NEX-*Pten* KO brains (n=5) weighed significantly more than WT brains (n=5) immediately after birth [$t(8)=3.428$, $p<0.01$] (Figure 2e). NEX-*Pten* Het brains (n=17) were similar in weight to WT brains. ANOVA analysis revealed an overall effect of *Pten* deficiency on brain weight [$F(2,24)=14.15$, $p<0.0001$]. Post hoc Dunnett's multiple comparison test revealed that this effect was driven by complete loss of Pten [WT vs. KO, $p<0.05$].

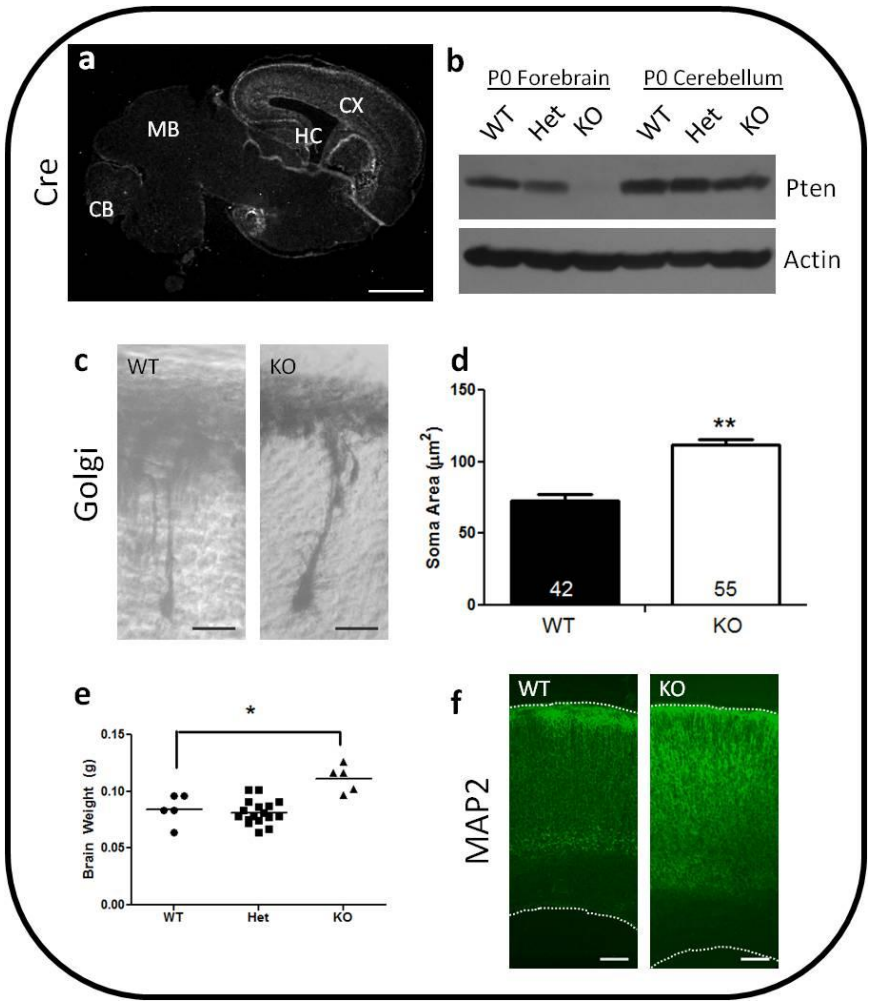

Figure 2. *Pten* deletion in the excitatory cortical neurons of the forebrain results in increased soma size, brain weight and MAP2 staining.

a) Low magnification image of a NEX-*Pten* wildtype (WT) sagittal brain slice at postnatal day 0 (P0) processed for Cre immunofluorescence, demonstrating widespread expression in the cerebral cortex (CX) and hippocampus (HC), but not the midbrain (MB) or cerebellum (CB). b) Representative Western blot of forebrain and cerebellum of NEX-*Pten* WT, heterozygous (Het) and knockout (KO) P0 mice. Lysate was probed with antibodies for Pten and actin and revealed the progressive reduction of Pten in the forebrain of NEX-*Pten* Het and KO mice. c) High magnification brightfield images of cortical neurons in Golgi impregnated NEX-*Pten* WT and KO brains. d) Quantification of the soma size of Golgi impregnated cortical neurons in the upper

third of the cerebral cortex. NEX-*Pten* KO cortical neurons (n=55) have significantly larger somas than WT cortical neurons (n=42) (**p<0.0001). e) NEX-*Pten* KO brains weighed significantly more than NEX-*Pten* WT brains at birth (* p<0.05). f) Low magnification confocal images of MAP2 immunofluorescence labeling in NEX-*Pten* WT and KO cortex. Scale bars = 1 mm (a), 30 μm (c), 100 μm (f).

Histological staining of comparable P0 brain sections showed a specific enlargement of forebrain structures in NEX-*Pten* KO brains compared to WT littermates (Figure 3), which is consistent with Cre expression, and thus Pten loss, in this model. Forebrains of NEX-*Pten* Het mice were unaffected by Pten heterozygosity and were indistinguishable from WT mice (data not shown). In addition to having a larger cortex and hippocampus, cellular layers were less compact in NEX-*Pten* KO structures (Figure 3c-f). The size of the cerebellum and other hindbrain structures did not differ between genotypes (Figure 3g-h).

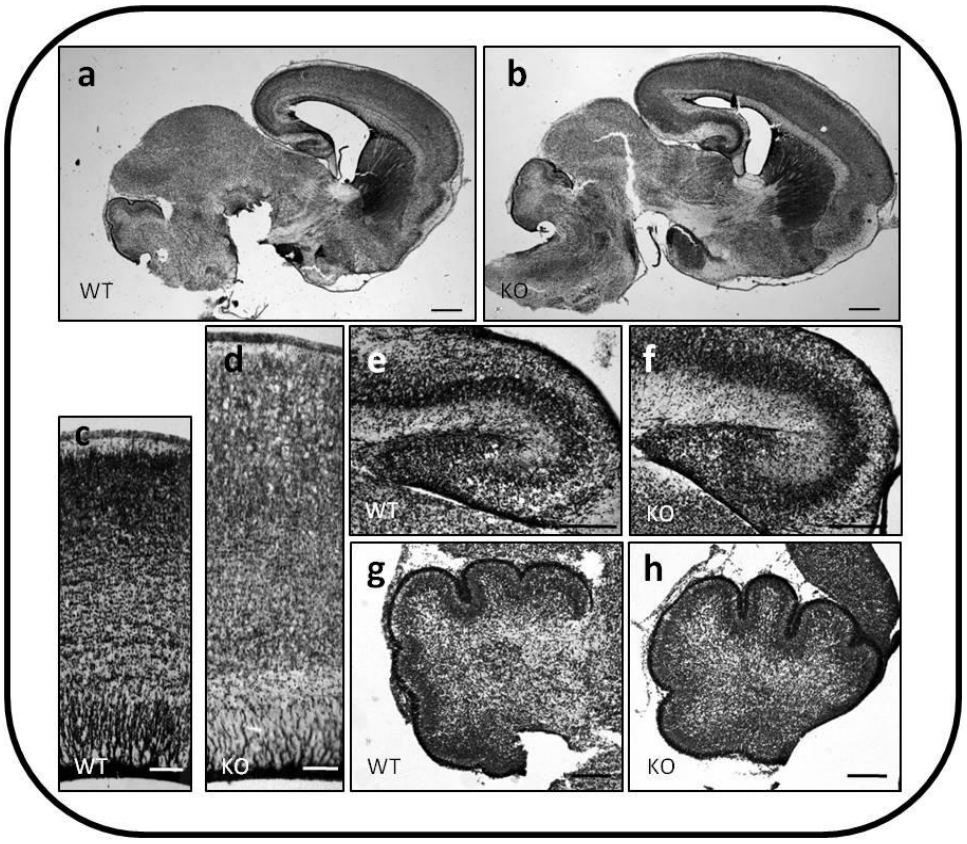

Figure 3. Histological staining of brain structures in newly born NEX-*Pten* mice.

Sagittal sections of postnatal day 0 (P0) NEX-*Pten* wildtype (WT) and knockout (KO) littermates were stained with thionin. Low magnification images of NEX-*Pten* WT (a) and KO (b) brains revealed an enlarged forebrain in KO mice at P0. Comparable higher magnification images of the lateral cerebral cortex (c, d), hippocampus (e, f) and cerebellum (g, h) revealed a specific enlargement of the forebrain structures in NEX-*Pten* KO mice. Scale bars = 500 μm (a, b), 100 μm (c, d), 200 μm (e-h).

To determine if Pten loss affected the migration or positioning of excitatory neurons in the forebrain, immunofluorescence labeling was performed to evaluate cortical layer development in NEX-*Pten* P0 KO mice. Reelin (Reln), an extracellular glycoprotein secreted by Cajal-Retzius cells in the marginal zone near the surface of the cortex, is involved in the regulation of principal

cortical neuron migration (D'Arcangelo, 2005). In both NEX-*Pten* WT and KO mice, the Reln signal was predominantly found in the marginal zone of the cortex (Figure 4a-b). The size and position of Reln-positive Cajal-Retzius cells did not differ between genotypes, although the distribution of the Reln signal appeared less uniform in the NEX-*Pten* KO marginal zone. Labeling with Tbr1, a marker of early-born neurons, identified principal cortical neurons in the deep layers of WT cortex (Figure 4c). In NEX-*Pten* KO cortex, the majority of Tbr1-positive neurons were correctly positioned in deep cortical layers, similar to WT, but were less compact than the Tbr1-positive layers in WT controls (Figure 4d). In addition, some Tbr1-positive neurons in the NEX-*Pten* KO cortex were present near or within the marginal zone at the surface of the cortex. BrdU administration at embryonic day 15.5 (E15.5) labeled late-born cortical neurons, which migrated properly to the upper layers of both NEX-*Pten* WT and KO P0 cortices (Figure 4e and g). Cux1, an upper cortical layer marker, also did not differ between genotypes (Figure 4f and h), suggesting that Pten loss in excitatory neurons in the cortex did not significantly alter cortical layer formation or radial migration in the young neocortex.

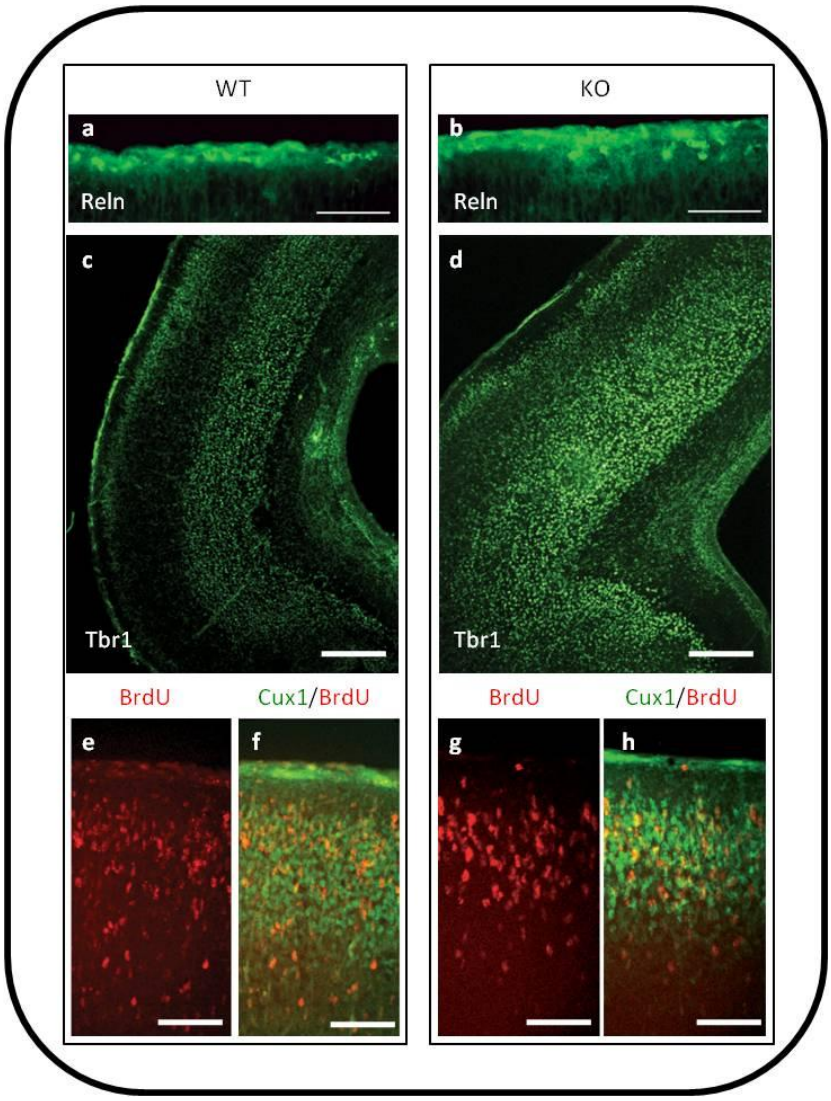

Figure 4. Analysis of cortical layer formation in NEX-*Pten* mice at postnatal day 0.

Brain sections from postnatal day 0 (P0) NEX-*Pten* wildtype (WT) and knockout (KO) mice were processed for immunofluorescence staining using Reln (a, b) or Tbr1 (c, d) antibodies. BrdU was injected into a pregnant dam to label dividing cells at E15.5. Brain sections were processed for immunofluorescence staining using BrdU and Cux1 antibodies (e-h). Confocal images revealed that Reln is predominantly expressed in the marginal zone of the cortex. Tbr1-labeled neurons are present in the deep layers of the caudal cerebral cortex in NEX-*Pten* WT and KO mice. Cells labeled with BrdU (red) and Cux1 (green) are predominantly in the upper layers of the cerebral cortex in both genotypes. Scale bars = 100 µm (a, b), 200 µm (c, d), 100 µm (e-h).

Analysis of the PI3K/Akt/mTOR Pathway and other Signaling Cascades in NEX-Pten Forebrain

Since Pten is a negative regulator of the PI3K/Akt/mTOR pathway, loss of Pten function should result in altered signaling in the forebrain of NEX-*Pten* KO mice. Using semi-quantitative Western blot analyses, P0 forebrain lysate from multiple mice (n=3-6 per genotype) were analyzed to evaluate several components of this signaling cascade. Western blot values for proteins of interest were normalized to appropriate loading controls (e.g., actin, total Akt, total S6) to take into account potential protein translation increases (due to mTORC1's involvement in protein translation and synthesis) or loading variability. In NEX-*Pten* P0 forebrain lysate, there was a progressive reduction of Pten levels in Het and KO mice compared to WT controls (Figure5a, b, d). NEX-*Pten* KO mice had significantly less Pten than WT littermates [$t(4)=3.851$, $p<0.02$]. ANOVA analysis revealed an effect of genotype due to loss of Pten [$F(2,6)=9.862$, $p<0.02$], with significant differences between NEX-*Pten* WT and KO mice [Dunnett's post hoc test, $p<0.05$]. While Pten was modestly decreased in NEX-*Pten* Het forebrain (0.7 fold of WT), this was not statistically different than WT Pten levels. Loss of Pten in NEX-*Pten* KO mice led to dramatic increases in Akt phosphorylation at two separate sites, serine 473 (Ser473; mediated by mTORC2) and threonine 308 (Thr308; target of PDK1), which were significantly increased compared to WT [$t(4)=5.848$ and 5.044, respectively, $ps<0.01$] (Figure5a, c). ANOVA analyses revealed an overall effect of genotype for both Akt phosphorylation sites [$F(2,6)=28.49$ and 25.06, for Ser473 and Thr308, respectively, $ps<0.002$], with NEX-*Pten* KO mice having significantly higher levels than WT controls [Dunnett's post hoc test, $p<0.05$]. While Pten deficiency increased phosphorylation of Akt, total levels of Akt were not affected (Figure5a, c). These data indicate that loss of Pten results in increased activity of PI3K and mTORC2 in NEX-*Pten* KO mice without affecting the gross level of Akt protein.

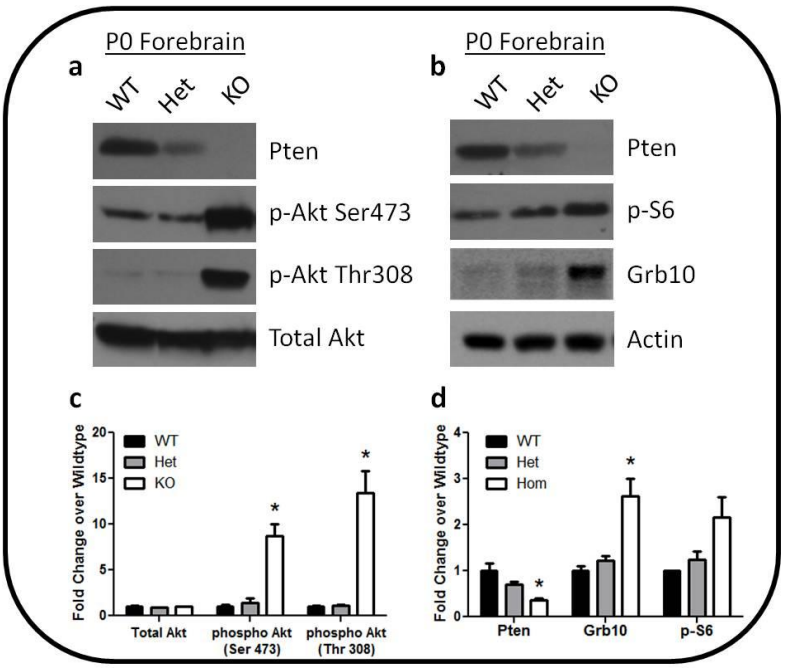

Figure 5. The PI3K/Akt/mTOR signaling pathway is upregulated in the postnatal day 0 forebrain of NEX-*Pten* knockout mice.

a) Representative Western blots of Pten, phospho-Akt serine 473 (p-Akt Ser473), phospho-Akt threonine 308 (p-Akt Thr308) and total Akt proteins in NEX-*Pten* wildtype (WT), heterozygous (Het) and knockout (KO) forebrain at postnatal day 0 (P0). b) Representative Western blots of Pten, phospho-S6 serine 240/244 (p-S6), Grb10 and actin proteins in P0 NEX-*Pten* WT, Het and KO forebrain lysate. Semi-quantitative analyses reveals that loss of Pten (normalized to actin) in NEX-*Pten* KO forebrain results in significantly increased phosphorylation of Akt (c) (normalized to total Akt) and downstream targets of mTORC1 (d) (normalized to actin) compared to WT forebrain (*$p<0.05$). Images represent data from 3-6 mice per genotype.

Next, Western blot analyses evaluated downstream targets of mTORC1, including ribosomal protein S6 and Grb10, a newly identified substrate of mTORC1 (Hsu et al., 2011; Yu et al., 2011). Phospho-S6 protein expression was increased in NEX-*Pten* KO forebrain, although

this did not reach statistical significance when analyzed by Student's t-test (WT vs. KO) or one-way ANOVA (Figure5b, d). Grb10, which is stabilized through phosphorylation, was significantly elevated in NEX-*Pten* KO mice compared to WT littermates [$t(8)=4.084$, $p<0.004$] (Figure5b, d). There was an overall effect of gene dosage on Grb10 [ANOVA: $F(2,12)=14.02$, $p<0.001$], with NEX-*Pten* KO levels being significantly higher than WT levels [Dunnett's post hoc test, $p<0.05$]. Loss of Pten did not alter mTOR phosphorylation at Ser2448 (Figure6a, b). This phosphorylation event is thought to be mediated by p70 S6 kinase (S6K1) (Chiang and Abraham, 2005), although earlier reports suggest it is mediated by Akt (Nave et al., 1999). Phosphorylation of S6K1 at threonine 389 (Thr389), which correlates with p70 kinase activity *in vivo* (Weng et al., 1998), tended to be increased in NEX-*Pten* KO forebrain, but this did not reach statistical significance (Figure6a, b). Similarly, phosphorylation of the translational repressor 4EBP1 was increased in NEX-*Pten* KO mice, although this was not statistically significant (Figure 6a, b). Phosphorylation of the translational initiation factor eIF4E, however, was significantly increased in NEX-*Pten* KO forebrain lysate compared to WT controls [$t(8)=2.954$, $p<0.02$] (Figure 6 a, b). There was also a marginal effect of genotype on eIF4E phosphorylation levels [ANOVA: $F(2,6)=4.683$, $p<0.06$]. 4EBP1 binds to eIF4E to inhibit cap-dependent translation, but phosphorylation of 4EBP1 disrupts this interaction, allowing the activation of cap-dependent translation (Pause et al., 1994). Given this, and that increased levels of phosphorylated eIF4E are correlated with translational upregulation (Furic et al., 2010; Shveygert et al., 2010), these data suggest that loss of Pten leads to increased protein translation via these mTORC1 downstream effectors.

The PI3K/Akt/mTOR pathway is integral for many functions, including cellular growth and protein synthesis. mTORC1, a central mediator of these processes, is regulated by a number of upstream signaling cascades outside of Akt, including the extracellular-regulated kinase (Erk1/2; also known as p44/42 MAP kinase) (Carlson et al., 2001; Winter et al., 2011), which promotes mTORC1 signaling through TSC2 phosphorylation. Here, Western blot analysis

revealed that NEX-*Pten* KO mice have increased phosphorylation of Erk1/2 in the forebrain compared to WT mice [t(8)=2.954, p<0.02] (Figure 6c, d). There was also an effect of Pten deficiency on Erk phosphorylation [F(2,12)=4.657, p<0.04]. NEX-*Pten* Het mice were significantly higher than WT mice, while KO mice were marginally elevated compared to WT [Dunnett's post hoc: WT vs. Het, p<0.05; WT vs. KO, p<0.1]. This is in line with previous *in vitro* studies that have shown Pten can inhibit Erk1/2 phosphorylation (Weng et al., 2001; Gupta and Dey, 2012). Akt has many targets outside of mTOR, one of which is GSK3β, a critical regulator of glycogen synthesis and cell fate (Welsh et al., 1996). Phosphorylation of GSK3β at Ser9 by Akt inhibits its activity (Cross et al., 1995) and has been noted in other *Pten* conditional mutant mouse models (Zhou et al., 2009). However, despite robust active//tion of Akt, no increase in GSK3β phosphorylation levels was detected in the NEX-*Pten* KO forebrain (Figure 6c, d). Taken together, these data suggest Pten deficiency in excitatory neurons of the forebrain leads to excessive activation of many components of the PI3K/Akt/mTOR signaling pathway, as well as other signaling cascades, such as the MAPK pathway leading to Erk1/2 phosphorylation.

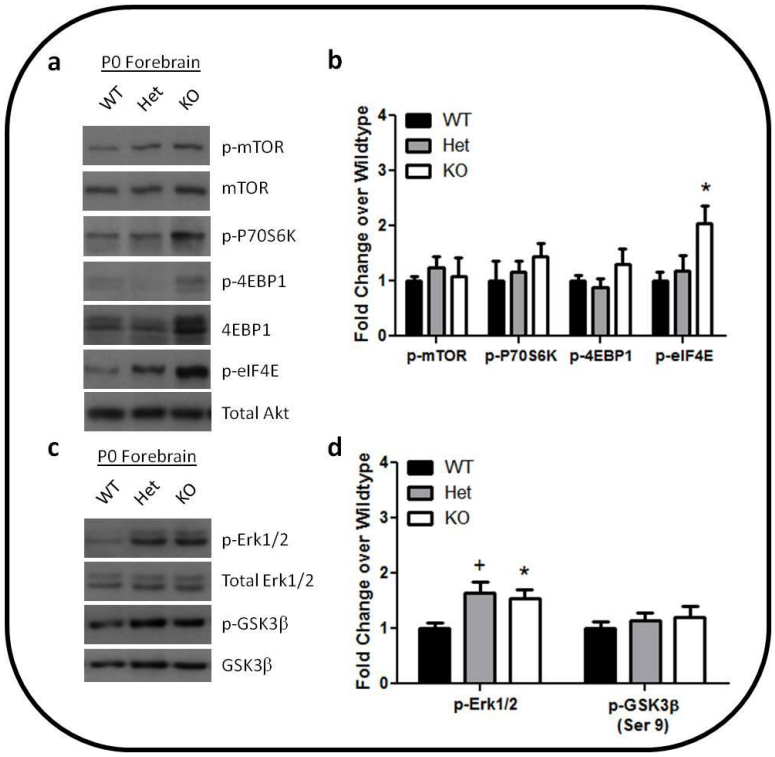

Figure 6. Effect of Pten deficiency on additional components of the PI3K/Akt/mTOR signaling cascade and the MAPK pathway.

a) Representative Western blots of phospho-mTOR serine 2448 (p-mTOR), mTOR, phospho-p70 S6 kinase threonine 389 (p-S6K1), phospho-4EBP1 (p-4EBP1), 4EBP1, phospho-eIF4E serine 209 (p-eIF4E) and total Akt proteins in NEX-*Pten* wildtype (WT), heterozygous (Het) and knockout (KO) forebrain lysate at postnatal day 0 (P0). b) Semi-quantitative analysis of Western blots reveal that NEX-*Pten* KO forebrains have higher levels of p-eIF4E (normalized to total Akt) than WT forebrain (*$p<0.05$). Loss of Pten did not alter levels of p-mTOR (normalized to mTOR), p-S6K1 (normalized to total Akt), or p-4EBP1 (normalized to 4EBP1). c) Representative Western blots of phospho-Erk1/2 threonine 202/204 (p-Erk), total Erk1/2, phospho-GSK3β serine 9 (p-GSK3β), and total GSK3β from NEX-*Pten* WT, Het and KO forebrain lysate at P0. d) Semi-quantitative analysis of Western blots indicate that NEX-*Pten* Het KO forebrains have higher levels of p-Erk1/2 (normalized to total Erk1/2), but not p-GSK3β (normalized to total GSK3β) compared to WT forebrain (Student's t-test, WT vs. KO, *$p<0.05$; Dunnett's post hoc test, WT vs. Het, +, $p<0.05$). Images represent data from 5-6 mice per genotype.

Increased activity of the PI3K/Akt/mTOR pathway may result in alterations in signaling cascades that are important for other brain functions, such as migration, neuronal differentiation and synaptic function. Dab1 is an adaptor protein which acts as the main effector of Reln signaling for proper cortical layer formation during development. Levels of Dab1 were significantly increased in NEX-*Pten* KO, but not Het, mice [one-sample t-test: $t(2)=5.267$, $p<0.04$] (Figure 7a,b). The one-sample t-test was used for this analysis because samples were run on different blots with one WT per blot and therefore, no variability could be calculated for the WT samples. Dab1 increases may have resulted in the cellular layer distortion seen in the NEX-*Pten* KO cortex (Figures 3 and 4). To determine if loss of Pten had consequences on neuronal

differentiation, the mature neuron markers MAP2 and NeuN were evaluated. While no changes in NeuN were detected in NEX-*Pten* mutants, MAP2 protein expression was significantly increased in NEX-*Pten* KO forebrain compared to WT mice [$t(10)=2.473$, $p<0.04$] (Figure 7c, d). The effect of genotype on MAP2 was marginal [ANOVA: $F(2,15)=3.098$, $p<0.08$]. In immunofluorescence studies, MAP2 from NEX-*Pten* KO cortex appeared to have a qualitatively higher fluorescent signal than WT cortex when images were taken at the same exposure (Figure 2f).

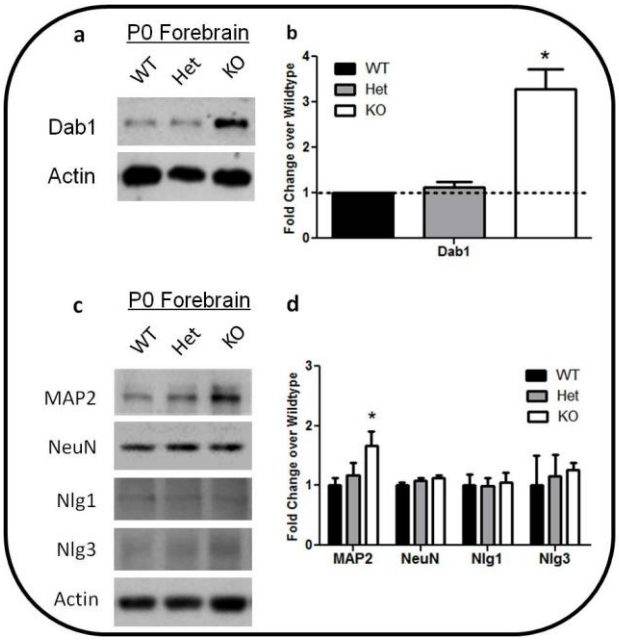

Figure 7. Altered expression of proteins involved in brain development and synapse formation. a) Representative Western blots of Dab1 and actin proteins in NEX-*Pten* wildtype (WT), heterozygous (Het) and knockout (KO) forebrain at postnatal day 0 (P0). b) Semi-quantitative analysis of Western blots revealed that NEX-*Pten* KO mice have higher levels of Dab1 (normalized to actin) in the forebrain (one-sample t-test, *$p<0.05$). c) Representative Western blots of MAP2, NeuN, neuroligin 1 (Nlg1), neuroligin 3 (Nlg3) and actin levels in P0 NEX-*Pten* WT, Het and KO forebrain. d) Semi-quantitative Western blot analyses indicates that NEX-*Pten* KO mice have significantly higher levels of MAP2, but not NeuN, Nlg1 or Nlg3 (normalized to

actin), compared to NEX-*Pten* WT mice (*p<0.05). Data were obtained from 3-6 mice per genotype.

Characterization of Synaptic Proteins and Ionotropic Glutamate Receptor Protein Expression

To investigate if Pten deficiency affects synapse formation, Western blot analyses of neuroligin 1 (Nlg1) and neuroligin 3 (Nlg3) were performed. Neuroligins are postsynaptic cell adhesion proteins which aid in the maintenance of neuronal synapses by acting as ligands for neurexins, located on the presynaptic membrane (Fabrichny et al., 2007). Neither Nlg1 nor Nlg3 were changed by *Pten* deletion (Figure 7c, d). Further, ionotropic glutamate receptor subunits were analyzed to determine if loss of Pten altered synaptic function in excitatory neurons. Three NMDA receptor subunits, NR2A, NR2B and NR1, were significantly increased in the forebrain of NEX-*Pten* KO mice compared to WT controls [$t(10)=2.627$, $p<0.03$; $t(8)=3.659$, $p<0.01$; $t(4)=3.038$, $p<0.04$, respectively] (Figure 8a, c). Although there was no overall effect of genotype on NR2A levels, there was an overall effect of genotype on NR2B and NR1 due to loss of Pten [NR2B: $F(2,12)=5.323$, $p<0.03$; NR1: $F(2,6)=5.646$, $p<0.05$]. NEX-*Pten* KO forebrains had significantly more of each of these receptor subunit proteins compared to WT [Dunnett's post hoc tests, ps<0.05). Although the loss of one *Pten* allele in NEX-*Pten* Het forebrain increased NR2A, NR2B and NR1 levels, these were not significantly different from WT controls (i.e., Pten was haplosufficient). Conversely, NEX-*Pten* KO mice had significantly lower protein levels of NR3A, but not NR3B, in the forebrain, compared to WT mice [$t(4)=2.982$, $p<0..05$] (Figure 8b, d). There was also an effect of gene dosage on NR3A protein levels [$F(2,5)=8.129$, $p<0.03$], such that both NEX-*Pten* Het and KO mice differed significantly from WT mice [Dunnett's post hoc tests, WT vs. Het, WT vs. KO, ps<0.05]. Levels of the AMPA receptor subunit GluR1 were not affected by *Pten* deficiency (Figure 9). However, protein levels of GluR2/3 AMPA receptor subunits were increased in NEX-*Pten* KO mice compared to WT [$t(4)=3.049$, $p<0.04$], with no overall effect of genotype on GluR2/3 levels (Figure 9). These data suggest that loss of *Pten* in

forebrain excitatory neurons selectively affects the protein expression of several, but not all, NMDA and AMPA subunits.

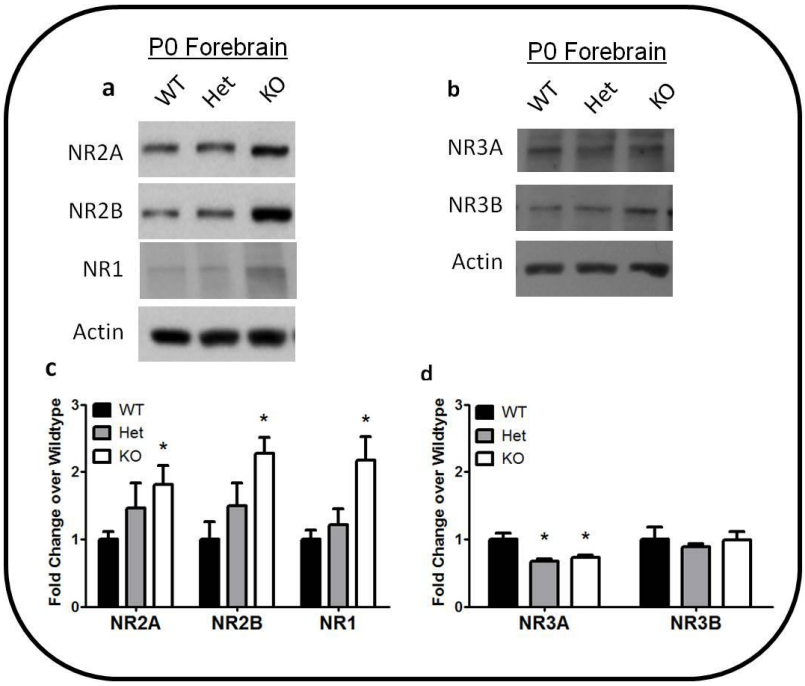

Figure 8. Abnormal expression of NMDA receptor subunits in the forebrains of newborn NEX-*Pten* mice.

a) Representative Western blots of the NMDA receptor subunits NR2A, NR2B, NR1 and actin in P0 NEX-*Pten* wildtype (WT), heterozygous (Het) and knockout (KO) forebrain at postnatal day 0 (P0). b) Representative Western blots of the NMDA receptor subunits NR3A, NR3B and actin in P0 NEX-*Pten* WT, Het and KO forebrain. c) Semi-quantitative Western blot analyses revealed that NR2A, NR2B and NR1 (normalized to actin) are significantly increased in NEX-*Pten* KO forebrain compared to WT. d) Semi-quantitative analyses of Western blots indicate that NR3A is significantly decreased in NEX-*Pten* Het and KO forebrain compared to WT, but that NR3B remains unchanged between genotypes. NR3A and NR3B were normalized to actin. Data were obtained from 3-6 mice per genotype. *$p<0.05$.

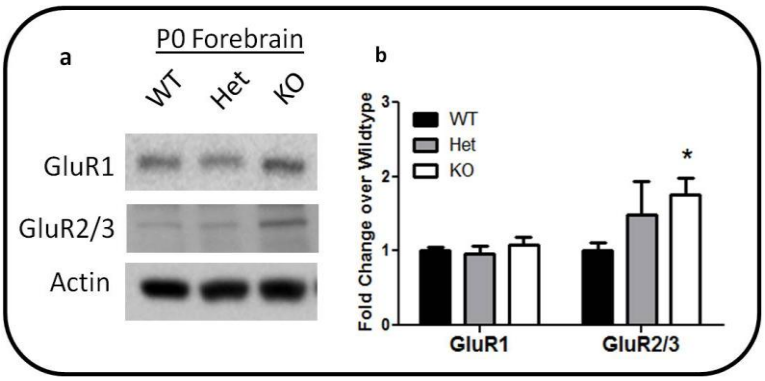

Figure 9. Altered expression of AMPA receptor subunits in newborn NEX-*Pten* mice.

a) Representative Western blots of AMPA receptor subunits GluR1, GluR2/3 and actin protein levels in NEX-*Pten* wildtype (WT), heterozygous (Het) and knockout (KO) forebrain at postnatal day 0 (P0). b) Semi-quantitative Western blot analyses demonstrate that while GluR1 is unchanged by loss of Pten in NEX-*Pten* KO forebrain, levels of GluR2/3 (normalized to actin) are significantly increased in NEX-*Pten* KO forebrain at P0. Data were obtained from 3-6 mice per genotype. *p<0.05.

Quantitative Real-Time PCR of Ionotropic Glutamate Receptor Subunits

The altered protein expression of NMDA and AMPA receptor subunits could be due to several factors, such as increased/decreased translation, alterations in protein trafficking or changes in protein degradation. Quantitative real-time polymerase chain reaction (qRT-PCR) was used to measure gene expression of NMDA (*Grin)* and AMPA (*Gria)* subunits, as well as Dab1, in P0 cortex to determine if gene expression changes could account for alterations in protein levels (n=3-5 per genotype). Gene expression of *Grin2A*, *Grin2B*, *Grin3A* and *Grin3B* were not significantly different in NEX-*Pten* mutant mice compared to WT mice (Figure 10a). Only *Grin1* gene expression was significantly increased in the cortex of NEX-*Pten* KO mice at P0 [$t(4)=2.925$, $p<0.05$] (Figure 10a). Further, ANOVA analysis revealed that *Pten* deficiency had an overall effect on *Grin1* gene expression [$F(2,8)=7.553$, $p<0.02$], which was driven by

complete loss of Pten [Dunnett's post hoc test, WT vs. KO, $p<0.05$]. There were no differences between genotypes for *Gria1*, *Gria2* or *Gria3* gene expression in P0 cortex (Figure 10b). Finally, *Dab1* gene expression was also unchanged in NEX-*Pten* mutant mice (Figure 10c). Together, these data suggest that *Pten* deficiency during brain development generally does not have global effects on glutamate receptor gene expression, but rather selectively increases gene expression for the NR1 subunit in NEX-*Pten* KO cortex.

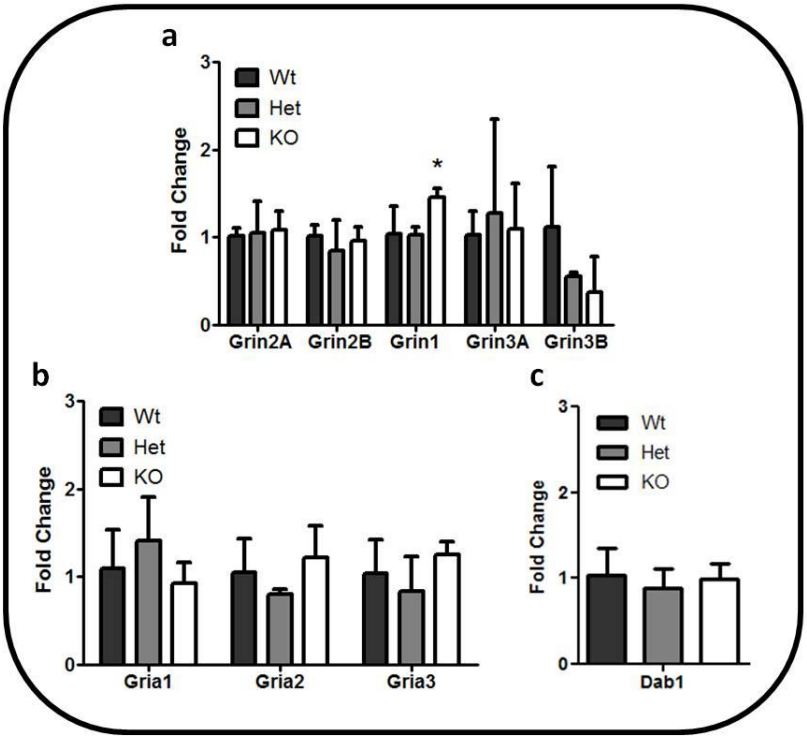

Figure 10. Quantitative real-time PCR (qRT-PCR) analyses of ionotropic glutamate receptor expression and Dab1 in newborn NEX-*Pten* cortex.

a) Quantitative qRT-PCR analyses of NMDA receptor subunits NR2A (*Grin2A*), NR2B (*Grin2B*), NR1 (*Grin1*), NR3A (*Grin3A*) and NR3B (*Grin3B*) normalized to the housekeeping gene *Gapdh* in NEX-*Pten* wildtype (WT), heterozygous (Het) and knockout (KO) cortex at postnatal day 0 (P0). Only *Grin1* is significantly upregulated in NEX-*Pten* KO cortex compared to WT (*$p<0.05$). b) Quantitative qRT-PCR analyses of NEX-*Pten* P0 cortex indicate loss of Pten does not affect gene expression of AMPA receptor subunits GluR1 (*Gria1*), GluR2 (*Gria2*), and

GluR3 (*Gria3*) normalized to *Gapdh*. c) Quantitative aRT-PCR analysis indicates *Dab1* gene expression (normalized to *Gapdh*) is unchanged in NEX-*Pten* P0 cortex. Data were obtained from 3-5 mice per genotype.

Characterization of mTOR Signaling and Glutamate Receptor Subunit Expression in Embryonic NEX-Pten mice

The NEX promoter induces Cre expression in the neocortex and hippocampus starting around E11.5 (Goebbels et al., 2006). NEX-*Pten* mice were analyzed at E17.5 to determine if PI3K/Akt/mTOR signaling is altered shortly after loss of Pten. At E17.5, Pten was significantly reduced in NEX-*Pten* KO forebrain, compared to WT mice [$t(4)=4.269$, $p<0.02$] (Figure 11b, d). There was an overall effect of genotype on Pten deficiency [$F(2,6)=9.027$, $p<0.05$], such that NEX-*Pten* KO mice had significantly less Pten protein than WT mice [Dunnett's post hoc test, $p<0.05$]. Consequently, Akt phosphorylation was significantly increased at both Ser473 and Thr308 phosphorylation sites in NEX-*Pten* KO forebrain at E17.5 [Ser473: $t(4)=10.66$, $p<0.0005$; Thr308: $t(4)=5.639$, $p<0.001$] (Figure 11a, d). Genotype had an overall effect on Akt phosphorylation [Ser473: $F(2,6)=110.1$, $p<0.0001$; Thr308: $F(2,6)=26.7$, $p<0.002$], with NEX-*Pten* KO mice having significantly more phosphorylated Akt at both sites compared to WT mice [Dunnett's post hoc tests, $ps<0.05$]. Two of mTORC1's downstream targets, phospho-S6 and phospho-4EBP1, were also examined. Levels of phosphorylated S6 were significantly increased in NEX-*Pten* KO mice [$t(4)=6.705$, $p<0.003$] (Figure 11b, d). Phospho-S6 was significantly affected by genotype [$F(2,6)=39.38$, $p<0.0005$], with NEX-*Pten* KO mice having significantly elevated levels compared to WT mice [Dunnett's post hoc test, $p<0.05$]. Phosphorylated 4EBP1 was marginally increased in embryonic NEX-*Pten* KO forebrain [$t(4)=2.363$, $p<0.08$] (Figure 11c, e). ANOVA analysis revealed a significant effect of genotype on phospho-4EBP1 [$F(2,6)=6.463$, $p<0.04$], but there were no significant differences between genotypes during post hoc analysis. Additionally, while phosphorylated Erk1/2 did not differ between genotypes,

GSK3β phosphorylation was significantly increased in embryonic NEX-*Pten* KO mice [t(4)=3.346, p<0.03], suggesting that GSK3β activity is inhibited shortly after *Pten* deletion (Figure 11c, e). There was an overall effect of genotype on levels of phosphorylated GSK3β [F(2,6)=16.86, p<0.004], with NEX-*Pten* KO mice having significantly higher levels of phosphorylated GSK3β than WT mice [Dunnett's post hoc test, p<0.05]. Therefore, several components of the PI3K/Akt/mTOR signaling cascade were upregulated in embryonic NEX-*Pten* KO forebrain, similar to the hyperactivation seen at P0. The effects of *Pten* deficiency on other phosphorylated proteins, however, differed between the E17.5 and P0 time points, suggesting the signaling cascades affected by chronic Pten loss may be homeostatically regulated over time.

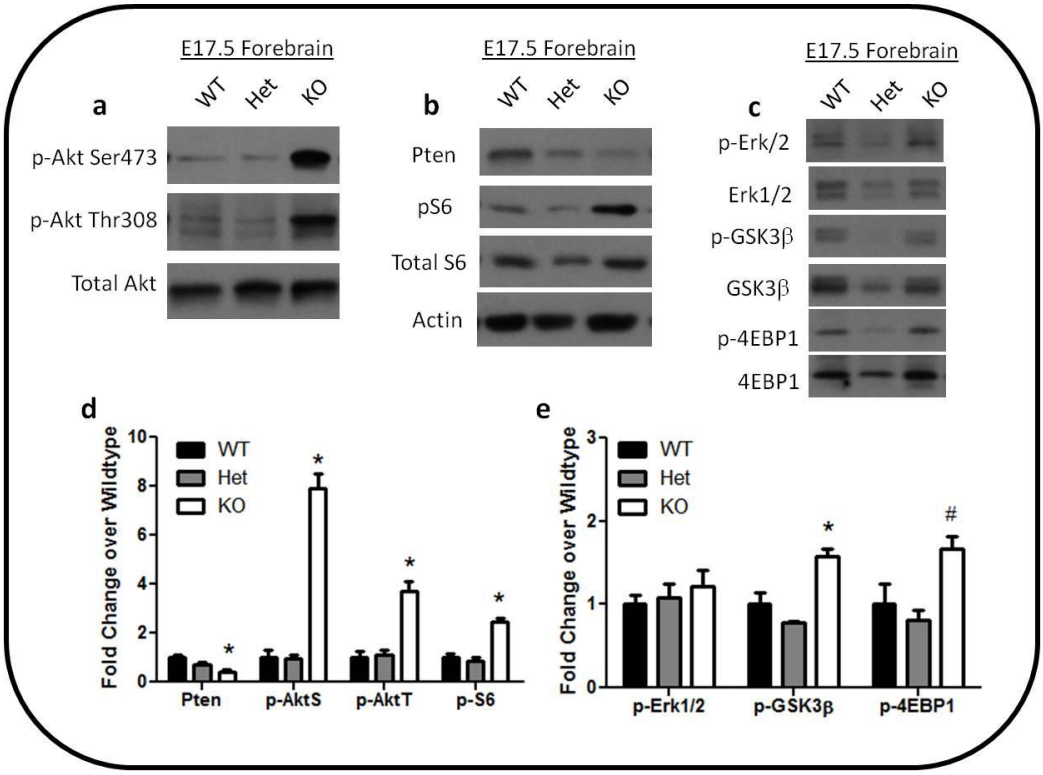

Figure 11. Characterization of the PI3K/Akt/mTOR signaling cascade and other related pathways in embryonic NEX-*Pten* forebrains.

a) Representative Western blots of phospho-Akt serine 473 (p-Akt Ser473), phospho-Akt threonine 308 (p-Akt Thr308) and total Akt protein levels in embryonic day 17.5 (E17.5) NEX-

Pten wildtype (WT), heterozygous (Het) and knockout (KO) forebrain. b) Representative Western blots of Pten, phospho-S6 serine 235/236 (p-S6), total S6 and actin protein levels in E17.5 NEX-*Pten* WT, Het and KO forebrain. c) Representative Western blots of phospho-Erk1/2 threonine 202/204 (p-Erk), total Erk1/2, phospho-GSK3β serine 9 (p-GSK3β), total GSK3β, phospho-4EBP1 threonine 37/46 (p-4EBP1) and 4EBP1 protein levels from E17.5 NEX-*Pten* WT, Het and KO forebrain lysate. d) Semi-quantitative Western blot analysis revealed a significant reduction in Pten (normalized to actin) and increased phosphorylation of Akt (normalized to total Akt) and S6 (normalized to total S6) in E17.5 NEX-*Pten* KO forebrain compared to WT. e) Semi-quantitative Western blot analyses revealed significantly increased phosphorylated GSK3β (normalized to GSK3β) and marginally increased phosphorylated 4EBP1 (normalized to 4EBP1) in E17.5 NEX-*Pten* KO forebrain compared to WT. Levels of phosphorylated Erk1/2 (normalized to total Erk) did not differ between genotypes. Data were obtained from 3 mice per genotype. *$p<0.05$, #$p<0.1$.

NMDA and AMPA receptor protein expression patterns were examined in embryonic NEX-*Pten* forebrain lysate to determine if ionotropic glutamate receptor subunits were altered prior to birth, since components of the PI3K/Akt/mTOR pathway were upregulated at this time point. Although NEX-*Pten* KO NR2A levels were not significantly elevated compared to WT mice at E17.5, there tended to be an overall genotype effect on increasing NR2A levels [$F(2,6)=4.048$, $p<0.08$] (Figure 12a, c). NR2B levels also increased in a genotype-dependent fashion. E17.5 NEX-*Pten* KO mice had higher NR2B protein levels than WT animals, but this was not statistically significant (Figure 12a, c). Both NR1 and NR3A did not differ among genotypes (Figure 12a-c). Similarly, there were no significant changes in GluR1 protein levels among embryonic NEX-*Pten* mice, although levels were non-significantly higher in KO animals (Figure 12b, d). Western blot membranes were probed for NR3B and GluR2/3, but no bands

were detected in NEX-*Pten* embryonic samples. This was most likely due to low expression levels in the embryonic forebrain, as an adult WT cortex control sample (ICR/CD-1 WT strain) did produce bands of the expected size with both NR3B and GluR2/3 antibodies when analyzed concurrently with NEX-*Pten* embryonic samples (data not shown). Finally, Dab1 levels were increased in NEX-*Pten* mutants, but this did not reach statistical significance (Figure 12 b, e). These data suggest that several of the significantly upregulated glutamate receptor subunits found in P0 NEX-*Pten* KO began to increase their protein expression in embryonic NEX-*Pten* KO mice, although they were not statistically significant at this earlier time point.

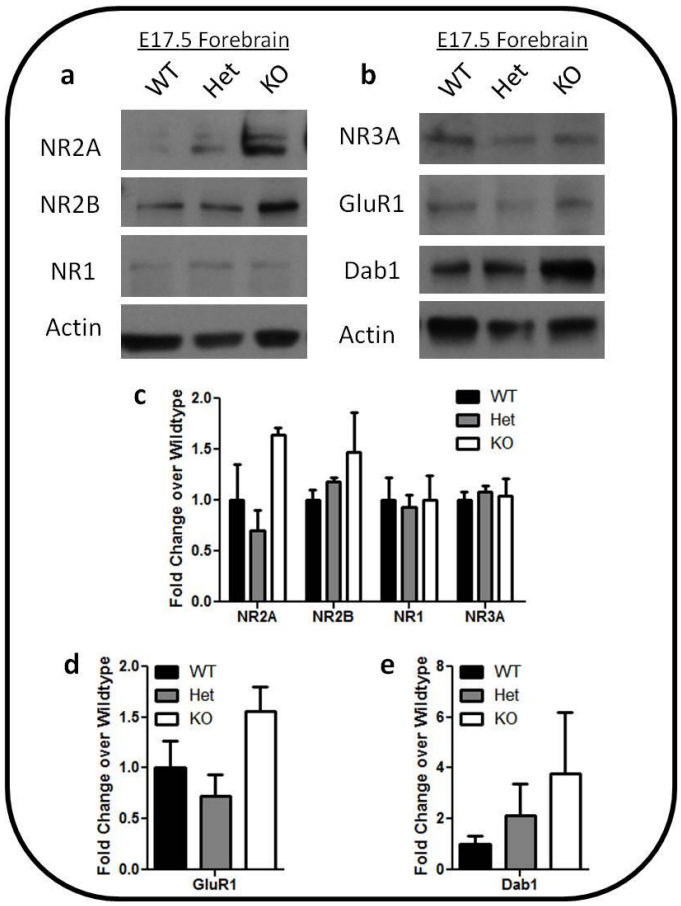

Figure 12. Ionotropic glutamate receptor expression in embryonic NEX-*Pten* forebrain.

a) Representative Western blots of NMDA subunits NR2A, NR2B, NR1 and actin protein levels in embryonic day 17.5 (E17.5) NEX-*Pten* wildtype (WT), heterozygous (Het) and knockout (KO)

forebrains. b) Representative Western blots of the NMDA receptor subunit NR3A, AMPA receptor subunit GluR1, Dab1 and actin protein levels in E17.5 NEX-*Pten* WT, Het and KO forebrain. c) Semi-quantitative Western blot analyses revealed no significant changes in NR2A, NR2B, NR1 or NR3A (normalized to actin) in E17.5 NEX-*Pten* KO forebrain compared to WT. Neither GluR1 (d) nor Dab1 (e) (normalized to actin) were significantly altered by loss of Pten in E17.5 NEX-*Pten* forebrain samples. Data were obtained from 3 mice per genotype.

Analysis of Adult NEX-Pten Heterozygous Crude Synaptosome Fractionation

NEX-*Pten* KO mice die shortly after birth, limiting the study of how chronic loss of *Pten* in excitatory neurons of the forebrain affects glutamate receptor expression. NEX-*Pten* Het mice have increased NR2 and NR1 protein levels at P0, although these effects are not statistically significant. To examine the synaptic localization of these subunits in adult NEX-*Pten* Het mice, crude synaptosome fractionation was performed on the cortex and hippocampus of 6 month old NEX-*Pten* WT (n=4) and Het mice (n=3). In the cortex, Pten levels were significantly lower in NEX-*Pten* Het homogenate lysate, but not the synaptic fraction, compared to WT mice [$t(10)=2.762$, $p<0.02$] (Figure 13a-c). Although Pten was decreased, mTORC2-mediated Akt phosphorylation at Ser473 was not significantly upregulated in either NEX-*Pten* Het cortical homogenate or synaptic fraction, suggesting that chronic Pten haplosufficiency does not significantly upregulate PI3K/Akt/mTOR signaling in the NEX-*Pten* Het adult cortex. None of the NMDA receptor subunits were significantly changed in the cortical homogenate or synaptic fraction of NEX-*Pten* Het adult mice (Figure 13e-g). While NR2A protein levels were higher in the cortical homogenate of NEX-*Pten* Het adult mice, this was not statistically significant (Figure 13e, f). The AMPA receptor subunit GluR1 remained unchanged in NEX-*Pten* Het cortical homogenate and synaptic fraction. GluR2/3 protein levels, however, were significantly decreased in the cortical homogenate of adult NEX-*Pten* Het mice [$t(4)=8.429$, $p<0.002$], but did not differ between genotypes in the synaptic fraction (Figure 13e-g).

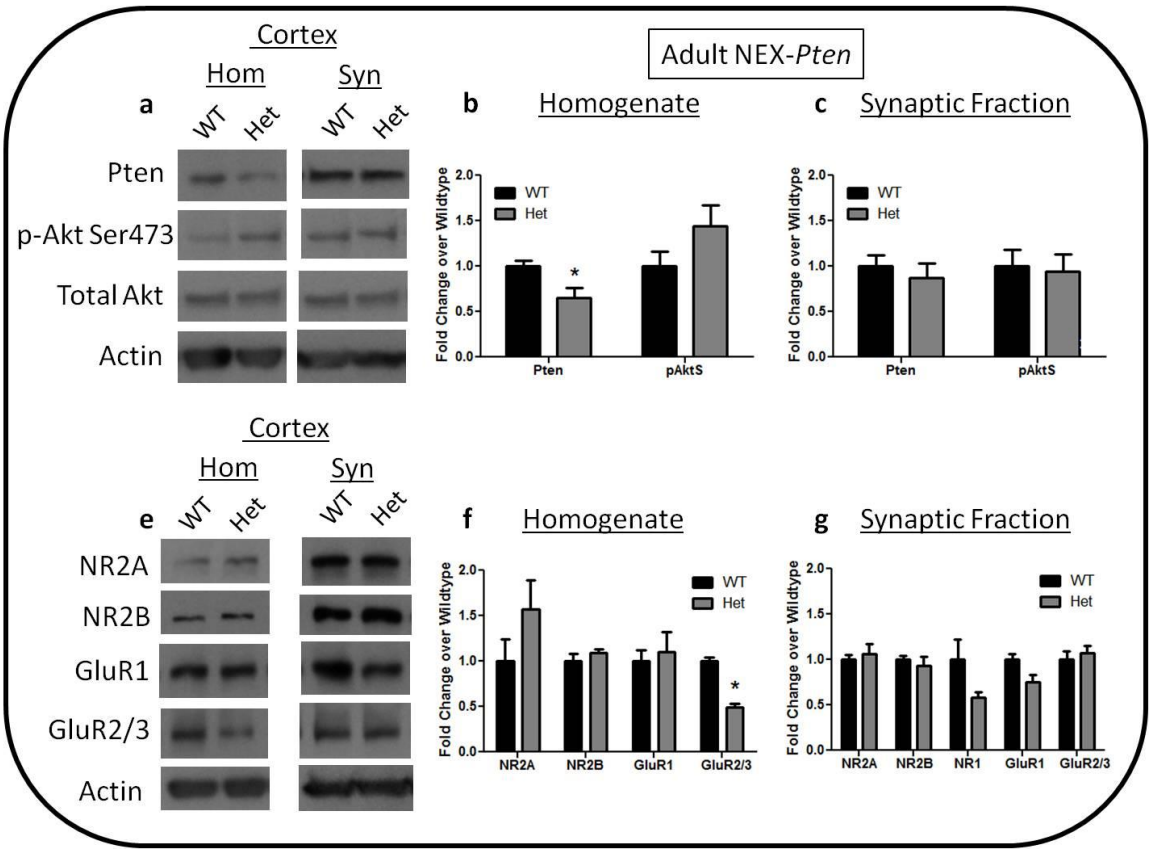

Figure 13. Characterization of PI3K/Akt/mTOR signaling and glutamate receptor expression in the cortex of adult NEX-*Pten* heterozygous mice.

a) Representative Western blots of Pten, phospho-Akt serine 473 (pAktS), total Akt and actin protein levels in homogenate (Hom) and synaptic fractions (Syn) of 6 month old adult NEX-*Pten* wildtype (WT) and heterozygous (Het) cortex. b) Semi-quantitative Western blot analyses revealed that Pten (normalized to actin) was significantly reduced in NEX-*Pten* Het homogenate. Phosphorylated levels of Akt (normalized to total Akt) did not differ between genotypes. c) Semi-quantitative Western blot analyses revealed that Pten and pAktS did not differ between genotypes in the cortical synaptic fraction of adult NEX-*Pten* WT and Het mice. e) Representative Western blots of the NDMA receptor subunits NR2A and NR2B, the AMPA receptor subunits GluR1 and GluR2/3 and actin protein levels in homogenate and synaptic fractions of adult NEX-*Pten* WT and Het cortex. f) Semi-quantitative Western blot analyses revealed no significant changes in

NR2A, NR2B, or GluR1 in adult NEX-*Pten* cortical homogenate. GluR2/3 protein levels were significantly reduced in adult NEX-*Pten* cortical homogenate. All proteins were normalized to actin. g) No significant differences were found in NR2A, NR2B, NR1, GluR1 or GluR2/3 (normalized to actin) in the cortical synaptic fraction of adult NEX-*Pen* WT and Het mice. Data were obtained from 3-4 mice per genotype. *$p<0.05$.

In the adult hippocampus, there were no significant decreases in Pten protein levels in NEX-*Pten* Het homogenate lysate or synaptic fraction, although Pten levels were lower in the Het compared to WT mice (0.72 and 0.74 fold decrease of WT, respectively) (Figure 14a-c). Consequently, phosphorylation of Akt at Ser473 remained unchanged in the hippocampal homogenate and synaptic fraction of adult NEX-*Pten* Het mice (Figure 14a-c). Hippocampal levels of all NMDA and AMPA receptor subunits were not significantly different between NEX-*Pten* WT and Het mice in either homogenate or synaptic fraction samples (Figure 14e-g). Similar to the cortex, NR2A levels were higher in hippocampal homogenate lysate in adult NEX-*Pten* Het mice, but this was not statistically significant (Figure 14e, f). NEX-*Pten* Het mice had significantly lower levels of NR3A at P0. However, synaptosomal fractionation samples were not available to evaluate NR3A or NR3B levels in the NEX-*Pten* adult Het at this later time point. Together, these data suggest that chronic Pten haplosufficiency in adult NEX-*Pten* Het mice does not significantly upregulate the PI3K/Akt/mTOR pathway or alter glutamate receptor subunit protein levels in the cortex or hippocampus.

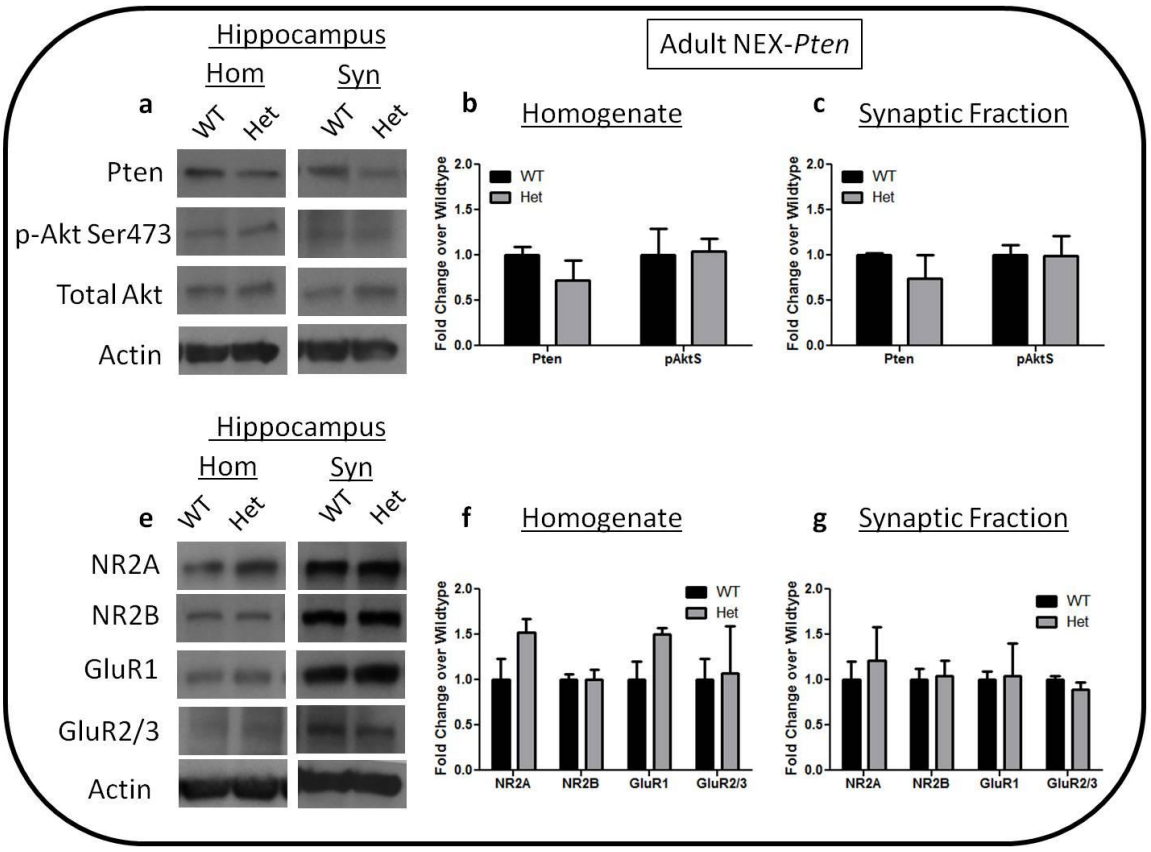

Figure 14. Characterization of PI3K/Akt/mTOR signaling and glutamate receptor expression in the hippocampus of adult NEX-*Pten* heterozygous mice.

a) Representative Western blots of Pten, phospho-Akt serine 473 (pAktS), total Akt and actin protein levels in homogenate (Hom) and synaptic fractions (Syn) of 6 month old adult NEX-*Pten* wildtype (WT) and heterozygous (Het) hippocampus. b) Semi-quantitative Western blot analyses revealed no significant differences in Pten (normalized to actin) or pAktS (normalized to total Akt) between genotypes in hippocampal homogenate. c) Semi-quantitative Western blot analyses revealed that Pten and pAktS did not differ between genotypes in the hippocampal synaptic fraction of adult NEX-*Pten* WT and Het mice. e) Representative Western blots of the NDMA receptor subunits NR2A and NR2B, the AMPA receptor subunits GluR1 and GluR2/3 and actin protein levels in homogenate and synaptic fractions of adult NEX-*Pten* WT and Het hippocampus. f) Semi-quantitative Western blot analyses revealed no significant changes in

NR2A, NR2B, GluR1 or GluR2/3 (normalized to actin) in adult NEX-*Pten* hippocampal homogenate. g) No significant differences were found in NR2A, NR2B, NR1, GluR1 or GluR2/3 (normalized to actin) in the hippocampal synaptic fraction of adult NEX-*Pen* WT and Het mice. Data were obtained from 3-4 mice per genotype.

Evaluation of Prenatal Rapamycin Treatment in NEX-Pten Mice

In order to determine if the increased levels of NMDA receptor subunits in NEX-*Pten* KO forebrain were due to mTORC1 activity, pregnant NEX-*Pten* Het dams were administered rapamycin by IP injection twice during gestation, at E13.6 and E16.5. These time points were chosen because of rapamycin's pharmacokinetic profile and long half-life in order to reduce mTORC1 activity throughout embryonic development (Meikle et al., 2008; Anderl et al., 2011),. When administered low doses of rapamycin, NEX-*Pten* females continued to gain weight during pregnancy and birthed pups of all genotypes at the expected time point (E19), similar to vehicle-treated dams (data not shown). As expected, vehicle-treated NEX-*Pten* KO forebrains (n=4) had higher levels of phospho-S6 (2.7 fold increase over WT) and phospho-S6K1 (3.9 fold increase over WT) than vehicle-treated WT samples (n=4), although these were not statistically significant (Figure 15a,b). NR2A protein levels were significantly higher in vehicle-treated NEX-*Pten* KO mice compared to WT [$t(6)=2.876$, $p<0.03$] (Figure 15c). Western blot analyses revealed phospho-S6 was reduced in NEX-*Pten* KO mice after administration of 1 mg/kg (n=3) and 3 mg/kg (n=4) of rapamycin (0.6 and 0.66 fold change of Veh-KO, respectively) compared to vehicle-treated NEX-*Pten* KO mice (Figure 15a, b). Rapamycin (1 and 3 mg/kg) also reduced phospho-S6K1 levels in NEX-*Pten* KO mice compared to vehicle-treated KO mice (0.47 and 0.51 fold change of Veh-KO, respectively). Although reduced by rapamycin, levels of phospho-S6 and phospho-S6K1 in NEX-*Pten* KO mice were not statistically different between drug groups and vehicle. Levels of NR2A remained unchanged in rapamycin-treated NEX-*Pten* KO mice compared to vehicle-treated KO mice (Figure 15c). In subcutaneous (SC) dosing studies,

vehicle-treated NEX-*Pten* KO mice had higher levels of phospho-S6 in the forebrain compared to vehicle-treated WT mice (n=4) (Figure 15d). SC injection of 3 mg/kg of rapamycin to pregnant NEX-*Pten* females did not reduce phospho-S6 levels in NEX-*Pten* KO mice (n=2), compared to vehicle-treated KO mice (Figure 15d). Higher doses of rapamycin (e.g., 5 mg/kg and 10 mg/kg) and increased frequency of administration (i.e., E13, E16 and E18) resulted in loss of pregnancy.

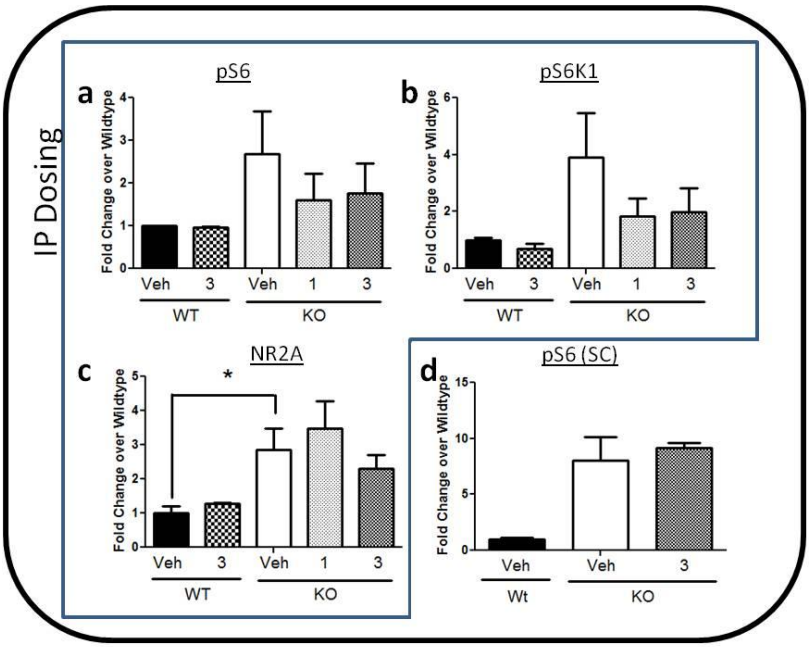

Figure 15. Evaluation of prenatal rapamycin treatment in NEX-*Pten* postnatal day 0 forebrain. Pregnant NEX-Pten heterozygous females were administered rapamycin either intraperitoneally (IP) or subcutaneously (SC) at embryonic day 13.5 and 16.5. Semi-quantitative Western blot analyses revealed non-significantly elevated levels of phospho-S6 serine 235/236 (pS6) (a) and phospho-p70 S6 kinase (pS6K1) (b) in vehicle-treated NEX-Pten knockout (KO) forebrain (n=4), compared to vehicle-treated WT forebrain (n=4) at postnatal day 0 (P0). 3 mg/kg of prenatal rapamycin treatment (IP) did not change pS6 or pS6K1 levels in NEX-Pten WT forebrain (n=2). Although levels of pS6 and pS6K1 were reduced by prenatal IP administration of rapamycin at 1and 3 mg/kg (n=3 and 4, respectively) in NEX-Pten KO forebrain, this was not statistically significant. c) Semi-quantitative Western blot analyses revealed that NR2A levels were

significantly increased in vehicle-treated NEX-Pten KO forebrain compared to vehicle-treated WT forebrain (*p<0.05). Prenatal rapamycin treatment did not alter NR2A levels in either genotype. d) Subcutaneously administered prenatal rapamycin treatment did not alter pS6 levels in NEX-Pten KO forebrain (n=2 per group). Vehicle-treated NEX-Pten KO mice had higher levels of pS6 than vehicle-treated NEX-Pten WT mice (n=4).

---

4. Discussion

In the present studies, NEX-*Pten* mice were evaluated for ionotropic glutamate receptor expression, since mutations in human *PTEN* and mouse *Pten* are associated with increased seizure liability. Protein levels of specific NMDA and AMPA receptor subunits were altered by Pten deficiency, while others were unchanged, suggesting that loss of Pten selectively modifies glutamate receptor subunit protein expression. NEX-*Pten* KO mice exhibited higher levels of NR2A, NR2B and NR1, but decreased levels of NR3A, in the forebrain. NR2A and NR2B differ in their pharmacokinetic properties, and relative levels of each receptor subunit can affect NMDA electrophysiological properties (Vicini et al., 1998), potentially contributing to increased neuronal excitability and seizure. NR1, the obligatory NMDA receptor subunit required for receptor function, is specifically required for surface expression of NR2 subunits (Fukaya et al., 2003). In the embryonic forebrain of NEX-*Pten* KO mice, NR2A and NR2B tended to be increased, while NR1 levels did not differ among genotypes. qRT-PCR analyses confirmed that elevated protein levels of NR2A and NR2B were not due to increased gene expression. Interestingly, NR1 gene expression levels were significantly higher in P0 cortex of NEX-*Pten* KO mice. Together, these data suggest that embryonic loss of Pten begins to increase NR2A and NR2B levels, which are significantly elevated by P0, compared to WT mice. NR2 subunit increases, in turn, likely drive the increased gene expression of NR1 at P0, and the subsequent increased protein expression of NR1, which is needed for surface expression of NR2-NR1 receptor complexes.

While the NR2 subunits were elevated in NEX-*Pten* KO mice, NR3A protein levels were decreased without any accompanying changes in gene expression. As opposed to the glutamate binding site located on NR2 subunits, NR3 subunits possess glycine and D-serine binding sites, similar to NR1 (Low and Wee, 2010; Pachernegg S, 2011). NR3 can form receptor complexes with NR1 and NR2 or NR1 alone to alter NMDA receptor electrophysiological properties (Das et al., 1998; Nishi et al., 2001; Al-Hallaq et al., 2002). NR3A mRNA is expressed early in postnatal development but declines in the adult brain (Sucher et al., 1995). Here, in NEX-*Pten* KO mice, NR3A levels were decreased at P0, while NR3B levels were not altered, without accompanying changes in gene expression. Genetic deletion of NR3A has been shown to accelerate glutamatergic receptor maturation by increasing expression of NR1 and NR2A (but not NR2B), as well as GluR1, in early postnatal mice (Henson et al., 2012). These studies support the idea that glutamate receptors concentrate at synapses earlier if NR3A is not present, and would be consistent with the current studies demonstrating lower NR3A, but higher NR1 and NR2A, levels in early postnatal NEX-*Pten* KO mice.

NMDA receptors are involved in synaptic plasticity, learning and memory (Tsien et al., 1996a; Chen and Tonegawa, 1997; Nakazawa et al., 2004). AMPA receptors are responsible for the rapid neuronal membrane depolarization and fast synaptic transmission that are thought to be required to activate NMDA receptors (Malinow and Malenka, 2002). In newly born NEX-*Pten* KO mice, loss of Pten did not alter GluR1, but did upregulate GluR2/3 protein levels, with no changes in gene expression. GluR2/3 could not be detected in embryonic NEX-*Pten* KO forebrain, so it is unknown if the increases in GluR2, GluR3 or both GluR2 and 3 occur shortly after Pten deletion. Both GluR2 and GluR3 are important for the stabilization of AMPA receptors at the synapse and hippocampal LTD (Lee and Kirkwood, 2011; Asrar and Jia, 2013). Mice lacking GluR2 and GluR3 are severely impaired in basal synaptic transmission (Meng et al., 2003). In contrast, GluR2 knockout mice have normal basal transmission, but elevated LTP (Jia et al., 1996; Jia et al., 2001), supporting the role for this AMPA receptor subunit in synaptic

plasticity. GluR2 regulates AMPA receptor calcium permeability, such that if GluR2 is not present, the AMPA receptor is calcium permeable (Lerma et al., 1994; Dingledine et al., 1999). This has important functional consequences for receptor kinetics and other signaling events responsive to calcium influx (e.g., LTP) (Fukunaga, 1993; Fukunaga et al., 1995). Upregulation of GluR3, which is calcium permeable, may contribute to cell death due to excitotoxicity from increased calcium load upon activation (Rembach et al., 2004). High levels of GluR3 may result from low levels of GluR2, or vice versa. Additional analyses are needed to determine which AMPA receptor, GluR2 and/or GLuR3, is upregulated and how it contributes to the phenotype seen in NEX-*Pten* KO forebrain. In addition to examining glutamate receptor subunits, neuroligin 1 and neuroligin 3 were analyzed due to their importance in proper synapse formation (Fabrichny et al., 2007). Normal levels of neuroligin 1 and neuroligin 3 were observed in NEX-*Pten* KO mice, suggesting that this aspect of synaptic formation is unaffected in these animals.

Newly born NEX-*Pten* Het mice appeared relatively normal in terms of survival and neuronal morphology. Therefore, these mice could be aged to determine how chronic loss of one *Pten* allele affects ionotropic glutamate receptor expression. At P0, NEX-*Pten* Het mice had modest increases in NR2A, NR2B and NR1 and significant decreases in NR3A levels. However, at 6 months of age, adult NEX-*Pten* Het mice did not have any significant abnormalities in NR2, NR1 or GluR1 subunits, suggesting partially intact Pten signaling was sufficient to maintain normal/WT levels of downstream protein targets. Although GluR2/3 levels were reduced in cortical homogenate in NEX-*Pten* Het mice, it is difficult to know if these changes were due to GluR2 or GluR3 alterations. Since mice lacking GluR2 and GluR3 are impaired in basal synaptic transmission (Meng et al., 2003), these data suggest that older NEX-*Pten* Het mice may have synaptic transmission abnormalities. Additional studies are required to determine if either or both of these receptors are responsible for the total reduction seen here in adult NEX-*Pten* Het mice and their functional consequences.

Aside from glutamate receptor abnormalities, developmental loss of *Pten* resulted in macrocephaly and neuronal hypertrophy in NEX-*Pten* KO mice at birth. NEX-*Pten* KO mice were born in approximately the expected Mendelian ratio, but the mutation produced lethality shortly after birth. Although *Pten* was deleted in excitatory forebrain neurons, these neurons were able to migrate and position themselves approximately in the appropriate cellular layers. However, some distortion of cortical layering was observed, and several neurons over-migrated into the marginal zone near the surface of the cortex in NEX-*Pten* KO mice. Reln and Dab1 are required for proper cortical layer formation and radial migration of newly born neurons (Curran and D'Arcangelo, 1998). NEX-*Pten* KO mice had significantly higher levels of Dab1 in their forebrains, as determined by Western blot analyses. Although Reln immunofluorescent labeling was relatively similar between genotypes, the striking increase in Dab1 protein levels could be responsible for the overmigration seen in some Pten-negative neurons. The protein overexpression of Dab1 was not due to an increase in gene expression, since qRT-PCR analysis did not find any alterations in Dab1 mRNA levels. Therefore, it may be that some of the components of the PI3K/Akt/mTOR signaling cascade are responsible for the increased levels of Dab1, possibly through alterations in protein degradation (Li et al., 2005), stability(Choi et al., 2010) or translation (Gingras et al., 1998).

Pten deletion in NEX-*Pten* cortical excitatory neurons led to increased cell size, which is consistent with previous reports (Backman et al., 2001; Kwon et al., 2001; Backman et al., 2002; Ljungberg et al., 2009). Biochemical analyses revealed that loss of Pten resulted in specific increases in the dendritic marker MAP2, but not the nuclear marker NeuN, suggesting that the neurons are larger in the NEX-*Pten* KO forebrain, but similar in number compared to NEX-*Pten* WT forebrain. Immunofluorescence labeling of MAP2 also resulted in qualitatively higher fluorescent signal in NEX-*Pten* KO cortex. These results are most likely due to increased neuronal hypertrophy from loss of Pten's regulatory role on the PI3K/Akt/mTOR signaling

pathway, and are consistent with previous reports of dendritic hypertrophy in other conditional Pten mutant models (Fraser et al., 2008; Chow et al., 2009; Zhou et al., 2009).

Due to the importance of mTOR's functions in cell size and protein synthesis, the PI3K/Akt/mTOR pathway interacts with a host of other signaling cascades to effectively regulate cellular growth and function. Several components of the PI3K/Akt/mTOR pathway were upregulated in the NEX-*Pten* KO forebrain. PI3K and Akt have other downstream targets outside of mTOR, two of which, Erk1/2 and GSK3β, were examined because of the importance of their roles in cellular functions (Roux and Blenis, 2004; Hur and Zhou, 2010). Erk1/2 (also known as p44/42 kinase) can be activated in response to a wide range of extracellular stimuli, such as growth factors, ion channels and receptor tyrosine kinases (Fukunaga and Miyamoto, 1998; Kyosseva, 2004; Mebratu and Tesfaigzi, 2009). Erk1/2 and Akt have a cooperative and complex relationship, such that both are required to activate eIF4E-initiated cap-dependent translation via 4EBP1 (Ye et al., 2013). Akt and Erk1/2 synergistically promote this mTORC1-mediated event through phosphorylation of TSC2 on different sites that decrease TSC2-mediated inhibition of this pathway (Winter et al., 2011). In NEX-*Pten* mice, Akt phosphorylation was significantly upregulated in both embryonic and early postnatal NEX-*Pten* KO forebrains. Additionally, increased levels of phosphorylated Erk1/2 were found in the forebrain of newly born Het and KO mice. Together, these data suggest that the increases seen in phospho-4EBP1 and phospho-eIF4E may be due to the additive effects of Akt and Erk activity in the NEX-*Pten* KO forebrain.

As a critical component of the PI3K/Akt cell survival pathway, GSK3β can be inhibited by phosphorylation via Akt at serine 9 (Ser9) (Plyte et al., 1992; Cross et al., 1995). Phospho-GSK3β (Ser9) was significantly increased in embryonic NEX-*Pten* KO forebrain, but was unchanged shortly after birth compared to wildtype littermates. Since phosphorylation of GSK3β inhibits its function, this could be detrimentally affecting cell survival in NEX-*Pten* KO mice. Alternatively, increased phospho-GSK3β levels in NEX-*Pten* KO mice could be due to the substantial increases in Akt activation at the embryonic time point. Since NEX-*Pten* KO mice do

survive until birth with normal phospho-GSK3β levels, GSK3β phosphorylation may normalize regardless of Akt status as part of a homeostatic mechanism over time.

To determine if the glutamate receptor abnormalities were due to mTORC1 hyperactivation, pregnant NEX-*Pten* Het dams were prenatally administered rapamycin, the canonical mTORC1 inhibitor. Although low doses of prenatal rapamycin treatment were well tolerated, they were not sufficient to significantly lower mTORC1 targets in rapamycin-treated NEX-*Pten* KO mice. These subthreshold doses did not significantly ameliorate the elevated levels of NR2A in NEX-*Pten* KO mice, suggesting increased exposure of rapamycin is needed to thoroughly evaluate if mTORC1 is involved in the ionotropic glutamate receptor abnormalities in NEX-*Pten* KO mice. Increased frequency of dosing or administration of higher doses of rapamycin both resulted in loss of pregnancy, limiting the evaluation of prenatal rapamycin treatment. Investigation of mTORC1's role in the glutamate receptor abnormalities in newborn NEX-*Pten* KO mice was therefore limited due to rapamycin effects on prenatal viability.

Overall, these data indicate that loss of Pten in NEX-*Pten* mice results in a selective alteration of glutamate receptor subunit protein levels, most likely in principal excitatory neurons. Subtype selective abnormalities in NMDA and AMPA subunit expression due to Pten deficiency may have functional consequences on synaptic activity and excitability. Germline *PTEN* mutations are implicated in a subset of individuals with autism and increased seizure liability, so it may be that abnormal glutamate receptor function contributes to these phenotypes. In support of this, glutamate antagonists have shown some efficacy in ameliorating autism-relevant symptoms (Erickson and Chambers, 2006; Niederhofer, 2007). Further biochemical and behavioral analyses are necessary to elucidate a more detailed mechanism behind the relationship between Pten and glutamate receptor expression and function.

Acknowledgements

Data from this chapter has appeared in Kazdoba et al., 2012.

I would like to thank the following people for their contributions to the work presented in this chapter of my dissertation: Beth Crowell for her assistance in mating NEX-*Pten* mice for these studies and thionin staining of NEX-*Pten* tissue; and Gum Hwa Lee for running the Dab1 Western blot and her help in designing primers for the qRT-PCR studies.

Chapter 3. Characterization of NEX-*Pten* dissociated neuronal cultures

1. Introduction

The subunit composition of the NMDA receptor changes as synapses mature, such that more NR2A-containing receptors are present in mature neurons compared to NR2B-containing receptors, which are primarily found in immature neurons (Cline et al., 1996; Kew et al., 1998; Stocca and Vicini, 1998; Tovar and Westbrook, 1999). Protein levels of several NMDA subunits (i.e., NR2A, NR2B and NR1) were upregulated in the early postnatal NEX-*Pten* KO forebrain (Chapter 2). It is possible that loss of Pten in forebrain excitatory neurons shifted the developmental switch between NR2A and NR2B, either by accelerating the appearance of NR2A-containing receptors or delaying reductions in NR2B-containing receptors.

NEX-*Pten* KO mice die prematurely, limiting the evaluation of chronic loss of Pten in excitatory neurons and its effects on ionotropic glutamate receptor expression. However, the developmental switch between NR2A- and NR2B-containing NMDA receptors that occurs *in vivo* as synapses mature also occurs *in vitro* as neurons mature in culture (Williams et al., 1993). Therefore, NEX-*Pten* cortical and hippocampal neurons from KO mice were developed in culture for several weeks after dissociation at P0. Since the PI3K/Akt/mTOR pathway is involved in neuronal development, the morphology of NEX-*Pten* cortical and hippocampal neurons was characterized, including cell size, dendrite branching and axon number. Dissociated cortical neurons were analyzed by Western blot to assess how loss of *Pten* altered PI3K/Akt/mTOR signaling *in vitro*. Biochemical analyses also evaluated ionotropic glutamate receptor expression in NEX-*Pten* KO cortical neurons at 7 and 14 days *in vitro* (DIV). The PI3K inhibitor LY294002 and the mTORC1 inhibitor rapamycin were evaluated in WT and NEX-*Pten* KO cultures to determine how inhibition of these components of the PI3K/Akt/mTOR signaling pathway affected cellular morphology and ionotropic glutamate receptor subunits. Together, this series of experiments characterized NEX-*Pten* dissociated cultures to determine if this *in vitro* model could be used for future pharmacology and mechanism of action studies.

2. Materials and Methods

Dissociated Culture Preparation and Analysis

Cortical and hippocampal tissue was isolated from NEX-*Pten* mouse pups at P0 immediately after birth, and prepared with a papain dissociation kit (Worthington, Lakewood, NJ). Pup body weight was recorded prior to brain removal, and brain weights were recorded prior to dissection. For Western blot analyses, immunocytochemistry and inhibitor studies, neuronal cultures were prepared from individual NEX-*Pten* brains. For co-culture studies (soma size characterization), cortical tissue from individual pups was combined and dissociated together to create cortical cultures containing neurons from NEX-*Pten* Wt, Het and KO mice. For inhibitor studies, WT cortical cultures were prepared from embryos of pregnant CD-1 mice (Charles River Laboratories) and harvested at E16.5. Tissue was dissected in cold Hank's Balanced Salt Solution (HBSS; Invitrogen), sliced into small pieces, and incubated in a prepared papain solution in a 37°C water bath for 30 min. Cells were then titurated and centrifuged for 5 min at 300xg to form a pellet. The pellet was re-suspended in a solution of Earle's Balanced Salt Solution (EBSS)/deoxyribonuclease I (DNase)/ovomucoid protease inhibitor, according to the manufacturer's instructions. The re-suspension was layered on top of ovomucoid protease inhibitor solution, centrifuged for 6 min at 100xg, and then centrifuged for an additional 6 min at 200xg to evenly coat the cells with the ovomucoid solution. Pelleted cells were then re-suspended in a mixture of 98% Neurobasal media, 2% B-27 supplement, 0.5mM glutamine and 0.5 mM PenStrep (Invitrogen). Cells were plated onto poly-L-lysine coated glass coverslips for immunocytochemistry experiments or 6 well plates for Western blot studies, and maintained at 37°C in 5% CO_2 in a water-jacketed incubator. Half the culture media was replaced with freshly prepared B-27-supplemented Neurobasal media every 2-4 days for maintenance.

Western Blot Analyses

Dissociated cortical cultures of individual pups were plated across 3 wells per mouse at 1-3 million cells per well, and harvested at either early (4 days *in vitro* (4 DIV)), mid (7 DIV) or late (12-15 DIV) time points. Wells were washed twice with warmed sterile phosphate buffered saline (DPBS) and then collected by adding RIPA lysis buffer with phosphatase and protease inhibitors (as described above) to the well and gently removing cells with a cell scraper. Cells were lysed in RIPA buffer for 10 min on ice and then centrifuged at 3000xg for 5 min at 4°C. Supernatant was collected, measured by the Bradford method for protein concentration and stored at -80°C until further use. Western blot analyses were performed as described in Chapter 2.

Immunocytochemistry

For immunolabeling, hippocampal cultures were washed with warmed DPBS and immediately fixed with 4% paraformaldehyde (in PBS) for 15 min at room temperature. Cells were then washed 3 times for 5 min with phosphate buffered saline (PBS), permeabilized with 0.1% Triton-X (in PBS) for 10 min and blocked with blocking buffer (10% normal goat serum albumin in 0.1% Triton-X/PBS) for 30 min. Samples were incubated with primary antibodies diluted in blocking buffer overnight at 4°C (Table 1). Subsequently, cells were washed with PBS and incubated with Alexa-Fluor conjugated secondary antibodies in 0.1% Triton-X/PBS for 1 hr at room temperature (Table 2). After PBS washes (3 x 5 min), coverslips were mounted with Vectashield Mounting Medium containing DAPI (Vector Laboratories) and imaged.

Characterization of Soma Size

To label actin, rhodamine-conjugated phalloidin (10 µl; Invitrogen) was added to blocking buffer for 15 min, followed by 3 PBS washes. To identify Pten-positive and Pten-negative somas in co-cultured cortical neurons, Pten was also immunolabeled with Alexa Fluor 488 secondary antibody. Cortical neurons were then imaged with a Leica DM5000B

epifluorescent microscope, using a 20x objective (HC PLAN APO; N.A. 0.7). Somas of Pten-positive and Pten-negative neurons were traced from merged images of phalloidin and Pten labeled cells using the Freehand Selection tool in ImageJ (NIH, Bethesda, MD) to measure their size.

Dendrite Arborization (Scholl Analysis)

Neurons were immunolabeled with MAP2 (with Alexa Fluor 488 secondary antibody) and imaged using a Yokogawa CSU-10 spinning disk confocal head attached to an inverted fluorescence microscope (Olympus IX50). Cell soma and dendrites were traced using the Paintbrush tool in ImageJ. Dendritic branching was analyzed using the SchollAnalysis plugin in FIJI (ImageJ bundle).

Axon Characterization

Neurons were immunolabeled with MAP2 and neurofilament-heavy (NFH) as described above. Processes that were MAP2(-)/NFH(+) were considered axons, while processes that were MAP2(+)/NFH(+) were considered dendrites. Neurons were imaged using a Yokogawa CSU-10 spinning disk confocal head attached to an inverted fluorescence microscope (Olympus IX50). Axons were counted manually; axon number was averaged and compared between genotypes.

Drug Preparation

LY294002 and rapamycin were prepared as described in Chapter 2. For *in vitro* studies, LY294002 or rapamycin were added to the culture medium for either 1 or 24 hrs, and then cells were collected for Western blot analysis. Any changes to culture medium color (indicating pH change) or cell viability were noted.

Statistical Analyses

For *in vitro* morphology studies, soma size and axon number of individual neurons within genotype were averaged and analyzed using a Student's t-test ($p<0.05$). Dendrite branching was analyzed by a multifactorial ANOVA, with either genotype or inhibitor treatment as the between-subjects factor and distance from the soma as the within-subjects factor. Bonferroni post hoc analysis compared Scholl radius of Het or KO to WT. For Western blot studies using NEX-*Pten* WT, Het and KO mice, a planned comparison Student's t-test evaluated if loss of Pten in NEX-*Pten* KO mice resulted in abnormalities compared to NEX-*Pten* WT mice ($p<0.05$). This was followed by a one-way ANOVA to determine if there was an effect of gene dosage, and Dunnett's post hoc tests to compare all genotypes (i.e., Het and KO) to WT. Normalized protein values in Western blot analyses were analyzed first by Student's t-test and then by one-way ANOVA with post hoc Dunnett's tests. One sample t-tests were used for LY294002 inhibitor studies in WT neurons because samples were run on different blots with one vehicle per time point per blot and therefore, no variability could be calculated for the vehicle samples. A one way ANOVA was used for LY294002 inhibitor studies in NEX-*Pten* KO neurons, with a Dunnett's post hoc test to compare all doses to vehicle. Effect size was calculated for NMDA and AMPA receptor subunit results, along with a power analysis (Appendix).

3. Results

Characterization of NEX-Pten Morphology In Vitro

In Chapter 2, soma size characterization revealed that somas of Pten-negative principal excitatory neurons from NEX-*Pten* KO mice were significantly enlarged compared to NEX-*Pten* WT mice. To further investigate the neuronal morphology of NEX-*Pten* KO neurons, cortical neurons were co-cultured from P0 embryos produced by the mating of two NEX-*Pten* Het mice. Pten was fluorescently immunolabeled to distinguish Pten-negative neurons from Pten-positive neurons after 15 days *in vitro* (15 DIV). Cortical neurons were then labeled with rhodamine-conjugated phalloidin to stain F-actin in the cell body and dendrites, as well as DAPI to visualize

the nuclei (Figure 16a). Soma size was measured by tracing cell bodies of Pten-negative (n=22) and Pten-positive neurons (n=35) and calculating the area of each soma. Cortical neurons lacking Pten were significantly larger than Pten-positive neurons [$t(55)=7.413$, $p<0.0001$] (Figure 16b). These findings are consistent with the NEX-*Pten* KO *in vivo* findings described in Chapter 2 as well as other reports of neuronal hypertrophy in conditional *Pten* mutant mice (Backman et al., 2001; Kwon et al., 2001; Ljungberg et al., 2009; Kazdoba et al., 2012).

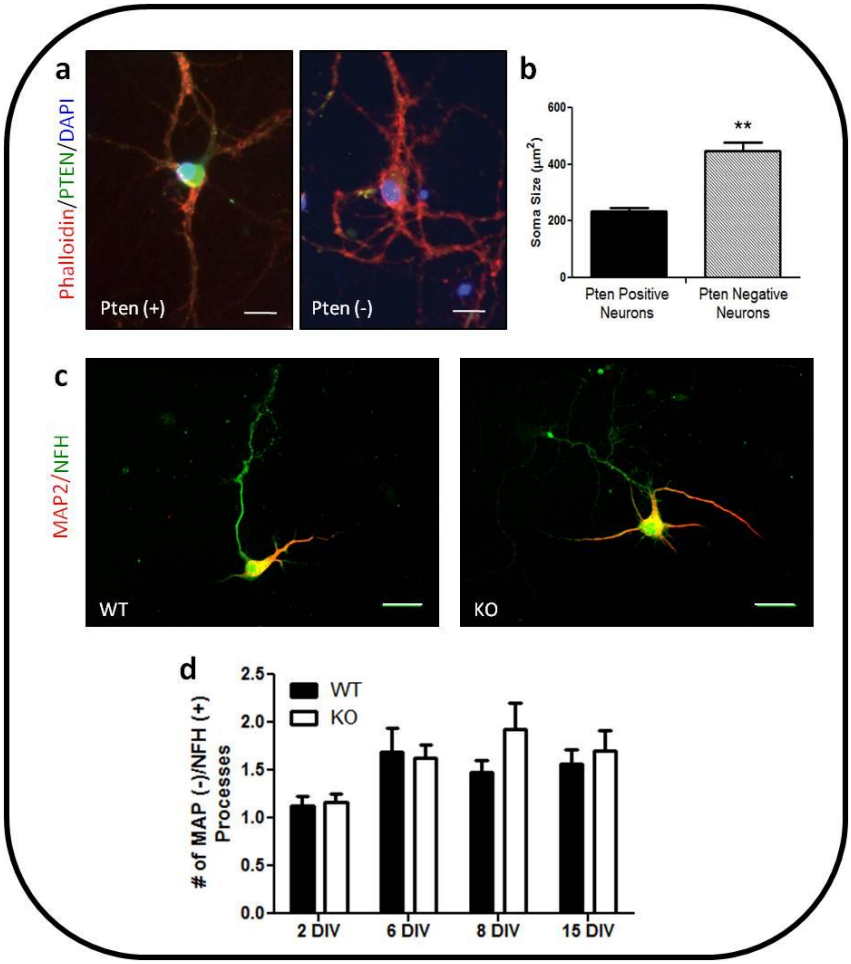

Figure 16. Characterization of soma size and axon number of NEX-*Pten* dissociated cultures. a) Representative fluorescent images of NEX-*Pten* dissociated cortical neurons cultures for 15 days *in vitro* (DIV) and triple labeled with rhodamine-conjugated phalloidin to label actin (red), Pten antibodies (green) and DAPI nuclear stain (blue). b) Quantification of soma size of reveals

that Pten-negative (n=22) cortical neurons have significantly larger cell bodies than Pten-positive neurons (n=35) (**p<0.0001). c) Representative confocal images of 6 DIV NEX-*Pten* wildtype (WT) and knockout (KO) hippocamapal neurons double labeled for MAP2 (red) and neurofilament-heavy (NFH) (green). Dendrites were defined as MAP2(+)/NFH(+) processes, while axons were defined as MAP2(-)/NFH(+) processes. d) The number of MAP2(-)/NFH(+) axons in NEX-*Pten* WT and KO dissociated hippocampal cultures at several ages (n=15-30 per group) were not significantly different. Scale bar = 20 μm (a), 30 μm (c).

NEX-*Pten* dissociated neuronal cultures provided an opportunity to examine how loss of Pten affects neuronal morphology in more detail. Individually cultured NEX-*Pten* WT and KO dissociated hippocampal neurons were fluorescently immunolabeled for MAP2, which binds to tubulin and stabilizes microtubules, and neurofilament-heavy (NFH), cytoskeletal filaments that provide structural support to dendrites and axons. Dendrites were defined as neuritic processes that were MAP2(+)/NFH(+), while axons were defined as MAP2(-)/NFH(+) processes. The number of axons were counted at several different ages (i.e., 2, 6, 8, 15 DIV; n=15-30 neurons per group). While several individual neurons in each genotype displayed multiple axons, there were no significant differences between NEX-*Pten* WT and KO hippocampal neurons in overall axon number (Figure 16c, d). To further characterize neuronal morphology, dendritic arborization was analyzed by automated Scholl analysis on MAP2-immunolabeled hippocampal neurons at 4 and 10 DIV (n=10-13 neurons per group) (Figure 17a, b). At 4 DIV, a multifactorial ANOVA with Genotype (3) as a between-subjects factor and Scholl Radius (10) as a within-subjects factor revealed that there was a main effect of Genotype [$F(2,306)=6.274$, $p<0.004$], a main effect of Scholl Radius [$F(9,306)=36.22$, $p<0.0001$] and a Genotype by Scholl Radius interaction [$F(18,306)=1.7$, $p<0.04$] (Figure 17c). Dendritic branching differed depending on the genotype, such that NEX-*Pten* KO neurons had a significantly greater number of dendrite branches 20 μm away from the soma compared to WT neurons [Bonferroni post hoc test,

p<0.01]. Similarly, at 10 DIV, a multifactorial ANOVA with Genotype (3) as a between-subjects factor and Scholl Radius (10) as a within-subjects factor found a main effect of genotype [F(2,279)=7.12, p<0.003], a main effect of Scholl Radius [F(9,279)=37.86, p<0.0001] and a Genotype by Scholl Radius interaction [F(18,279)=3.05, p<0.0001] (Figure 17d). NEX-*Pten* KO hippocampal neurons at 10 DIV had significantly greater dendritic arborization compared to WT neurons at several distances (i.e., 20-50 μm) from the soma [Bonferroni's post hoc test (20, 30, 40, 50 μm) ps<0.05]. Therefore, these data provide evidence that genetic deletion of *Pten* in NEX-*Pten* KO neurons does not affect axon formation *in vitro* but does increase dendrite branching near the soma (≤50 μm) by 10 DIV.

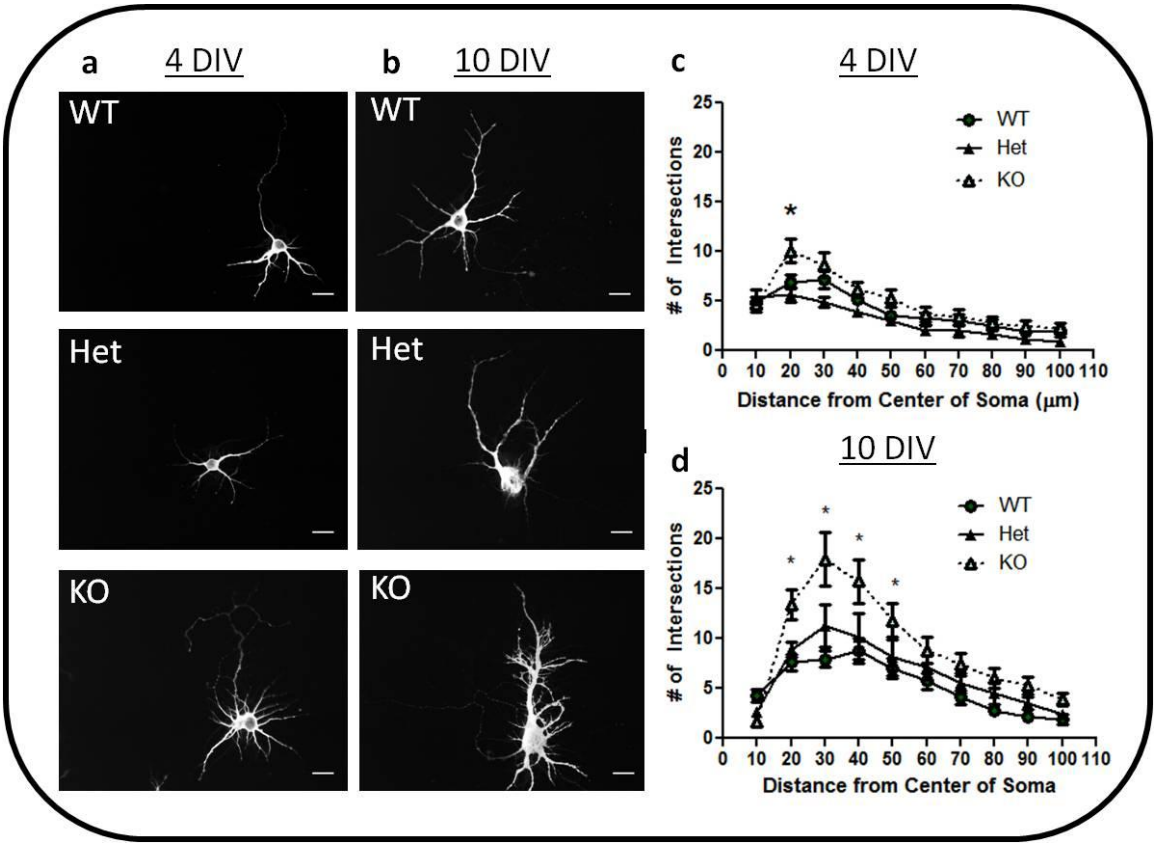

Figure 17. Characterization of dendrite arborization in NEX-*Pten* dissociated hippocampal cultures.

Representative confocal images of NEX-*Pten* wildtype (WT), heterozygous (Het) and knockout (KO) hippocampal cultures at 4 days *in vitro* (DIV) (a) and 10 DIV (b) immunolabeled with

MAP2. c) A multifactorial ANOVA of dendrite branching in NEX-*Pten* 4 DIV hippocampal neurons revealed an interaction between genotype and dendrite branching. NEX-*Pten* KO hippocampal neurons had more dendrite crossings 20 μm from the soma compared to WT hippocampal neurons, as automatically measured by Scholl analysis. (Bonferroni post hoc test, WT vs. KO, *p<0.01). d) A multifactorial ANOVA of dendrite branching in NEX-*Pten* 10 DIV hippocampal neurons revealed an interaction between genotype and Scholl analysis of dendrite branching. NEX-*Pten* KO hippocampal neurons had more dendrite crossings 20-60 μm from the soma compared to WT hippocampal neurons. (Bonferroni post hoc test, WT vs. KO at 20, 40, 50, 60 μm, *ps<0.01). Scale bars = 20 μm.

Western Blot Analyses of mTOR Signaling in NEX-Pten Cultures

NEX-*Pten* cortical neurons were individually cultured from each genotype and then analyzed by Western blot at selected time points to determine how Pten deficiency may alter glutamate receptor expression as neurons mature and undergo this developmental switch in NMDA receptor subunits. At 4 DIV, hyperactivation of the mTOR signaling pathway, as measured by Akt phosphorylation at Ser473 and phospho-S6 levels, was greatly increased in NEX-*Pten* KO cortical neurons compared to WT neurons (data not shown). At 7 and 14 DIV, levels of Pten were significantly reduced in NEX-*Pten* KO neurons compared to WT cultures [7 DIV: $t(6)=11.06$; 14 DIV: $t(4)=31.18$; ps<0.0001] (Figure 18a, c, e). ANOVA analyses revealed that loss of Pten was significantly affected by genotype at both 7 and 14 DIV [7 DIV: $F(2,9)=30.29$, $p<0.0001$; 14 DIV: $F(2,7)=15.36$, $p<0.003$], such that NEX-*Pten* KO cortical neurons had significantly less Pten then WT neurons at both ages [Dunnett's post hoc tests, ps<0.05]. Consequently, 7 DIV and 14 DIV NEX-*Pten* KO cortical cultures had significantly higher levels of Akt phosphorylation at Ser473 [7 DIV: $t(10)=13.05$, $p<0.0001$; 14 DIV: $t(11)=3.465$, $p<0.001$] and Thr308 [7 DIV: $t(7)=4.814$, $p<0.002$; 14 DIV: $t(7)=4.863$, $p<0.002$] than WT cultures. ANOVA analyses revealed that the levels of Akt phosphorylation at Ser473

[7DIV: $F(2,14)=158.2$, $p<0.0001$; 14 DIV: $F(2,16)=11.84$, $p<0.001$] and Thr308 [7 DIV: $F(2,11)=27.29$, $p<0.0001$; 14 DIV: $F(2,11)=24.87$, $p<0.0001$] were significantly affected by genotype at both ages (Figure 18a, c, f, g). These genotype effects were driven by significant increases in phosphorylation in NEX-*Pten* KO cultures compared to WT neurons (Dunnett's post hoc tests, $ps<0.05$). Together, these data demonstrate that *Pten* is significantly reduced in 7 and 14 DIV NEX-*Pten* KO hippocampal cultures. The removal of Pten's regulatory role on the PI3K/Akt/mTOR pathway led to elevated levels of phosphorylation of Akt at both the PDK1- and mTORC2-mediated sites, which parallels the elevating signaling in NEX-*Pten* KO lysate discussed in Chapter 2.

Characterization of Ionotropic Glutamate Receptor Expression in NEX-Pten Cultures

NR2A and NR2B could not be reliably detected in NEX-*Pten* neurons at 4 DIV. Therefore, it was not possible to perform a complete characterization of ionotropic glutamate receptor subunits in NEX-*Pten* cortical neurons at this age. However, both subunits could be detected in older cultures. At 7 DIV, there was a marginal effect of genotype on NR2A [$F(2,6)=3.623$, $p<0.09$], such that NEX-*Pten* KO cortical cultures had higher NR2A protein levels, although this was not statistically significant (Figure 18b, h). NR2B protein levels were significantly higher in NEX-*Pten* KO cortical cultures at 7 DIV compared to WT neurons [$t(4)=2.991$, $p<0.04$] (Figure 18b, i). GluR1 did not differ between genotypes at 7 DIV (Figure 18b, j). In 14 DIV cortical neurons, NR2A and NR2B did not differ between genotypes (Figure 18d, h, i). The AMPA receptor subunit, GluR1, tended to be reduced in NEX-*Pten* KO hippocampal neurons compared to WT neurons [$t(5)=2.22$, $p<0.08$] (Figure 18d, j). ANOVA analysis also revealed that there was a marginal effect of genotype on GluR1 in 14 DIV neurons [$F(2,7)=3.375$, $p<0.1$]. NR1 and GluR2/3 were not detectable by Western blot in cortical neurons at either 7 or 14 DIV, and therefore, could not be analyzed. Overall, the ionotropic glutamate receptor characterization in NEX-*Pten* cortical cultures demonstrated that there were elevated

protein levels of NR2A and NR2B in younger neurons, but these increases are no longer present in older neurons.

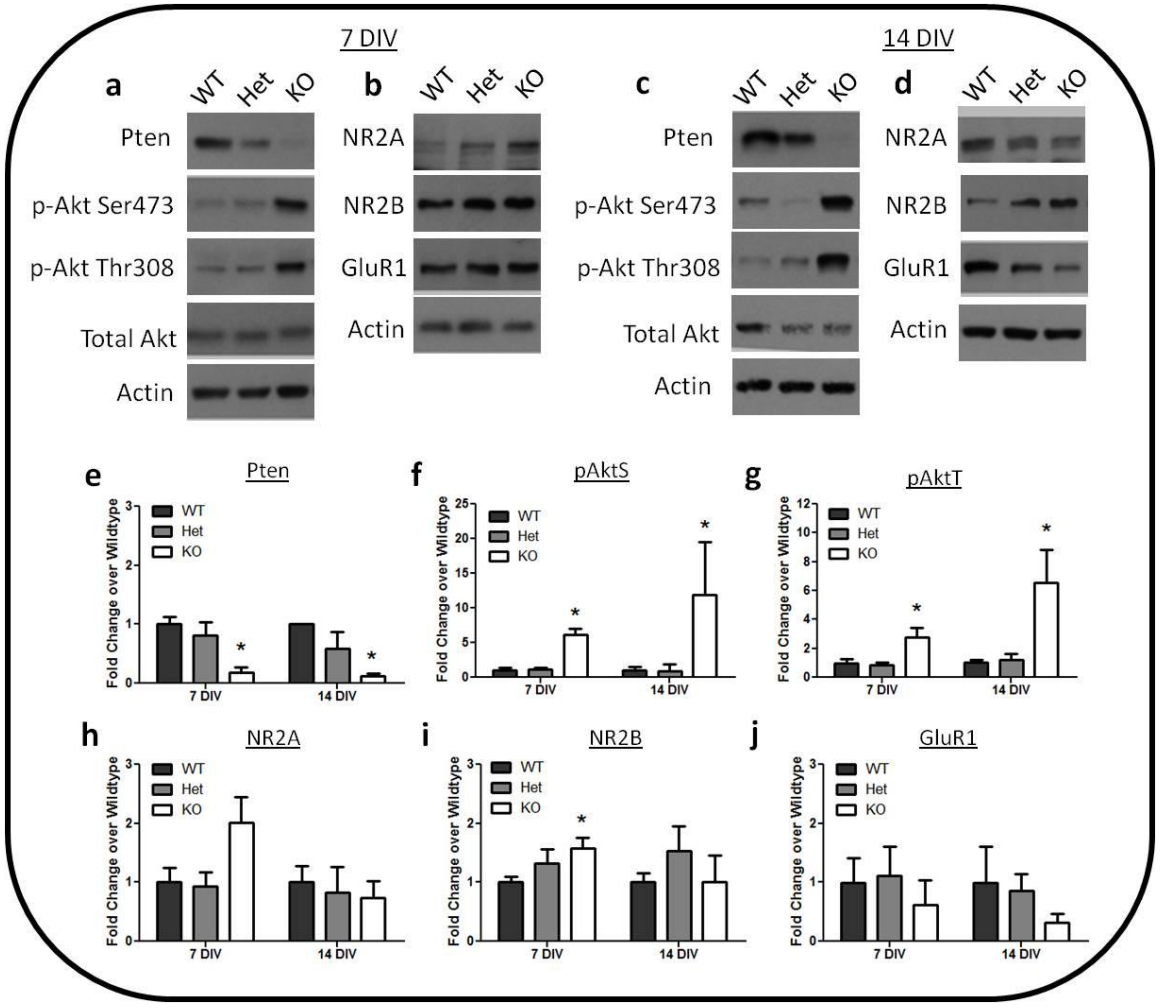

Figure 18. Characterization of the PI3K/Akt/mTOR pathway and glutamate receptor expression in NEX-*Pten* dissociated cortical cultures.

a) Representative Western blots of Pten, phospho-Akt serine 473 (p-Akt Ser473; pAktS), phospho-Akt threonine 308 (p-Akt Thr308; pAktT), total Akt and actin proteins in NEX-*Pten* wildtype (WT), heterozygous (Het) and knockout (KO) dissociated cortical cultures aged 7 days *in vitro* (DIV). b) Representative Western blots of NR2A, NR2B, GluR1 and actin protein levels in 7 DIV NEX-*Pten* WT, Het and KO dissociated cortical cultures. c) Representative Western blots of Pten, p-Akt Ser473, p-Akt Thr308, total Akt and actin proteins in 14 DIV NEX-*Pten* WT,

Het and KO dissociated cortical cultures. d) Representative Western blots of NR2A, NR2B, GluR1 and actin protein levels in 14 DIV NEX-*Pten* WT, Het and KO dissociated cortical cultures. d) Western blot analysis indicates that Pten (normalized to actin) is significantly reduced in NEX-*Pten* KO dissociated cortical cultures at 7 and 14 DIV compared to WT cultures. Akt phosphorylation at Ser473 (f) and Thr308 (g) (normalized to total Akt) are significantly increased in 7 and 14 DIV NEX-*Pten* KO dissociated cortical cultures. h) NR2A protein levels (normalized to actin) in NEX-*Pten* cortical cultures do not significantly differ between genotypes at either 7 or 14 DIV. i) NR2B protein levels (normalized to actin) are significantly increased in 7 DIV, but not 14 DIV, NEX-*Pten* KO cortical neurons compared to WT. j) GluR1 protein levels (normalized to actin) are unchanged in NEX-*Pten* dissociated cortical cultures at 7 and 14 DIV. Data were obtained from 3-7 individual cortical cultures per genotype. *$p<0.05$.

Evaluation of PI3K Inhibition using LY294002 in Wildtype and NEX-Pten Dissociated Cultures

LY294002, a highly selective PI3K inhibitor, can specifically reduce PI3K activity without affecting other protein kinases (Vlahos et al., 1994). A one-sample t-test was used for the following analyses because samples were run on different blots with one vehicle per time point (i.e., 1 hr or 24 hrs) per blot and therefore, no variability could be calculated for the vehicle samples. Using 14 DIV dissociated cortical cultures from WT (ICR/CD-1) mice, 1 hr treatment of 20 and 75 µM LY294002 significantly reduced Akt phosphorylation at Ser473 [one-sample t-test: 20 µM: $t(2)=34.39$, $p<0.001$; 75 µM: $t(2)=40.29$, $p<0.001$] and Thr308 [one-sample t-test: 20 µM: $t(2)=8.859$, $p<0.021$; 75 µM: $t(2)=9.296$, $p<0.02$] compared to vehicle-treated neurons (Figure 19a, e). Although LY294002 was able to reduce Akt phosphorylation after 1 hr, there were no significant changes in NR2A, NR2B or GluR1 protein levels at either dose (Figure 19b, g). 14 DV WT cortical cultures were then treated with 20 and 75 µM LY294002 for 24 hrs to evaluate if sustained PI3K inhibition would affect NMDA and AMPA subunit protein levels. After 24 hrs, WT neurons treated with 20 and 75 µM LY294002 had significantly lower levels of

Akt phosphorylation at Ser473 [one-sample t-test: 20 µM: t(2)=9.295, p<0.02; 75 µM: t(2)=12.7, p<0.007], but not Thr308 (Figure 19c, f). Dab1 protein levels were also significantly reduced at 20 µM [one-sample t-test: t(2)=87.60, p<0.0001] and 75 µM [one-sample t-test: t(2)=81.92, p<0.0001] (Figure 19c, f). After 24 hr LY294002 treatment, 14 DIV WT cortical neurons had significantly reduced protein levels of NR2A [one-sample t-test: 20 µM: t(2)=7.359, p<0.02; 75 µM: t(2)=8.187, p<0.02], but not NR2B (Figure 19d, h). GluR1 was also significantly reduced by 20 µM [one-sample t-test: t(2)=11.32, p<0.008], but not 75 µM (Figure 19d, h).

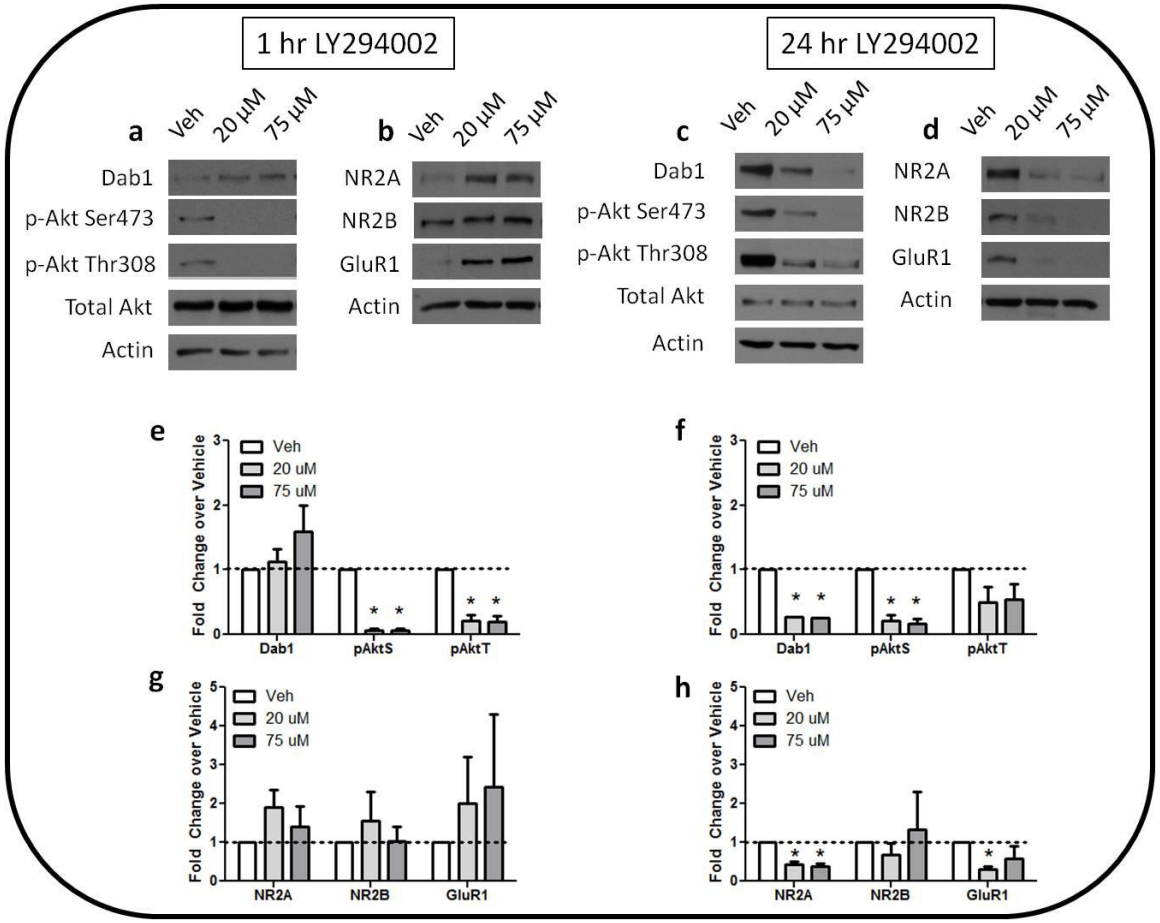

Figure 19. Evaluation of 1 hour and 24 hour treatment of the PI3K inhibitor LY294002 in wildtype dissociated cortical cultures.

a) Representative Western blots of Dab1, phospho-Akt serine 473 (p-Akt Ser473; pAktS), phospho-Akt threonine 308 (p-Akt Thr308; pAktT), total Akt and actin proteins in wildtype (WT) dissociated cortical cultures from ICR/CD-1 embryos aged 14 days *in vitro* (DIV) and treated

with LY294002 for 1 hr. b) Representative Western blots of the NMDA receptor subunits NR2A and NR2B, the AMPA receptor subunit GluR1 and actin protein levels in dissociated WT cortical neurons treated with LY294002 for 1 hr at 14 DIV. c) Representative Western blots of Dab1, p-Akt Ser47, p-Akt Thr308, total Akt and actin proteins in 14 DIV WT dissociated cortical cultures from ICR treated with LY294002 for 24 hr. b) Representative Western blots of NR2A, NR2B, GluR1 and actin protein levels in 14 DIV WT cortical cultures treated with LY294002 for 24 hr. e) 1 hr treatment of LY294002 did not alter Dab1 protein levels (normalized to actin), but did significantly lower phosphorylation of Akt (normalized to total Akt) in 14 DIV WT dissociated cortical neurons. f) 24 hr treatment of LY294002 significantly reduced Dab1 levels (normalized to actin) and phosphorylation of Akt at serine 473 (normalized to total Akt. Although Akt phosphorylation at threonine 308 (normalized to total Akt) was reduced, this was not statistically significant. g) 1 hr treatment of LY294003 did not alter protein levels of NR2A, NR2B or GluR1 (normalized to actin) in 14 DIV WT dissociated cortical cultures. h) 24 hr treatment of 20 or 75 µM LY294002 significantly reduced NR2A, but not NR2B protein levels in 14 DIV WT cortical cultures. 20 µM LY294002 significantly reduced GluR1 levels in 14 DIV WT dissociated cortical neurons. Data were obtained from 3 separate sets of cultures per dose and treatment time. one-sample t-test, *$p<0.05$.

Next, LY294002 was evaluated in 15 DIV NEX-*Pten* KO cortical cultures to determine if the activation of the PI3K/Akt/mTOR pathway previously observed could be reduced pharmacologically in this NEX-*Pten in vitro* model. After 24 hrs, LY294002 treatment significantly affected Akt phosphorylation at Ser473 [$F(2,6)=27.09$, $p<0.001$] and Thr308 [$F(2,6)=10.14$, $p<0.02$] (Figure 20a, c). Dunnett's post hoc tests revealed that both 50 µM and 75 µM significantly reduced Ser473 and Thr308 phosphorylation of Akt compared to vehicle-treated NEX-*Pten* KO neurons (ps<0.05). In addition, levels of phospho-S6 were affected by 24 hr LY294002 treatment [$F(2,6)=20.02$, $p<0.003$], such that NEX-*Pten* KO cortical neurons that were

treated with 50 µM and 75 µM had significantly lower levels of phospho-S6 compared to vehicle-treated neurons [Dunnett's post hoc, Veh. vs. dose, ps<0.05] (Figure 20a, c). Levels of Dab1 were not changed by 24 hrs of LY294002 treatment (Figure 20a, c). Although NR2A and NR2B protein expression was not significantly changed by 24 hr LY294002 treatment, NEX-*Pten* KO cortical neurons tended to have lower levels of NR2A and NR2B when PI3K activity was inhibited (Figure 20b, d). In NEX-*Pten* KO cortical neurons, GluR1 levels followed a similar pattern as WT neurons when treated with 50 µM and 75 µM LY294002 for 24 hrs, such that both doses, particularly 50 µM-treated neurons, had lower levels of GluR1, but this did not reach statistical significance (Figure 20b, d).

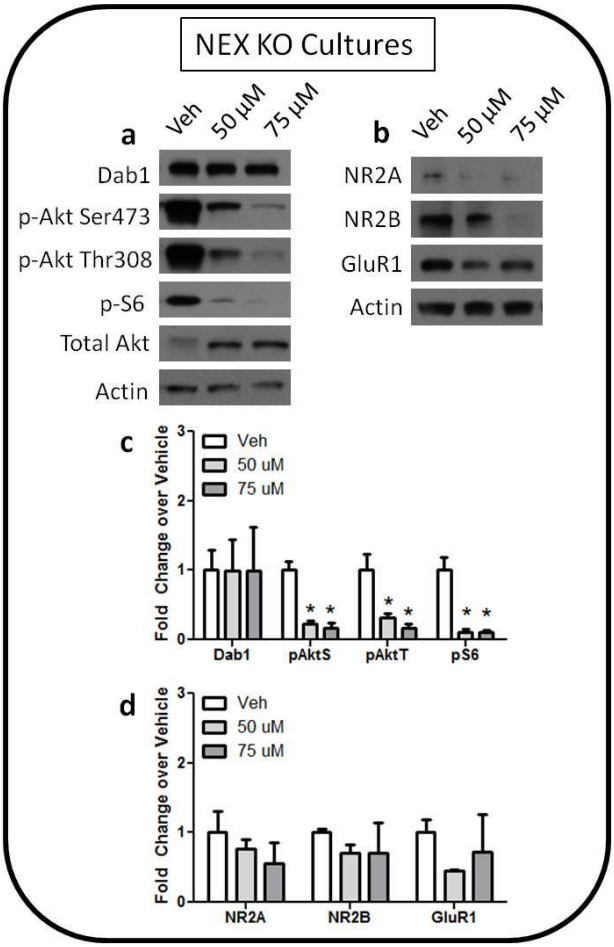

Figure 20. Evaluation of 24 hour treatment of the PI3K inhibitor LY294002 in NEX-*Pten* knockout dissociated cortical cultures.

a) Representative Western blots of Dab1, phospho-Akt serine 473 (p-Akt Ser473; pAktS), phospho-Akt threonine 308 (p-Akt Thr308; pAktT), phospho-S6 serine 235/235 (p-S6), total Akt and actin proteins in NEX-*Pten* knockout (KO) dissociated cortical cultures aged 15 days *in vitro* (DIV) and treated with LY294002 for 24 hr. b) Representative Western blots of the NMDA receptor subunits NR2A and NR2B, the AMPA receptor subunit GluR1 and actin protein levels in 15 DIV dissociated NEX-*Pten* KO cortical neurons treated with LY294002 for 24 hr. c) Semi-quantitative Western blot analyses revealed that 24 hr treatment with LY294002 did not alter Dab1 protein levels (normalized to actin), but did significantly reduce phosphorylation of Akt (normalized to total Akt) and S6 (normalized to actin) in 15 DIV NEX-*Pten* KO dissociated cortical neurons. d) NR2A, NR2B and Dab1 (normalized to actin) remain unchanged after 24 hr LY294002 treatment in NEX-*Pten* KO cortical cultures. Data were obtained from 3 sets per treatment group. $p<0.05$.

NEX-*Pten* KO hippocampal neurons had larger cell bodies and greater dendritic arborization compared to NEX-*Pten* WT neurons at 4 and 10 DIV (Figure 16a, b & 17). Since *Pten* deletion led to increased cellular growth, 15 DIV NEX-*Pten* KO neurons were treated with LY294002 for 24 hrs to determine if PI3K inhibition would reduce dendrite branching and soma size. A multifactorial ANOVA with LY294002 dose (4) as a between-subjects factor and Scholl Radius (10) as a within-subjects factor found a main effect of Scholl Radius [$F(9,477)=34.49$, $p<0.0001$] and an interaction between LY294002 treatment and Scholl Radius [$F(27,477)=1.71$, $p<0.02$] (Figure 21a-f). 24 hr treatment of 75 µM LY294002 (n=15 neurons) significantly reduced dendritic branching at 70 and 80 µm from the soma compared to vehicle-treated NEX-*Pten* KO neurons (n=16 neurons) [Bonferroni's post hoc test, $ps<0.05$] (Figure 21f). Although 100 µM of LY294002 (n=10 neurons) reduced the number of dendrite crossings 50 – 100 µm away from the soma, these reductions were not significantly reduced compared to vehicle-treated neurons. Soma size was significantly affected by 24 hr LY294002 treatment [$F(3,108)=7.034$,

p<0.0002], such that all doses of LY294002 significantly reduced cell body size compared to vehicle-treated cultures (n=26-30 neurons per dose) [Dunnett's post hoc tests, ps<0.05] (Figure 21g).

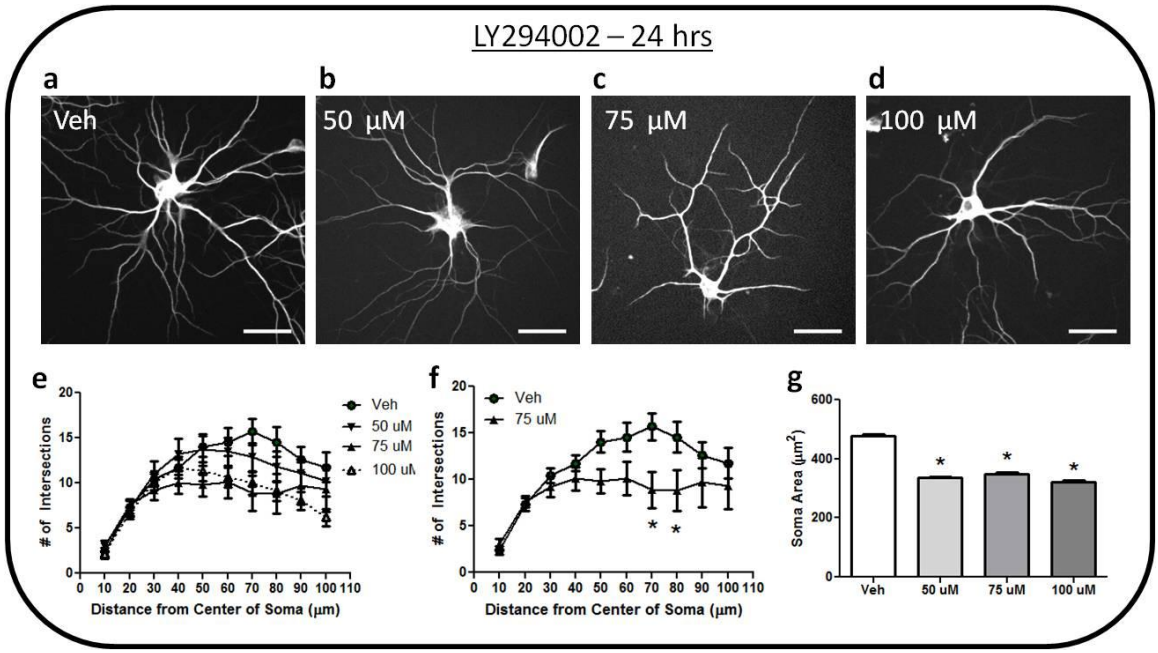

Figure 21. Characterization of dendrite branching in NEX-*Pten* knockout dissociated hippocampal cultures after 24 hr LY294002 treatment.

a-d) Representative confocal images of NEX-*Pten* knockout (KO) dissociated hippocampal neurons aged 15 days *in vitro* (DIV) and labeled with MAP2. e) Quantification of dendritic arborization of 15 DIV dissociated NEX-*Pten* KO hippocampal neurons treated with LY294002 for 24 hrs using automated Scholl analysis. A multifactorial ANOVA revealed an interaction between LY294002 treatment and dendrite branching. Data were obtained from 10-16 neurons per dose. f) A Bonferroni corrected post hoc test indicated that 24 hr treatment of 75 µM LY294002 significantly reduced the number of dendrite crossings 70-80 µm away from the soma, compared to vehicle treated NEX-*Pten* KO dissociated hippocampal neurons. g) 24 hr LY294002 significantly reduced soma size of treated NEX-*Pten* KO dissociated hippocampal cultures

compared to vehicle-treated NEX-*Pten* KO cultures (n=26-30 neurons per group). Scale bar = 50 µm. *p<0.05.

Evaluation of Rapamycin on Neuronal Morphology in Dissociated NEX-Pten KO Cultures

The canonical mTORC1 inhibitor, rapamycin, was evaluated in 14 DIV WT cortical neurons at several doses (i.e., 75 nM, 100 nM, 50 µM and 75 µM). None of the doses tested robustly reduced levels of phospho-S6, a downstream effector of mTORC1 (data not shown). NEX-*Pten* cortical neurons were not available for Western blot analysis of rapamycin treatment. To determine if rapamycin altered dendritic arborization in the NEX-*Pten* culture model, 15 DIV NEX-*Pten* KO hippocampal neurons (n=20 neurons per dose) were treated with 75 or 100 nM of rapamycin for 24 hrs and were analyzed by Scholl analysis. A multifactorial ANOVA with Rapamycin dose (3) as a between-subjects factor and Scholl Radius (10) as a within-subjects factor found a main effect of Rapamycin treatment [$F(2,513)=4.97$, $p<0.01$], main effect of Scholl Radius [$F(9,513)=36.85$, $p<0.0001$] and an interaction between Rapamycin treatment and Scholl Radius [$F(18,477)=3.03$, $p<0.0001$] (Figure 22a-d). After 24 hrs, 75 nM of rapamycin significantly reduced branching 20 µm from the soma compared to vehicle-treated NEX-*Pten* KO neurons [Bonferroni post hoc test, $p<0.05$] (Figure 22e). Conversely, rapamycin significantly increased branching 60 µm from the soma in NEX-*Pten* KO neurons treated with 100 nM compared to vehicle-treated KO hippocampal neurons. Soma size of NEX-*Pten* KO hippocampal neurons (n=34-45 neurons per dose) was significantly affected by 24 hr rapamycin treatment [$F(2,120)=22.23$, $p<0.0001$], such that both doses of rapamycin significantly reduced cell body size [Dunnett's post hoc test, $ps<0.05$] (Figure 22f).

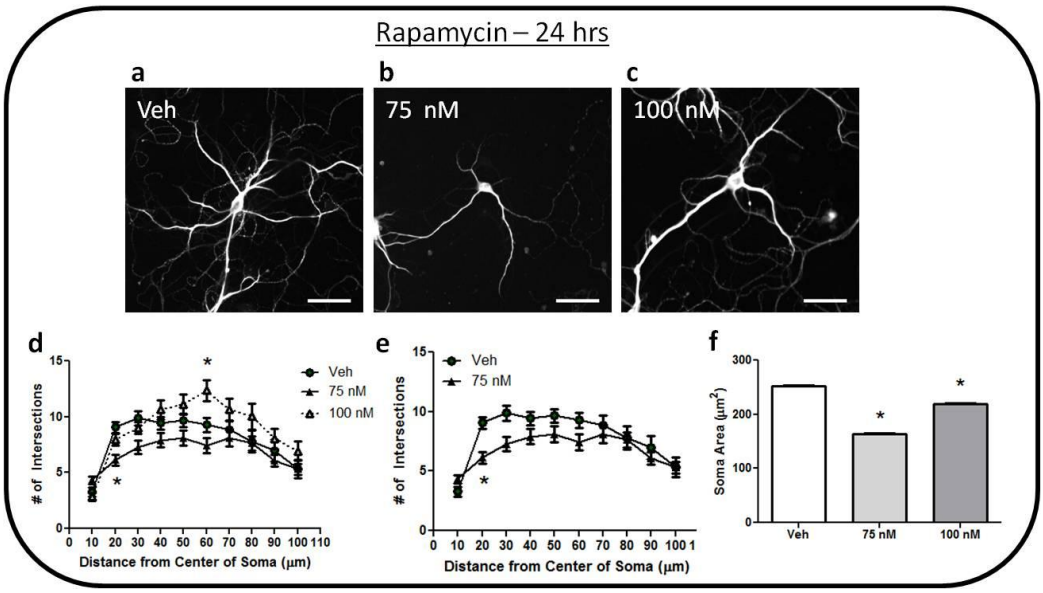

Figure 22. Characterization of dendrite branching in NEX-*Pten* knockout dissociated hippocampal cultures after 24 hr rapamycin treatment.

a-c) Representative confocal images of NEX-*Pten* knockout (KO) dissociated hippocampal neurons aged 15 days *in vitro* (DIV) and labeled with MAP2. d) Quantification of dendritic arborization of 15 DIV dissociated NEX-*Pten* KO hippocampal neurons treated with rapamycin for 24 hrs using automated Scholl analysis. A multifactorial ANOVA revealed an interaction between rapamycin treatment and dendrite branching. A Bonferroni corrected post hoc test indicated that 24 hr treatment of 100 nM rapamycin significantly increased the number of dendrite crossings 60 μm away from the soma, compared to vehicle treated NEX-*Pten* KO hippocampal neurons. Data were obtained from 20 neurons per dose. e) A Bonferroni post hoc test indicated that 24 hr treatment of 75 nM rapamycin significantly reduced the number of dendrite crossings 20 μm away from the soma, compared to vehicle treated NEX-*Pten* KO dissociated hippocampal neurons. g) 24 hr rapamycin significantly reduced soma size of treated NEX-*Pten* KO dissociated hippocampal cultures compared to vehicle-treated NEX-*Pten* KO cultures (n=34-45 neurons per group). Scale bar = 50 μm. *$p<0.05$.

4. Discussion

Dissociated hippocampal and cortical neurons from P0 NEX-*Pten* WT, Het and KO mice successfully grew in culture. NEX-*Pten* KO dissociated neurons had more complex dendrite patterning and larger somas, which is consistent with the findings in the NEX-*Pten* KO forebrain (Chapter 2). 24 hr inhibition of PI3K (LY294002) or mTORC1 (rapamycin) reduced dendrite complexity in NEX-*Pten* KO cultures, such that dendrite branching patterns were not as complex compared to vehicle treated neurons at select doses. Both inhibitors also reduced soma size after 24 hrs of treatment. These results are consistent with reports that mTOR regulates dendrite arborization (Jaworski et al., 2005; Kumar et al., 2005) and cell size (Fingar et al., 2002). Previous research found that Pten downregulation using short hairpin RNA (shRNA) or genetic *Pten* deletion enhanced the intrinsic ability of adult mouse corticospinal tract neurons to regenerate numerous axons in spinal cord lesion models (Liu et al., 2010; Zukor et al., 2013). In addition, small inhibitor RNA (siRNA) designed to downregulate *Pten* induced the formation of multiple axons in dissociated rat hippocampal neurons (Jiang et al., 2005). In the current studies, dissociated hippocampal cultures from NEX-*Pten* KO mice did not differ in axon number compared to WT cultures. The discrepancy between these results and reports detailing multiple axons from loss of *Pten* may be due to differences in magnitude of Pten loss, brain region examined or methodology between studies (e.g., shRNA/siRNA vs. genetic deletion). It is also possible there were differences in axon morphology, given that NEX-*Pten* hippocampal neurons had more elaborate dendritic branching patterns than WT neurons. Axon branching and thickness were not quantified in the present studies. These axonal characteristics did not seem qualitatively different between genotypes, but should be addressed in future studies. Therefore, although NEX-*Pten* KO neurons were larger and had more dendrite branches, they maintained a normal number of axons at several time points.

Dissociated cultures from NEX-*Pten* mice allowed a more detailed analysis of how Pten deficiency can affect glutamate receptor subunit expression *in vitro* as synapses mature.

Increased activation of the PI3K/Akt/mTOR pathway, as determined by Akt phosphorylation, could be detected in very young to older cultures. Glutamate receptor subunit expression was difficult to detect at 4 DIV, and therefore, could not be characterized. In moderately young cultures (i.e., 7 DIV), the NMDA receptor subunits NR2A and NR2B were readily detected and were increased in NEX-*Pten* KO cultures. By 14 DIV, however, these increases were no longer present. GluR1 protein expression was similar between genotypes at all time points tested. NR1, NR3A, NR3B and GluR2/3 could not be reliably detected *in vitro*, limiting the scope of glutamate receptor characterization. Therefore, although the mTOR pathway was elevated in all ages analyzed, NMDA receptor subunit protein abnormalities were normalized over time. The pattern of upregulation followed by normalization of NMDA subunit levels seen here is similar to the pattern described for NEX-*Pten* Het mice in Chapter 2. Although not statistically significant, increases in NR2A, NR2B and NR1 were found in NEX-*Pten* Het forebrain at P0, but these were no longer present by 6 months of age. The amelioration of abnormal NMDA receptor subunit levels may be due to compensatory mechanisms that ultimately normalize glutamate receptor protein levels.

One of the benefits of a NEX-*Pten in vitro* model is the ability to use PI3K/Akt/mTOR inhibitors to determine the mechanism responsible for the NEX-*Pten* KO glutamate receptor phenotype. The dissociated cultures allow for more flexibility in evaluating compounds, since several inhibitors of the mTOR pathway cannot be extensively tested *in vivo* but can be evaluated *in vitro*. The specific PI3K inhibitor LY294002 selectively reduces PI3K activity without affecting other protein kinases (Vlahos et al., 1994). In cortical cultures from WT animals, LY294002 robustly reduced Akt phosphorylation after 1 hr of treatment. While PDK1-mediated Akt phosphorylation at Thr308 was significantly reduced after 1 hr of LY294002, phosphorylation at this site was lower, but not significantly so, after 24 hrs of PI3K inhibition. This suggests that activity of some downstream components (e.g.., mTORC2) of the PI3K/Akt/mTOR pathway may remain suppressed as PI3K function begins to return to baseline

and take longer to normalize. Neither NR2A nor NR2B levels were changed after 1 hr of LY294002, but levels of NR2A were significantly decreased in WT cultures after 24 hrs. In 15 DIV NEX-*Pten* KO cultures, 24 hr treatment of LY294002 reduced Akt and S6 phosphorylation and tended to reduce NR2A levels, although this was not statistically significant. These data suggest PI3K may be necessary for increased expression of NR2A in NEX-*Pten* KO mice, but it is unclear if PI3K alone is sufficient to produce this phenotype. To be noted, the transient increase in NMDA receptor protein expression in NEX-*Pten* KO cortical cultures was greatest at 7 DIV, but here, the role of PI3K inhibition in the NMDA receptor phenotype was evaluated at 15 DIV. Ideally, studies with LY294002 should be repeated at earlier time points in dissociated NEX-*Pten* cortical cultures to determine if PI3K inhibition can suppress the increase in NMDA receptor subunits. Another possibility for the mild effect of LY294002 on NR2A is that more chronic inhibition of the PI3K/Akt/mTOR pathway is needed to significantly lower NR2A levels in NEX-*Pten* cortical cultures. Repeated administration of LY294002 and rapamycin (daily dosing for 2-4 days) was evaluated in WT cultures, but these chronic regimens led to reduction in cell viability and increased cell death (data not shown). Unfortunately, inhibitor studies in NEX-*Pten* KO cortical cultures were limited to LY294002 and the 15 DIV time point because of sample availability. Future studies with second generation inhibitors that are well tolerated chronically would prove useful in detailing which components of the PI3K/Akt/mTOR pathway are involved in the NEX-*Pten* KO phenotype *in vitro*. In addition, glutamate receptor expression may need to be evaluated at additional time points to determine the exact duration of the modest increases in NR2 subunits seen in NEX-*Pten* KO cultures.

Acknowledgements

I would like to thank Beth Crowell for her assistance in mating NEX-*Pten* mice for these studies.

Chapter 4. Investigation of ionotropic glutamate receptor expression in other *Pten* conditional knockout models

1. Introduction

While NEX-*Pten* KO mice die prematurely, homozygous mutants in other conditional Pten mouse lines survive longer. For example, unlike NEX-*Pten* KO mice, NS-*Pten* KO mice survive into early adulthood. In these animals, Cre expression deletes *Pten* in the majority of hippocampal and cerebellar neurons, as well as some cortical neurons (Kwon et al., 2001; Ljungberg et al., 2009). Thus, NS-*Pten* KO mice provide an opportunity to evaluate how loss of Pten can affect ionotropic glutamate receptor protein expression in early adulthood, when synapses are more mature. However, NS-*Pten* KO mice develop spontaneous seizures by 1-2 months of age. Therefore, because seizure development can alter glutamate receptor function and expression (Meldrum, 1994; Mathern et al., 1997), young NS-*Pten* (2-3 weeks of age) juvenile mice were used to analyze glutamate receptor subunit expression prior to seizure development. Young adult (1-2 months old) NS-*Pten* mice were also used to assess glutamate receptor expression after seizure development. Because the *Cre* reporter in the NS-*Pten* conditional model has greater Cre expression in the hippocampus than cortex, the present studies focused on this region due to greater loss of Pten.

To further investigate the role of Pten in the adult brain, the D'Arcangelo lab recently generated a colony of CaMKIIα-*Pten* mice, a conditional *Pten* knockout line driven by the CamKIIα-*Cre* promoter. The Cre recombinase expression begins approximately around postnatal day 16 (P16) in this model and is restricted primarily to the forebrain, specifically to excitatory neurons (Tsien et al., 1996b; Lan et al., 2007). Therefore, CaMKIIα-*Pten* mice provide an opportunity to analyze the effect of postnatal Pten deficiency on glutamate receptor expression in mature synapses. At time of this writing, a single conditional CaMKIIα-*Pten* KO mouse at 2 months of age was available for Western blot analyses.

2. Materials and Methods

Mice

Conditional NS-*Pten* (Gfap-*Cre*(+);Pten $^{loxP/loxP}$) mice were a gift from Dr. Suzanne Baker (St. Jude Children's Research Hospital, Memphis, TN) and have been previously described (Kwon et al., 2001; Ljungberg et al., 2009). Gfap-*Cre* (+);Pten $^{(+/loxP)}$ (Het) were mated to generate Wt (Gfap-*Cre* (+);Pten $^{(+/+)}$), Het and KO (Gfap-*Cre* (+);Pten $^{(loxP/loxP)}$) experimental animals. For CaMKIIα-*Pten* analyses, CaMKIIα-*Cre* (B6.Cg-Tg(Camk2a-cre)T29-1Stl/J) mice were obtained from The Jackson Laboratory (Bar Harbor, ME; stock number 005359) and crossed with Pten $^{(loxP/loxP)}$ mice to generate CaMKIIα -*Cre*(+/-);Pten $^{+/+}$ (WT), CaMKIIα–*Cre* (+/-);Pten $^{+/loxP}$ (Het) and CaMKIIα –*Cre* (+/-);Pten $^{loxP/loxP}$ (KO) mice. Housing conditions are described in Chapter 2.

Western Blot Analyses of Total Lysate and Crude Synaptosome Preparations

NS-*Pten* Wt, Het and KO hippocampi from littermate pairs were collected at pre-seizure (2-3 weeks) and post-seizure (1-2 months) time points. Cortex and hippocampus were collected from CaMKIIα-*Pten* at 2 months of age. Western blot analyses, lysate and crude synaptosome preparation protocols are described in Chapter 2.

Statistical Analyses

For studies using NS-*Pten* WT, Het and KO mice, a planned comparison Student's t-test evaluated if loss of Pten in NS-*Pten* KO mice resulted in abnormalities compared to NS-*Pten* WT mice ($p<0.05$). Subsequently, to determine if there was an effect of gene dosage, a one-way ANOVA was run with Dunnett's post hoc tests to compare all genotypes (i.e., Het and KO) to WT. Effect size was calculated for NMDA and AMPA receptor subunit results, along with a power analysis (Appendix).

3. Results

Characterization of NS-Pten Mice

Pre-seizure NS-*Pten* KO juvenile mice (2-3 weeks of age; n=3 per genotype) had reduced protein levels of Pten in hippocampal homogenate lysate (0.81 fold of WT) and synaptic fraction (0.82 fold of WT) compared to WT littermates, but these did not reach statistical significance (Figure 23a-c). Despite the modest reduction in Pten levels, further analysis of the PI3K/Akt/mTOR signaling pathway revealed that Akt phosphorylation in NS-*Pten* KO hippocampal homogenate was significantly increased at the Thr308 site compared to WT hippocampal homogenate [$t(4)=3.219$, $p<0.04$] (Figure 23a, b). ANOVA analysis revealed a gene dosage effect on Thr308 Akt phosphorylation levels [$F(2,6)=8.651$, $p<0.02$], with NS-*Pten* KO homogenate having significantly higher levels than WT [Dunnett's post hoc test, $p<0.05$]. There was a marginal effect of genotype on Akt phosphorylation at Ser473 in NS-*Pten* homogenate samples [$F(2,6)=4.004$, $p<0.08$] (Figure 23a, b). In the hippocampal synaptic fraction, both Thr308 and Ser473 phosphorylation levels were significantly increased in NS-*Pten* KO samples [Thr308: $t(4)=3.379$, $p<0.03$; Ser473: $t(4)=2.722$, $p<0.05$] (Figure 23a, c). There was a gene dosage effect on Akt phosphorylation levels at both sites [Thr308: $F(2,6)=6.697$, $p<0.03$; Ser473: $F(2,6)=11.42$, $p<0.01$] (Figure 23a, c). NS-*Pten* KO hippocampal synaptic fraction samples had significantly higher levels of Akt phosphorylation at Thr308 and Ser473 than WT samples [Dunnett's post hoc tests, $ps<0.05$]. Phospho-S6 levels were unchanged in NS-*Pten* KO mice in both the hippocampal homogenate and synaptic fraction compared to WT mice (Figure 23a-c). NR2A, NR2B and NR1 NMDA receptor subunits, as well as GluR1 and GluR2/3 AMPA receptor subunits, were not significantly affected by *Pten* deficiency in NS-*Pten* KO hippocampal homogenate or synaptic fraction (Figure 23d-f).

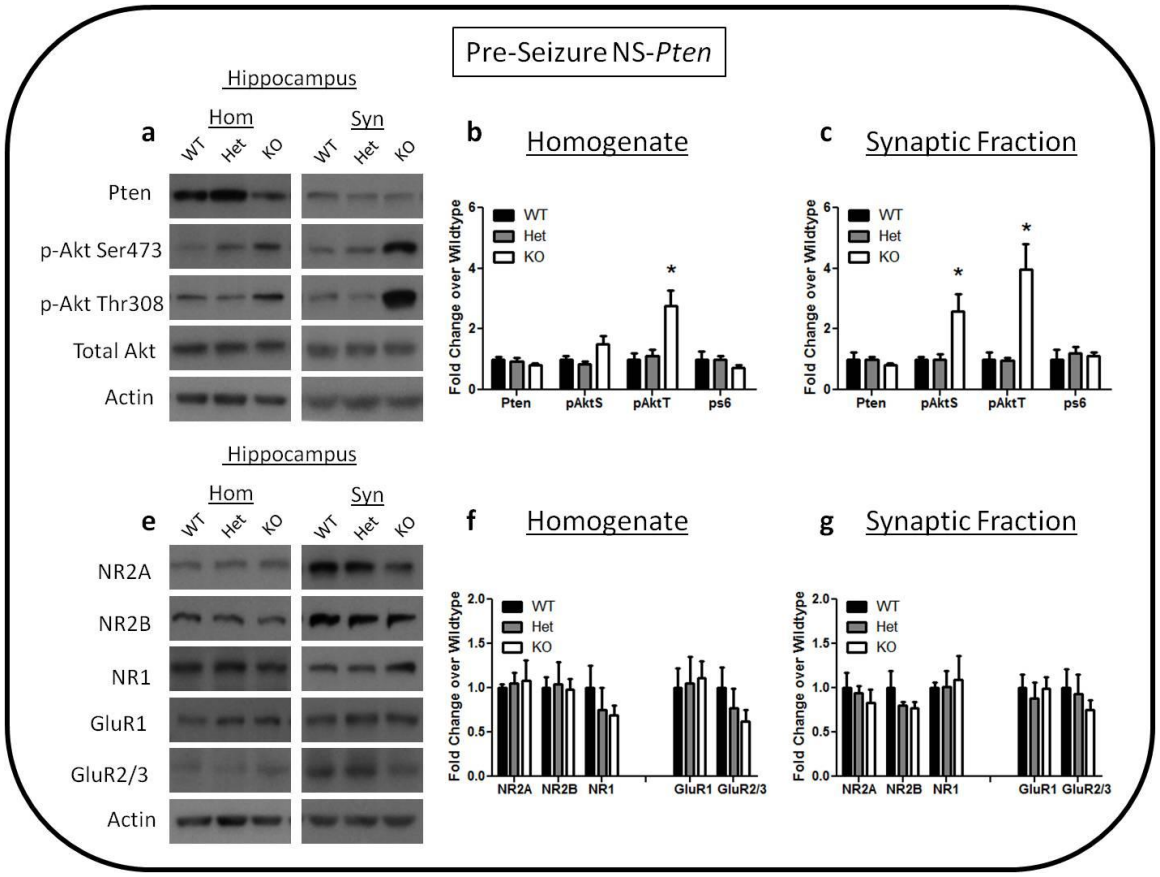

Figure 23. Characterization of PI3K/Akt/mTOR signaling and glutamate receptor expression in the hippocampus of pre-seizure NS-*Pten* heterozygous mice.

Crude synaptosome fractionation was performed on the hippocampus of 2-3 week old NS-*Pten* wildtype (WT), heterozygous (Het) and knockout (KO) mice (n=3-4 per genotype). a) Representative Western blots of Pten, phospho-Akt serine 473 (pAktS), total Akt and actin protein levels in homogenate (Hom) and synaptic fractions (Syn) of pre-seizure NS-*Pten* hippocampus. b) Semi-quantitative Western blot analyses revealed no significant differences in Pten (normalized to actin) or phosphorylation of Akt at serine 473 (normalized to total Akt) or S6 (normalized to actin) between genotypes in hippocampal homogenate. Phosphorylation of Akt at threonine 308 (normalized to total Akt) was significantly increased in hippocampal homogenate of pre-seizure NS-*Pten* KO mice. c) Semi-quantitative Western blot analyses revealed that Pten (normalized to actin) did not differ between genotypes in the hippocampal synaptic fraction of

young NS-*Pten* mice. Akt phosphorylation (normalized to total Akt) was significantly increased in the synaptic fraction of pre-seizure NS-*Pten* hippocampus. e) Representative Western blots of the NDMA receptor subunits NR2A, NR2B and NR1, the AMPA receptor subunits GluR1 and GluR2/3 and actin protein levels in homogenate and synaptic fractions of pre-seizure NS-*Pten* WT, Het and KO hippocampus. f) Semi-quantitative Western blot analyses revealed no significant changes in NR2A, NR2B, NR1, GluR1 or GluR2/3 (normalized to actin) in young NS-*Pten* hippocampal homogenate. g) No significant differences were found in NR2A, NR2B, NR1, GluR1 or GluR2/3 (normalized to actin) in the hippocampal synaptic fraction of young NS-*Pten* mice. *$p<0.05$.

In post-seizure NS-*Pten* KO hippocampus (4-6 weeks of age; n=3-4 per genotype), Pten was significantly reduced in the homogenate fraction (0.54 fold of WT) [$t(4)=11.48$, $p<0.004$], but not the synaptic fraction (0.76 fold of WT), (Figure 24a-c). Hippocampal homogenate from NS-*Pten* KO mice contained significantly higher levels of Akt phosphorylation at Thr308 [$t(5)=2.738$, $p<0.04$] and Ser473 [$t(5)=3.46$, $p<0.02$] compared to WT (Figure 24a, b). There was a gene dosage effect on both Akt phosphorylation sites as well [Thr308: $F(2,7)=7.264$, $p<0.02$; Ser473: $F(2,7)=12.4$, $p<0.006$], with NS-*Pten* KO mice having significantly higher levels of phosphorylation at Thr308 and Ser473 than WT [Dunnett's post hoc tests, $ps<0.05$]. Similarly, NS-*Pten* KO hippocampal synaptic fraction samples had higher levels of Akt phosphorylation at Thr308 [$t(5)=2.910$, $p<0.04$] and Ser473 [$t(5)=3.436$, $p<0.02$] compared to WT synaptic fraction (Figure 24a, c). ANOVA analyses revealed that genotype significantly affected Akt phosphorylation at Thr308 [$F(2,7)=8.598$, $p<0.02$] and Ser473 [$F(2,7)=12.13$, $p<0.006$]. ANOVA analyses revealed that hippocampal synaptic fractions from NS-*Pten* KO mice had significantly higher phosphorylation at both Akt sites compared to WT mice [Dunnett's post hoc tests, $ps<0.05$]. Although not statistically significant, NS-*Pten* KO hippocampal homogenate and

synaptic fraction had higher levels of phospho-S6 than WT controls (homogenate: 2.15 fold higher than WT; synaptic fraction: 2.20 fold higher than WT) (Figure 24a-c). In hippocampal homogenate, there were no significant changes in the NMDA or AMPA receptor subunits between genotypes (Figure 24d-f). In post-seizure NS-*Pten* synaptic fractions, there were also no significant changes in any of the glutamate receptor subunits evaluated, although NR2A levels were lower in NS-*Pten* KO samples compared to WT (0.67 fold lower than WT) (Figure 24d-f).

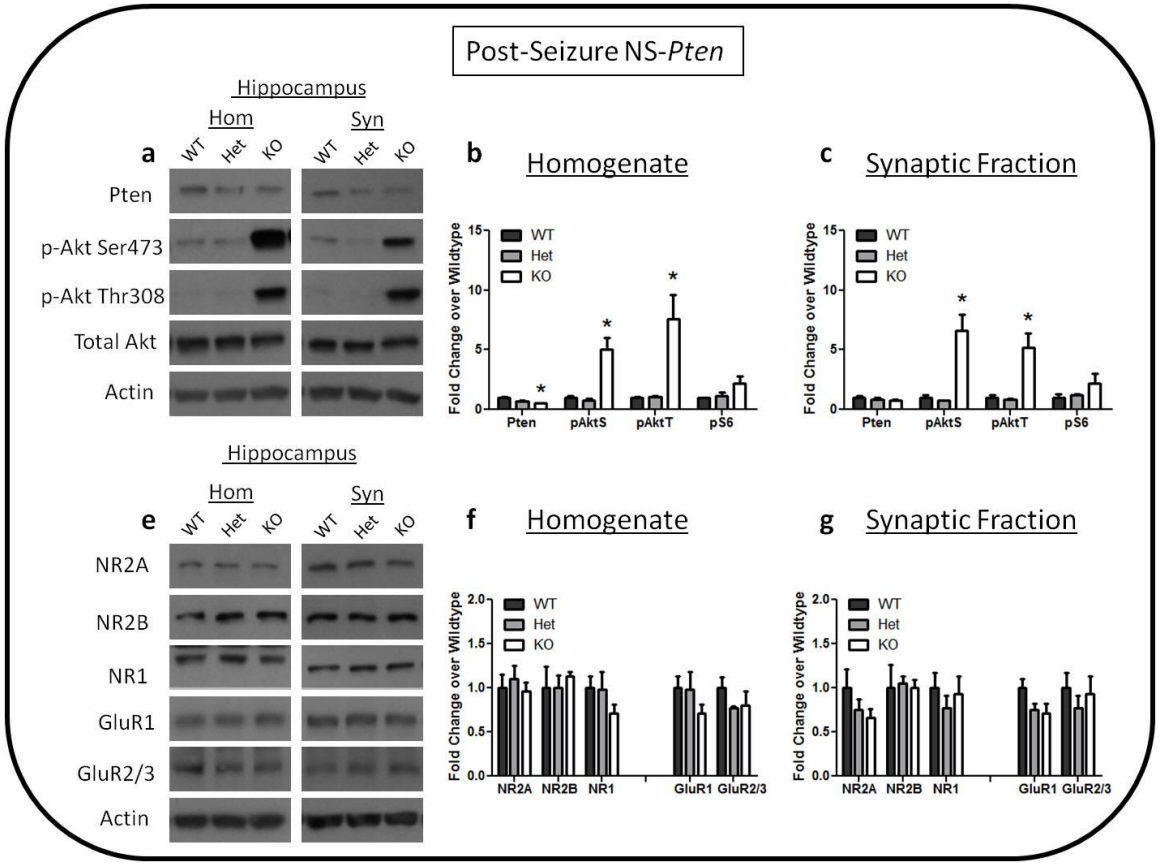

Figure 24. Characterization of PI3K/Akt/mTOR signaling and glutamate receptor expression in the hippocampus of post-seizure NS-*Pten* heterozygous mice.

Crude synaptosome fractionation was performed on the hippocampus of 4-6 week old NS-*Pten* wildtype (WT), heterozygous (Het) and knockout (KO) mice (n=3-4 per genotype). a) Representative Western blots of Pten, phospho-Akt serine 473 (pAktS), total Akt and actin protein levels in homogenate (Hom) and synaptic fractions (Syn) of post-seizure NS-*Pten*

hippocampus. b) Semi-quantitative Western blot analyses revealed that Pten (normalized to actin) was significantly reduced and Akt phosphorylation (normalized to total Akt) was significantly increased in young adult NS-*Pten* KO hippocampal homogenate compared to WT. No changes in phospho-S6 (normalized to actin) were detected. c) Semi-quantitative Western blot analyses revealed that Pten (normalized to actin) did not differ between genotypes in the hippocampal synaptic fraction of young adult NS-*Pten* mice. Akt phosphorylation (normalized to total Akt) was significantly increased in the synaptic fraction of post-seizure NS-*Pten* hippocampus. Phospho-S6 remained unchanged. e) Representative Western blots of the NDMA receptor subunits NR2A, NR2B and NR1, the AMPA receptor subunits GluR1 and GluR2/3 and actin protein levels in homogenate and synaptic fractions of post-seizure NS-*Pten* WT, Het and KO hippocampus. f) Semi-quantitative Western blot analyses revealed no significant changes in NR2A, NR2B, NR1, GluR1 or GluR2/3 (normalized to actin) in young adult NS-*Pten* hippocampal homogenate. g) Although NR2A was lower in NS-*Pten* KO mice, no significant differences were found in NR2A, NR2B, NR1, GluR1 or GluR2/3 (normalized to actin) in the hippocampal synaptic fraction of young adult NS-*Pten* mice. *$p<0.05$.

Characterization of CaMKIIα-Pten Mice

Due to low availability, only one CaMKIIα-*Pten* KO mouse was available at the 2 month time point. Because statistical analyses could not be performed, a semi-arbitrary cutoff of 0.5 or 1.5 fold change from WT was used to indicate a decrease or increase, respectively, from control levels. Pten protein levels were reduced in 2 month old CaMKIIα-*Pten* KO cortex and hippocampus compared to WT controls (Figure 25a-d). Akt phosphorylation at Thr308 and Ser 473 was substantially increased at both phosphorylation sites in 2 month CaMKIIα-*Pten* KO cortex and hippocampus compared to WT littermate (Figure 25a-d). Cortical and hippocampal phospho-S6 were increased in 2 month CaMKIIα-*Pten* KO cortex and hippocampus (Figure 25a-d). In the cortex, NR2A, NR2B and NR1 protein levels were increased in CaMKIIα-*Pten* KO

mice at 2 months, but were unchanged in the hippocampus (Figure 25a, b, e, f). GluR1 and GluR 2/3 protein levels were similar between genotypes in the cortex and hippocampus (Figure 25a, b, e, f).

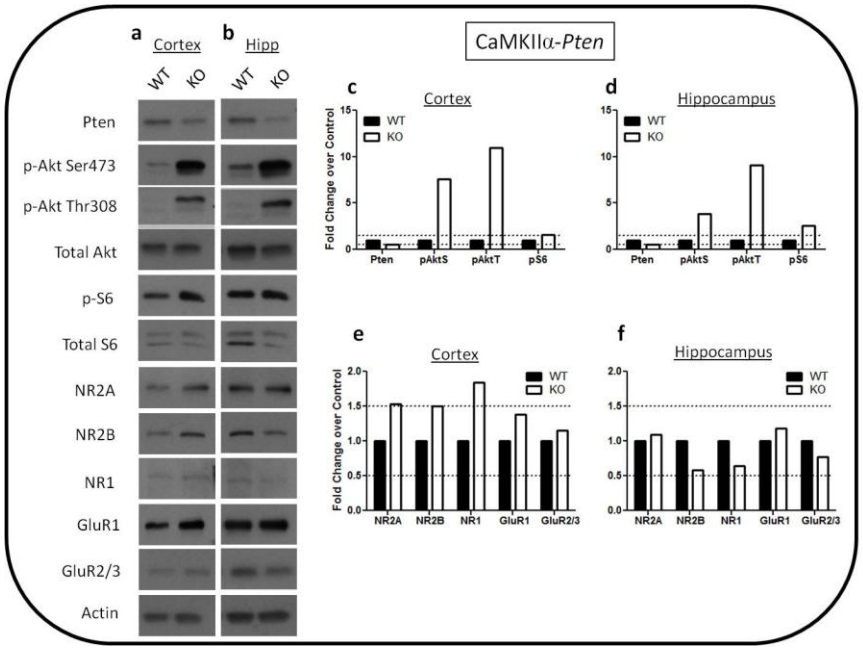

Figure 25. Characterization of PI3K/Akt/mTOR signaling and glutamate receptor expression in 2 month old CaMKIIα-*Pten* mice.

Only 1 CaMKIIα-*Pten* knockout (KO) mouse was available at 2 months of age. Therefore, although Western blots were quantified, no statistical analyses were performed (n=1 per genotype). An arbitrary cut-off of 1.5 fold change compared to control indicated an "increase" in protein levels, while a 0.5 fold change compared to control indicated a "decrease" in protein levels (indicated by the dotted lines on quantification graphs). a-b) Western blots of Pten, phospho-Akt serine 473 (pAktS), total Akt, phospho-S6 serine 235/236 (p-S6), total S6, the NDMA receptor subunits NR2A, NR2B and NR1, the AMPA receptor subunits GluR1 and GluR2/3 and actin protein levels in 2 month old CaMKIIα-*Pten* cortex (a) and hippocampus (b). c-f) Semi-quantitative Western blot analyses of cortex and hippocampus in CaMKIIα-*Pten* mice at 2 months of age. c-d) Pten levels were decreased in 2 month CaMKIIα-*Pten* KO cortex and hippocampus compared to controls. Phosphorylation of Akt and S6 were increased in CaMKIIα-

Pten KO cortex and hippocampus. e-f) At 2 months, NR2A, NR2B levels and NR1 protein levels were increased in the CaMKIIα-*Pten* KO cortex, but not the hippocampus. GluR1 and GluR2/3 were unchanged in the CaMKIIα-*Pten* KO cortex and hippocampus.

---

4. Discussion

NS-*Pten* and CaMKIIα-*Pten* mice were analyzed to determine if loss of Pten in conditional knockout models that survive to adulthood results in altered glutamate receptor subunit protein expression. Previously, Ventruti and colleagues (2011) found dramatically reduced levels of NR2A in adult NS-*Pten* KO hippocampal homogenate and synaptic fractions and NR2A reductions in adult NS-*Pten* Het hippocampal synaptic fractions. However, it is unclear whether the effects on NR2A levels were due to seizure activity or to Pten loss in mutant mice. To address this issue, in the current studies, both juvenile (pre-seizure) and adult (post-seizure) NS-*Pten* mice were utilized, and hippocampal homogenate and synaptic fractions were examined. Levels of Pten appeared to be unchanged in juvenile NS-*Pten* hippocampus, but Akt phosphorylation was increased in these samples, suggesting that even a small change in Pten levels can have dramatic effects on downstream targets. At the pre-seizure time point, no significant changes were found in NMDA or AMPA receptor subunits, although NR2A levels tended to be progressively decreased in the hippocampal synaptic fraction, in partial agreement with previous findings (Ventruti et al., 2011). Moreover, in post-seizure NS-*Pten* KO mice, Pten was significantly reduced and the PI3K/Akt/mTOR pathway was activated, but no significant decreases were detected in NMDA receptor subunits. NR2A levels tended to be progressively lower in NS-*Pten* Het and KO mice in hippocampal synaptic fractions, similar to the pre-seizure time point, but this did not reach significance. Mice from the NS-*Pten* line were on a mixed background, and were mated within the NS-*Pten* colony for many generations. Since these animals were not backcrossed to the original hybrid background strain, it is possible that genetic drift occurred during the period between the Ventruti et al. (2011) studies to the current

experiments (http://jaxmice.jax.org/manual/breeding_strategies_manual.pdf, p8). This could account for the differences seen here and previous reports on NR2A reductions in older NS-*Pten* mice. Although Pten was significantly reduced in post-seizure NS-*Pten* hippocampus in the current set of experiments, KO levels were only ~50% of WT levels, while Het levels were ~70% of WT. In the Ventruti et al. studies, Pten levels in the NS-*Pten* Het hippocampus were much lower (approximately 50% of WT). These differences in Pten reduction support the idea of genetic drift in the NS-*Pten* colony. Although the results reported here are quantitatively different than previous reports (Ventruti et al., 2011), they are qualitatively similar to previous findings.

One of the limitations of the NS-*Pten* mouse is that not all neurons in the NS-*Pten* KO hippocampus lack Pten. Therefore, this model represents more of a chimera of Pten function, rather than a complete reduction. In CaMKIIα-*Pten* mice, *Pten* is present during development and is deleted in most forebrain excitatory neurons beginning around P16, representing a more complete knockout of Pten. Therefore, the promoters in the CaMKIIα-*Pten* and NEX-*Pten* mice both drive *Pten* deletion in the same group of neurons, the forebrain excitatory neurons, but do so at different times (i.e., postnatal vs. embryonic, respectively). Previously characterized CaMKIIα-*Pten* KO mice exhibited deficits in excitatory synaptic transmission and impaired hippocampal-dependent spatial memory (Sperow et al., 2011). Analyses of KO animals from this mutant line are informative, as they could determine if postnatal loss of Pten also results in altered glutamate receptor protein expression. Only one KO sample from the CaMKIIα-*Pten* colony was available for analysis at the 2 month time point at time of this writing. Postnatal *Pten* deletion resulted in upregulation of the PI3K/Akt/mTOR pathway in the 2 month CaMKIIα-*Pten* KO cortex and hippocampus. These increases were accompanied by increases in NR2A, NR2B and NR1 levels in the 2 month CaMKIIα-*Pten* KO cortex, but not the hippocampus. The findings in the adult CaMKIIα-*Pten* KO cortex mirror the NMDA receptor subunit increases found in the early postnatal NEX-*Pten* KO forebrain. Additional animals are required to determine if these data

will be replicated and statistically significant. However, initial analysis of CaMKIIα-*Pten* KO suggests NMDA receptor protein levels are altered in these animals, similar to the NEX-*Pten* KO. It is likely these glutamate receptor increases contribute to the electrophysiological and behavioral abnormalities described by Sperow and colleagues (2011). Results from Chapter 2 demonstrate that developmental loss of Pten alters glutamate receptor protein expression, while the additional analysis of CaMKIIα-*Pten* KO mice reveals that postnatal deletion of *Pten* also alters NMDA receptor subunit levels. Together, these data support a role of Pten as a critical modulator of normal glutamate receptor protein expression. Further studies are required to determine if Pten itself is modulating NMDA receptor subunits, or if these changes are due to increased activity of the PI3K/Akt/mTOR pathway.

Acknowledgements

I would like to thank Ina Nikolaeva for providing the CaMKIIα-*Pten* samples.

Chapter 5. Conclusions and Future Directions

As a critical regulator of the PI3K/Akt/mTOR pathway, the Pten phosphatase is involved in many facets of cellular function, including neuronal development, cell size, dendrite branching, axon formation and synaptic plasticity (van Diepen and Eickholt, 2008). Germline *PTEN* mutations are associated with increased susceptibility to tumor formation, seizure susceptibility, and autism (Zhou and Parada, 2012). Several conditional *Pten* knockout mice have been generated and display morphological and behavioral abnormalities that mirror the phenotypes found in humans who have PTEN mutations (Kwon et al., 2006; Ljungberg et al., 2009; Napoli et al., 2012). The current set of studies sought to extend the literature by focusing on how Pten may be modulating components of synapses that contribute to excitatory activity.

In NEX-*Pten* KO mice, deletion of *Pten* is driven by the NEX-*Cre* promoter in postmitotic excitatory principal neurons in the cortex and hippocampus (Goebbels et al., 2006). Because NEX-*Pten* homozygous mutants die prematurely, biochemical and histological examination of development loss of *Pten* was limited to an early postnatal time point (postnatal day 0 (P0)). Initial characterization of the NEX-*Pten* mouse line revealed that homozygous mutant mice display macrocephaly and neuronal hypertrophy. Cortical layer formation was mostly normal, although there was some distortion in both the cortex and hippocampus, which appear larger and less compact than controls. Proper cortical layer formation requires Reln and Dab1 (Curran and D'Arcangelo, 1998; D'Arcangelo, 2001), and an increased level of Dab1 protein was observed in the NEX-*Pten* KO forebrain, which may contribute to the overmigration seen in some Pten-negative neurons in the cortex.

The progressive loss of Pten in NEX-*Pten* Het and homozygous KO mice was detected at embryonic day 17.5 (E17.5) and immediately after birth (P0), resulting in elevated activity of the PI3K/Akt/mTOR pathway. Specifically, Akt had substantially elevated levels of phosphorylation at serine 473 and threonine 308, sites which are phosphorylated by mTORC2 and PDK1, respectively. In addition, the activity of targets downstream of mTORC1, such as phosphorylated

S6, 4EBP1 and eIF4E, were increased in NEX-*Pten* KO mice compared to WT, suggesting that protein translation and synthesis may be upregulated in the homozygous mutant.

Given that Pten is implicated in seizure activity, ionotropic glutamate receptors were analyzed to determine if developmental loss of *Pten* altered synaptic proteins critical to neurotransmission. In the embryonic brain, there was a tendency for NR2A and NR2B subunits to be increased in NEX-*Pten* KO mice. In early postnatal brain, NEX-*Pten* KO mice had higher protein levels of NR2A, NR2B and NR1 subunits, while NR3A protein levels were decreased. Gene expression analyses revealed that only NR1 mRNA was increased in the cortex of newly born NEX-*Pten* KO mice, while the mRNA of other NMDA receptor subunits was unchanged compared to WT. These data revealed that NR2A and NR2B protein levels begin to rise in the embryonic forebrain of NEX-*Pten* KO mice shortly after *Pten* loss. Because NR1 is required for NR2 release from the ER and functional NMDA receptor formation (Fukaya et al., 2003), the increase in NR1 gene expression may be driven by the rising NR2 protein levels as part of a homeostatic mechanism. Since NR3A levels are unchanged in the embryonic NEX-*Pten* KO forebrain, but are decreased at P0, reduced NR3A protein levels may result from increased NR2 and NR1 protein levels, rather than from Pten loss directly. NR3B protein levels remained unchanged in early postnatal NEX-*Pten* KO mice. Thus, the upregulation of NR2 and NR1 protein subunits are not due to general increases in protein synthesis via mTORC1 activity.

Loss of one *Pten* allele has been previously shown to be insufficient to maintain WT conditions in several instances, such as PHTS and autoimmunity (Di Cristofano et al., 1999; Marsh et al., 1999; Pilarski et al., 2011; Nieuwenhuis et al., 2013). Shortly after birth, NEX-*Pten* Het mice tended to have higher levels of NR2A and NR2B compared to WT mice. To determine if chronic loss of one *Pten* allele would further exacerbate these abnormalities, forebrains of adult NEX-*Pten* WT and Het mice were analyzed. In the cortex, NEX-*Pten* Het mice had reduced Pten levels, and modestly elevated NR2A protein levels. A similar decrease in Pten and increase in NR2A were found in the hippocampus of NEX-*Pten* Het mice. No increases were seen in the

PI3K/Akt/mTOR pathway, as measured by Akt phosphorylation. These data suggest that long term, partial loss of Pten function in adult NEX-*Pten* Het forebrain is not sufficient to substantially elevate the PI3K/Akt/mTOR pathway or alter the protein expression of NMDA receptor subunits (i.e., Pten is haplosufficient).

AMPA receptors have also been implicated in excessive neuronal activity (Dingledine et al., 1990; Babb et al., 1996; Friedman and Veliskova, 1998; Doi et al., 2001; Zaccara et al., 2013). Similar to the results discussed earlier, the present studies revealed an increase in GluR2/3 protein levels in newly born NEX-*Pten* KO mice; GluR1 protein levels remained unchanged. Additionally, gene expression analyses did not detect any differences between genotypes in any of the three AMPA subunits, suggesting protein increases were not due to increased mRNA expression and subsequent protein translation. In the adult NEX-*Pten* Het cortex, GluR2/3 protein levels were reduced, but no changes were detected in hippocampal GluR2/3 levels or GluR1 in either region. Since the antibody used for these studies detects both GluR2 and GluR3, it is unclear if both receptor subunits were increased, decreased or differentially changed by Pten loss. These alterations seen in NEX-*Pten* mice may be due a homeostatic response to altered NMDA receptor levels, since AMPA receptors can accumulate in response to changes in the balance between excitation and inhibition (Turrigiano, 2008). Once activated, NMDA receptors allow calcium into the cell, which participates in many signaling processes critical for synaptic plasticity (i.e., LTP) (Nakazawa et al., 2004; Asrar and Jia, 2013). Levels of GluR2, whose absence confers AMPA receptor calcium permeability, may fluctuate to mitigate the amount of calcium entering the cell via NMDA receptors. Different compositions of AMPA receptor subunits have been reported in response to postsynaptic homeoplasticity-associated changes (e.g., increased GluR1 and GluR2 (O'Brien et al., 1998) vs. increased GluR1 only (Thiagarajan et al., 2005)). Therefore, additional studies with individual antibodies for GluR2 and GluR3 would be useful to determine which AMPA receptor subunits are changing in response to Pten deficiency and if this contributes to the excitatory function of the synapse.

Alterations in excitation/inhibition (E/I) balance in the synapse have been proposed to contribute to some neurodevelopmental disorders, including those that are due to loss of Pten function. For example, children with ASD exhibited increased region-specific elevations in several types of oscillatory activity, suggestive of a neural E/I imbalance, which was correlated with greater symptom severity (Cornew et al., 2012). Abnormal E/I balance has also been found in mouse models of autism, and are associated with autism-relevant behavioral deficits. A mouse lacking 4EBP2, an eIF4E repressor found downstream of mTOR, exhibited increased E/I balance and social interaction deficits, as well as repetitive behaviors and altered ultrasonic vocalizations (Gkogkas et al., 2013). Pharmacological inhibition of eIF4E activity normalized the E/I imbalance and ameliorated social deficits. Yizhar and colleagues (2011) demonstrated that increased cellular E/I balance in the medial prefrontal cortex via optogenetic activation impaired social preference in mice without affecting locomotor activity or anxiety. These impairments in social preference were partially rescued by optogenetic activation of inhibitory tone, suggesting that normalization or balancing of the E/I ratio ameliorates deficits in social dysfunction. Future studies with NEX-*Pten* KO mice are needed to determine if the alterations in ionotropic glutamate receptor protein levels lead to functional changes in synaptic activity, and therefore, E/I balance. Since NEX-*Pten* KO mice do not survive long after birth, *in vitro* evaluation of synaptic activity is possible by culturing NEX-*Pten* cortical neurons and plating them on multi-electrode arrays (MEAs). MEAs allow for the simultaneous recording of large populations of dissociated neurons or organotypic (three dimensional structure) slice cultures as well as the stimulation of excitable cells over periods of time without damaging the neurons' plasma membranes (Spira and Hai, 2013). NEX-*Pten* MEA studies would provide an opportunity to characterize synaptic activity in NEX-*Pten* neurons to determine if the alterations in NMDA and AMPA receptor subunits result in functional changes to neuronal activity.

Rapamycin, the canonical mTORC1 inhibitor, was administered prenatally to pregnant NEX-*Pten* Het mice to determine if NMDA and AMPA receptor abnormalities were due to

mTORC1, but there was not a sufficient therapeutic index due to rapamycin-induced lethality. Therefore, in order to further understand the mechanism behind the glutamate receptor abnormalities in NEX-*Pten* mice, hippocampal and cortical neurons were grown in culture for several weeks to establish an *in vitro* NEX-*Pten* model. NEX-*Pten* KO cortical cultures had larger somas, paralleling *in vivo* findings. Dissociated NEX-*Pten* KO hippocampal neurons also had more extensive dendrite branching, which correlates with the increased MAP2 immunofluorescence staining and protein levels seen in the NEX-*Pten* KO forebrain. Pten was decreased in NEX-Pten KO cortical cultures at mid and late time points, and Akt phosphorylation was increased, demonstrating that in culture, *Pten* deletion had substantial effects on PI3K/Akt/mTOR signaling. NR2A and NR2B were modestly and transiently increased in NEX-*Pten* KO cortical cultures. The selective PI3K inhibitor, LY294002, was used to determine if reduction of PI3K activity could reduce NMDA receptor subunit levels. NR2A levels were significantly reduced in WT cortical cultures at doses that also suppressed Akt phosphorylation. In addition, LY294002 treatment significantly reduced phosphorylation of Akt and S6 in older NEX-*Pten* KO cortical cultures, demonstrating that PI3K hyperactivation can be pharmacologically reduced. Levels of NR2A were also progressively reduced in NEX-*Pten* KO cultures treated with LY294002, indicating PI3K may be contributing to increased levels of NR2A in NEX-*Pten* KO cultures. These data suggest that since NEX-*Pten* KO cortical neurons have modestly increased NR2 subunits for a limited time period around 7 DIV, inhibitor studies should be performed at younger ages. Future pharmacological studies designed to investigate the mechanism behind NMDA receptor abnormalities in NEX-*Pten* cortical cultures should take this into account.

Given the limited therapeutic index of prenatal rapamycin treatment and the transient nature of NMDA receptor subunit increases in the NEX-*Pten* culture model, other conditional knockout mice can provide additional insight into the mechanism behind glutamate receptor abnormalities in NEX-*Pten* KO mice. The hippocampus of NS-*Pten* KO mice represents a

chimera of *Pten* loss, such that not all hippocampal neurons are Pten negative. Further, seizure onset in adult NS-*Pten* KO mice makes the interpretation of any glutamate receptor abnormalities difficult, given that epileptiform activity can alter NMDA and AMPA receptor composition (Dingledine et al., 1990; Meldrum, 1994; Mathern et al., 1997; Doi et al., 2001).

Since *Pten* is deleted during embryonic development in NEX-*Pten* KO mice, CaMKIIα-*Pten* KO mice provide an opportunity to investigate how postnatal deletion of *Pten* may affect glutamate receptor subunit expression. Although only one mutant animal was available for analysis, initial biochemical analyses suggest that NR2A, NR2B and NR1 are upregulated in the cortex, but not the hippocampus, of CaMKIIα-*Pten* KO mice. If these data are replicated with additional CaMKIIα-*Pten* KO samples, they support the idea that loss of *Pten*, either developmentally or postnatally, can alter NMDA receptor subunit composition.

Taken together, this series of studies demonstrate that *in vivo* activation of PI3K though loss of Pten function leads to increased protein expression of several NMDA receptor subunits in cortical neurons. This is further supported by *in vitro* studies which revealed that PI3K inhibition using LY294002 decreased NMDA receptor subunit expression, specifically NR2A. The opposite may be true in the hippocampus, given that *in vivo* NMDA receptor subunit expression was either unchanged or decreased with Pten deficiency. The mechanism behind these alterations in glutamate receptors is still unclear and the role of mTORC1 needs further clarification. Future studies using rapamycin and second generation mTOR inhibitors will provide evidence to determine if Pten affects glutamate receptor subunit expression in a manner that is dependent or independent from the PI3K/Akt/mTOR pathway. Other conditional knockout lines that target the mTOR pathway, such NEX-*Tsc2* KO mice, may also be informative. These results have implications for understanding the mechanism responsible for neural dysfunction and neurodevelopmental disorders associated with *PTEN* mutations and demonstrate promise in identifying novel treatments for these conditions.

Appendix

Effect Size and Power Analysis for NMDA and AMPA Receptor Results

Effect size was calculated for NMDA and AMPA receptor subunit data to measure the magnitude of the effect between WT and KO and WT and Het mice. Effect size can complement the reported inferential statistics (i.e., *p* values). A Cohen's *d* calculation, along with a power analysis, was used to estimate the required sample size for a statistically significant effect, assuming the initial data is representative of the final data set (i.e., similar mean and variability between samples). Cohen's *d* was calculated using the standardized differences between two sample means (e.g., WT and KO):

$$(Mean_1\text{-}Mean_2)/(\text{within-group sample standard deviation})$$

Cohen's *d* was calculated using an effect size calculator, while power analysis was performed using the program G*Power 3.1.6. Effect size was categorized by the following: No Effect (d<0.10), Small (d = 0.10 - 0.49), Medium (d = 0.5 - 0.79) and Large (d>0.8). Therefore, a lower Cohen's *d* value indicated the necessity of larger sample size.

	P0 Forebrain (vs. WT)			
	Effect	*d*	Effect	*d*
NMDAR	KO		Het	
NR2A	Large	1.66	Medium (n=31)	0.73
NR2B	Large	2.59	Large (n=24)	0.84
NR1	Large	3.04	Medium (n=29)	0.75
NR3A	Large	2.98	Large	3.5
NR3B	No effect	0.06	Medium (n=45)	0.60
AMPAR	KO		Het	
GluR1	Small (n=70)	0.48	Small (n=394)	0.20
GluR2/3	Large	3.05	Large	1.08

Appendix Table 1. Effect Size and Power Analyses for NMDA and AMPA Receptor Results in NEX-*Pten* Postnatal Day 0 Forebrain

All comparisons were made between NEX-*Pten* wildtype (WT) samples versus homozygous knockout (KO) or WT versus heterozygous (Het) samples. Green shaded rectangles indicate

significant result by Student's t-test ($p<0.05$). Number in parenthesis indicates required sample size group, as calculated by power analysis. P0 = Postnatal day 0.

	E17.5 Forebrain (vs. WT)			
	Effect	*d*	Effect	*d*
NMDAR	KO		Het	
NR2A	Large (n=5)	3.08	Large (n=17)	1.28
NR2B	Large (n=8)	2.00	Large (n=5)	2.80
NR1	No effect	0.03	Small (n=130)	0.45
NR3A	Small (n=182)	0.38	Large (n=15)	1.38
AMPAR	KO		Het	
GluR1	Large (n=5)	2.63	Large (n=15)	1.41

Appendix Table 2. Effect Size and Power Analyses for NMDA and AMPA Receptor Results in NEX-*Pten* Embryonic Forebrain

All comparisons were made between NEX-*Pten* wildtype (WT) samples versus homozygous knockout (KO) or WT versus heterozygous (Het) samples at embryonic day 17.5 (E17.5). Number in parenthesis indicates required sample size group, as calculated by power analysis.

	Gene Expression (vs. WT)			
	Effect	*d*	Effect	*d*
NMDAR	KO		Het	
Grin2A	Small (n=144)	0.43	Small (n=769)	0.184
Grin2B	Small (n=128)	0.45	Large (n=35)	0.884
Grin1	Large	2.41	No effect	0.04
Grin3A	Small (n=867)	0.17	No effect	0.04
Grin3B	Large (n=11)	1.67	Large (n=14)	1.43
AMPAR	KO		Het	
Gria1	Medium (n=75)	0.59	Large (n=42)	0.80
Gria2	Medium (n=97)	0.52	Large (n=21)	1.16
Gria3	Large (n=28)	0.99	Medium (n=63)	0.65

Appendix Table 3. Effect Size and Power Analyses for NMDA and AMPA Receptor Gene Expression Studies in NEX-*Pten* Postnatal Day 0 Cortex

All comparisons were made between NEX-*Pten* wildtype (WT) samples versus homozygous knockout (KO) or WT versus heterozygous (Het) samples. Green shaded rectangles indicate

significant result by Student's t-test ($p<0.05$). Number in parenthesis indicates required sample size group, as calculated by power analysis.

	NEX-*Pten* Het Cortex (vs. WT)			
	Effect	*d*	Effect	*d*
NMDAR	Homogenate		Synaptic Fraction	
NR2A	Large (n=7)	2.27	Large (n=41)	0.81
NR2B	Large (n=21)	1.54	Large (n=26)	1.04
NR1			Large (n=4)	3.21
AMPAR	Homogenate		Synaptic Fraction	
GluR1	Medium (n=68)	0.62	Large(n=4)	3.80
GluR2/3	Large	14.6	Large(n=26)	1.02

Appendix Table 4. Effect Size and Power Analyses for NMDA and AMPA Receptor Results in Adult NEX-*Pten* Cortex

All comparisons were made between NEX-*Pten* wildtype (WT) samples versus heterozygous (Het) samples. Green shaded rectangles indicate significant result by Student's t-test ($p<0.05$). Number in parenthesis indicates required sample size group, as calculated by power analysis.

	NEX-*Pten* Het Hippocampus (vs. WT)			
	Effect	*d*	Effect	*d*
NMDAR	Homogenate		Synaptic Fraction	
NR2A	Large (n=4)	3.09	Large (n=37)	0.86
NR2B	No effect	0.00	Small (n=290)	0.30
AMPAR	Homogenate		Synaptic Fraction	
GluR1	Large (n=4)	3.67	Small (n=721)	0.19
GluR2/3	Small (n=538)	0.22	Large (n=7)	2.15

Appendix Table 5. Effect Size and Power Analyses for NMDA and AMPA Receptor Results in Adult NEX-*Pten* Hippocampus

All comparisons were made between NEX-*Pten* wildtype (WT) samples versus heterozygous (Het) samples. Number in parenthesis indicates required sample size group, as calculated by power analysis.

	NEX-*Pten* Het 7 DIV Cortical Neurons (vs. WT)			
	Effect	*d*	Effect	*d*
NMDAR	KO		Het	
NR2A	Large (n=4)	3.54	Small (n=240)	0.33
NR2B	Large	5.18	Large (n=8)	2.06
AMPAR	KO		Het	
GluR1	Large (n=22)	1.12	Small (n=290)	0.30
	NEX-*Pten* Het 14 DIV Cortical Neurons (vs. WT)			
	Effect	*d*	Effect	*d*
NMDAR	KO		Het	
NR2A	Large (n=24)	1.09	Medium (n=76)	0.59
NR2B	No effect	0.02	Large (n=8)	1.98
AMPAR	KO		Het	
GluR1	Large (n=8)	2.01	Small (n=202)	0.36

Appendix Table 6. Effect Size and Power Analyses for NMDA and AMPA Receptor Results in NEX-*Pten* Cortical Cultures

All comparisons were made between NEX-*Pten* wildtype (WT) samples versus homozygous knockout (KO) or WT versus heterozygous (Het) samples. Green shaded rectangles indicate significant result by Student's t-test ($p<0.05$). Number in parenthesis indicates required sample size group, as calculated by power analysis. DIV = days *in vitro*.

Bibliography

Abel T, Nguyen PV, Barad M, Deuel TA, Kandel ER, Bourtchouladze R (1997) Genetic demonstration of a role for PKA in the late phase of LTP and in hippocampus-based long-term memory. Cell 88:615-626.

Aizenman CD, Cline HT (2007) Enhanced visual activity in vivo forms nascent synapses in the developing retinotectal projection. Journal of neurophysiology 97:2949-2957.

Al-Hallaq RA, Jarabek BR, Fu Z, Vicini S, Wolfe BB, Yasuda RP (2002) Association of NR3A with the N-methyl-D-aspartate receptor NR1 and NR2 subunits. Molecular pharmacology 62:1119-1127.

Ali IU, Schriml LM, Dean M (1999) Mutational spectra of PTEN/MMAC1 gene: a tumor suppressor with lipid phosphatase activity. Journal of the National Cancer Institute 91:1922-1932.

Anderl S, Freeland M, Kwiatkowski DJ, Goto J (2011) Therapeutic value of prenatal rapamycin treatment in a mouse brain model of tuberous sclerosis complex. Human molecular genetics 20:4597-4604.

Angurana SK, Angurana RS, Panigrahi I, Marwaha RK (2013) Proteus syndrome: Clinical profile of six patients and review of literature. Indian journal of human genetics 19:202-206.

Araghi-Niknam M, Fatemi SH (2003) Levels of Bcl-2 and P53 are altered in superior frontal and cerebellar cortices of autistic subjects. Cellular and molecular neurobiology 23:945-952.

Asrar S, Jia Z (2013) Molecular mechanisms coordinating functional and morphological plasticity at the synapse: role of GluA2/N-cadherin interaction-mediated actin signaling in mGluR-dependent LTD. Cellular signalling 25:397-402.

Babb TL, Mathern GW, Leite JP, Pretorius JK, Yeoman KM, Kuhlman PA (1996) Glutamate AMPA receptors in the fascia dentata of human and kainate rat hippocampal epilepsy. Epilepsy research 26:193-205.

Backman S, Stambolic V, Mak T (2002) PTEN function in mammalian cell size regulation. Current opinion in neurobiology 12:516-522.

Backman SA, Stambolic V, Suzuki A, Haight J, Elia A, Pretorius J, Tsao MS, Shannon P, Bolon B, Ivy GO, Mak TW (2001) Deletion of Pten in mouse brain causes seizures, ataxia and defects in soma size resembling Lhermitte-Duclos disease. Nature genetics 29:396-403.

Bassi C, Ho J, Srikumar T, Dowling RJ, Gorrini C, Miller SJ, Mak TW, Neel BG, Raught B, Stambolic V (2013) Nuclear PTEN controls DNA repair and sensitivity to genotoxic stress. Science (New York, NY 341:395-399.

Boehm J, Kang MG, Johnson RC, Esteban J, Huganir RL, Malinow R (2006) Synaptic incorporation of AMPA receptors during LTP is controlled by a PKC phosphorylation site on GluR1. Neuron 51:213-225.

Butler MG, Dasouki MJ, Zhou XP, Talebizadeh Z, Brown M, Takahashi TN, Miles JH, Wang CH, Stratton R, Pilarski R, Eng C (2005) Subset of individuals with autism spectrum disorders and extreme macrocephaly associated with germline PTEN tumour suppressor gene mutations. Journal of medical genetics 42:318-321.

Buxbaum JD, Cai G, Chaste P, Nygren G, Goldsmith J, Reichert J, Anckarsater H, Rastam M, Smith CJ, Silverman JM, Hollander E, Leboyer M, Gillberg C, Verloes A, Betancur C (2007) Mutation screening of the PTEN gene in patients with autism spectrum disorders and macrocephaly. Am J Med Genet B Neuropsychiatr Genet 144B:484-491.

Cantley LC, Neel BG (1999) New insights into tumor suppression: PTEN suppresses tumor formation by restraining the phosphoinositide 3-kinase/AKT pathway. Proceedings of the National Academy of Sciences of the United States of America 96:4240-4245.

Carlson CJ, Fan Z, Gordon SE, Booth FW (2001) Time course of the MAPK and PI3-kinase response within 24 h of skeletal muscle overload. J Appl Physiol (1985) 91:2079-2087.

Chen C, Tonegawa S (1997) Molecular genetic analysis of synaptic plasticity, activity-dependent neural development, learning, and memory in the mammalian brain. Annual review of neuroscience 20:157-184.

Chen N, Luo T, Raymond LA (1999) Subtype-dependence of NMDA receptor channel open probability. J Neurosci 19:6844-6854.

Chiang GG, Abraham RT (2005) Phosphorylation of mammalian target of rapamycin (mTOR) at Ser-2448 is mediated by p70S6 kinase. The Journal of biological chemistry 280:25485-25490.

Chippagiri P, Banavar Ravi S, Patwa N (2013) Multiple hamartoma syndrome with characteristic oral and cutaneous manifestations. Case reports in dentistry 2013:315109.

Choi YK, Kim CK, Lee H, Jeoung D, Ha KS, Kwon YG, Kim KW, Kim YM (2010) Carbon monoxide promotes VEGF expression by increasing HIF-1alpha protein level via two distinct mechanisms, translational activation and stabilization of HIF-1alpha protein. The Journal of biological chemistry 285:32116-32125.

Chow DK, Groszer M, Pribadi M, Machniki M, Carmichael ST, Liu X, Trachtenberg JT (2009) Laminar and compartmental regulation of dendritic growth in mature cortex. Nature neuroscience 12:116-118.

Chung JH, Ginn-Pease ME, Eng C (2005) Phosphatase and tensin homologue deleted on chromosome 10 (PTEN) has nuclear localization signal-like sequences for nuclear import mediated by major vault protein. Cancer research 65:4108-4116.

Chung JH, Ostrowski MC, Romigh T, Minaguchi T, Waite KA, Eng C (2006) The ERK1/2 pathway modulates nuclear PTEN-mediated cell cycle arrest by cyclin D1 transcriptional regulation. Human molecular genetics 15:2553-2559.

Cline HT, Wu GY, Malinow R (1996) In vivo development of neuronal structure and function. Cold Spring Harbor symposia on quantitative biology 61:95-104.

Cornew L, Roberts TP, Blaskey L, Edgar JC (2012) Resting-state oscillatory activity in autism spectrum disorders. Journal of autism and developmental disorders 42:1884-1894.

Courchesne E (2004) Brain development in autism: early overgrowth followed by premature arrest of growth. Mental retardation and developmental disabilities research reviews 10:106-111.

Courchesne E, Carper R, Akshoomoff N (2003) Evidence of brain overgrowth in the first year of life in autism. Jama 290:337-344.

Crino PB, Miyata H, Vinters HV (2002) Neurodevelopmental disorders as a cause of seizures: neuropathologic, genetic, and mechanistic considerations. Brain pathology (Zurich, Switzerland) 12:212-233.

Cross DA, Alessi DR, Cohen P, Andjelkovich M, Hemmings BA (1995) Inhibition of glycogen synthase kinase-3 by insulin mediated by protein kinase B. Nature 378:785-789.

Curran T, D'Arcangelo G (1998) Role of reelin in the control of brain development. Brain research 26:285-294.

Cybulski N, Hall MN (2009) TOR complex 2: a signaling pathway of its own. Trends in biochemical sciences 34:620-627.

D'Arcangelo G (2001) The role of the Reelin pathway in cortical development. Symposia of the Society for Experimental Biology:59-73.

D'Arcangelo G (2005) The reeler mouse: anatomy of a mutant. International review of neurobiology 71:383-417.

Das S, Sasaki YF, Rothe T, Premkumar LS, Takasu M, Crandall JE, Dikkes P, Conner DA, Rayudu PV, Cheung W, Chen HS, Lipton SA, Nakanishi N (1998) Increased NMDA current and spine density in mice lacking the NMDA receptor subunit NR3A. Nature 393:377-381.

Di Cristofano A, Pesce B, Cordon-Cardo C, Pandolfi PP (1998) Pten is essential for embryonic development and tumour suppression. Nature genetics 19:348-355.

Di Cristofano A, Kotsi P, Peng YF, Cordon-Cardo C, Elkon KB, Pandolfi PP (1999) Impaired Fas response and autoimmunity in Pten+/- mice. Science (New York, NY 285:2122-2125.

Dingledine R, McBain CJ, McNamara JO (1990) Excitatory amino acid receptors in epilepsy. Trends in pharmacological sciences 11:334-338.

Dingledine R, Borges K, Bowie D, Traynelis SF (1999) The glutamate receptor ion channels. Pharmacological reviews 51:7-61.

Doi T, Ueda Y, Tokumaru J, Mitsuyama Y, Willmore LJ (2001) Sequential changes in AMPA and NMDA protein levels during Fe(3+)-induced epileptogenesis. Brain Res Mol Brain Res 92:107-114.

Edinger AL, Linardic CM, Chiang GG, Thompson CB, Abraham RT (2003) Differential effects of rapamycin on mammalian target of rapamycin signaling functions in mammalian cells. Cancer research 63:8451-8460.

Erickson CA, Chambers JE (2006) Memantine for disruptive behavior in autistic disorder. The Journal of clinical psychiatry 67:1000.

Ewald RC CH (2009) NMDA Receptors and Brain Development. In: Biology of the NMDA Receptor (AM VD, ed). Boca Raton (FL): CRC Press.

Fabrichny IP, Leone P, Sulzenbacher G, Comoletti D, Miller MT, Taylor P, Bourne Y, Marchot P (2007) Structural analysis of the synaptic protein neuroligin and its beta-neurexin complex: determinants for folding and cell adhesion. Neuron 56:979-991.

Fidler DJ, Bailey JN, Smalley SL (2000) Macrocephaly in autism and other pervasive developmental disorders. Developmental medicine and child neurology 42:737-740.

Fingar DC, Salama S, Tsou C, Harlow E, Blenis J (2002) Mammalian cell size is controlled by mTOR and its downstream targets S6K1 and 4EBP1/eIF4E. Genes & development 16:1472-1487.

Fraser MM, Bayazitov IT, Zakharenko SS, Baker SJ (2008) Phosphatase and tensin homolog, deleted on chromosome 10 deficiency in brain causes defects in synaptic structure, transmission and plasticity, and myelination abnormalities. Neuroscience 151:476-488.

Friedman LK, Veliskova J (1998) GluR2 hippocampal knockdown reveals developmental regulation of epileptogenicity and neurodegeneration. Brain Res Mol Brain Res 61:224-231.

Fukaya M, Kato A, Lovett C, Tonegawa S, Watanabe M (2003) Retention of NMDA receptor NR2 subunits in the lumen of endoplasmic reticulum in targeted NR1 knockout mice. Proceedings of the National Academy of Sciences of the United States of America 100:4855-4860.

Fukunaga K (1993) [The role of Ca2+/calmodulin-dependent protein kinase II in the cellular signal transduction]. Nihon yakurigaku zasshi 102:355-369.

Fukunaga K, Miyamoto E (1998) Role of MAP kinase in neurons. Molecular neurobiology 16:79-95.

Fukunaga K, Muller D, Miyamoto E (1995) Increased phosphorylation of Ca2+/calmodulin-dependent protein kinase II and its endogenous substrates in the induction of long-term potentiation. The Journal of biological chemistry 270:6119-6124.

Furic L, Rong L, Larsson O, Koumakpayi IH, Yoshida K, Brueschke A, Petroulakis E, Robichaud N, Pollak M, Gaboury LA, Pandolfi PP, Saad F, Sonenberg N (2010) eIF4E phosphorylation promotes tumorigenesis and is associated with prostate cancer progression. Proceedings of the National Academy of Sciences of the United States of America 107:14134-14139.

Georgescu MM, Kirsch KH, Akagi T, Shishido T, Hanafusa H (1999) The tumor-suppressor activity of PTEN is regulated by its carboxyl-terminal region. Proceedings of the National Academy of Sciences of the United States of America 96:10182-10187.

Ghasemi M, Schachter SC (2011) The NMDA receptor complex as a therapeutic target in epilepsy: a review. Epilepsy Behav 22:617-640.

Gingras AC, Kennedy SG, O'Leary MA, Sonenberg N, Hay N (1998) 4E-BP1, a repressor of mRNA translation, is phosphorylated and inactivated by the Akt(PKB) signaling pathway. Genes & development 12:502-513.

Gkogkas CG, Khoutorsky A, Ran I, Rampakakis E, Nevarko T, Weatherill DB, Vasuta C, Yee S, Truitt M, Dallaire P, Major F, Lasko P, Ruggero D, Nader K, Lacaille JC, Sonenberg N (2013) Autism-related deficits via dysregulated eIF4E-dependent translational control. Nature 493:371-377.

Goebbels S, Bormuth I, Bode U, Hermanson O, Schwab MH, Nave KA (2006) Genetic targeting of principal neurons in neocortex and hippocampus of NEX-Cre mice. Genesis 44:611-621.

Goffin A, Hoefsloot LH, Bosgoed E, Swillen A, Fryns JP (2001) PTEN mutation in a family with Cowden syndrome and autism. Am J Med Genet 105:521-524.

Gupta A, Dey CS (2012) PTEN, a widely known negative regulator of insulin/PI3K signaling, positively regulates neuronal insulin resistance. Molecular biology of the cell 23:3882-3898.

Han SY, Kato H, Kato S, Suzuki T, Shibata H, Ishii S, Shiiba K, Matsuno S, Kanamaru R, Ishioka C (2000) Functional evaluation of PTEN missense mutations using in vitro phosphoinositide phosphatase assay. Cancer research 60:3147-3151.

Harding MW, Galat A, Uehling DE, Schreiber SL (1989) A receptor for the immunosuppressant FK506 is a cis-trans peptidyl-prolyl isomerase. Nature 341:758-760.

Hayashi Y, Shi SH, Esteban JA, Piccini A, Poncer JC, Malinow R (2000) Driving AMPA receptors into synapses by LTP and CaMKII: requirement for GluR1 and PDZ domain interaction. Science (New York, NY 287:2262-2267.

Henson MA, Larsen RS, Lawson SN, Perez-Otano I, Nakanishi N, Lipton SA, Philpot BD (2012) Genetic deletion of NR3A accelerates glutamatergic synapse maturation. PloS one 7:e42327.

Herman GE, Butter E, Enrile B, Pastore M, Prior TW, Sommer A (2007) Increasing knowledge of PTEN germline mutations: Two additional patients with autism and macrocephaly. American journal of medical genetics 143:589-593.

Hoeffer CA, Klann E (2010) mTOR signaling: at the crossroads of plasticity, memory and disease. Trends in neurosciences 33:67-75.

Hollmann M, Heinemann S (1994) Cloned glutamate receptors. Annual review of neuroscience 17:31-108.

Holmes GL, Stafstrom CE (2007) Tuberous sclerosis complex and epilepsy: recent developments and future challenges. Epilepsia 48:617-630.

Honore T, Lauridsen J, Krogsgaard-Larsen P (1982) The binding of [3H]AMPA, a structural analogue of glutamic acid, to rat brain membranes. Journal of neurochemistry 38:173-178.

Hopkins BD et al. (2013) A secreted PTEN phosphatase that enters cells to alter signaling and survival. Science (New York, NY 341:399-402.

Hsu PP, Kang SA, Rameseder J, Zhang Y, Ottina KA, Lim D, Peterson TR, Choi Y, Gray NS, Yaffe MB, Marto JA, Sabatini DM (2011) The mTOR-regulated phosphoproteome reveals a mechanism of mTORC1-mediated inhibition of growth factor signaling. Science (New York, NY 332:1317-1322.

Huang W, Zhu PJ, Zhang S, Zhou H, Stoica L, Galiano M, Krnjevic K, Roman G, Costa-Mattioli M (2013) mTORC2 controls actin polymerization required for consolidation of long-term memory. Nature neuroscience 16:441-448.

Huang X, Zhang H, Yang J, Wu J, McMahon J, Lin Y, Cao Z, Gruenthal M, Huang Y (2010) Pharmacological inhibition of the mammalian target of rapamycin pathway suppresses acquired epilepsy. Neurobiology of disease 40:193-199.

Hur EM, Zhou FQ (2010) GSK3 signalling in neural development. Nature reviews 11:539-551.

Jaworski J, Spangler S, Seeburg DP, Hoogenraad CC, Sheng M (2005) Control of dendritic arborization by the phosphoinositide-3'-kinase-Akt-mammalian target of rapamycin pathway. J Neurosci 25:11300-11312.

Jia Z, Lu YM, Agopyan N, Roder J (2001) Gene targeting reveals a role for the glutamate receptors mGluR5 and GluR2 in learning and memory. Physiology & behavior 73:793-802.

Jia Z, Agopyan N, Miu P, Xiong Z, Henderson J, Gerlai R, Taverna FA, Velumian A, MacDonald J, Carlen P, Abramow-Newerly W, Roder J (1996) Enhanced LTP in mice deficient in the AMPA receptor GluR2. Neuron 17:945-956.

Jiang H, Guo W, Liang X, Rao Y (2005) Both the establishment and the maintenance of neuronal polarity require active mechanisms: critical roles of GSK-3beta and its upstream regulators. Cell 120:123-135.

Jonas P, Burnashev N (1995) Molecular mechanisms controlling calcium entry through AMPA-type glutamate receptor channels. Neuron 15:987-990.

Jonas P, Racca C, Sakmann B, Seeburg PH, Monyer H (1994) Differences in Ca2+ permeability of AMPA-type glutamate receptor channels in neocortical neurons caused by differential GluR-B subunit expression. Neuron 12:1281-1289.

Jurado S, Benoist M, Lario A, Knafo S, Petrok CN, Esteban JA (2010) PTEN is recruited to the postsynaptic terminal for NMDA receptor-dependent long-term depression. The EMBO journal 29:2827-2840.

Jyoti A, Sethi P, Sharma D (2009) Curcumin protects against electrobehavioral progression of seizures in the iron-induced experimental model of epileptogenesis. Epilepsy Behav 14:300-308.

Kahan B (1998) A Phase III comparative efficacy trial of rapamune in renal allograft recipients. In: The Transplantation Society XVII World Congress. Montreal, Cnada.

Kazdoba TM, Sunnen CN, Crowell B, Lee GH, Anderson AE, D'Arcangelo G (2012) Development and characterization of NEX- Pten, a novel forebrain excitatory neuron-specific knockout mouse. Developmental neuroscience 34:198-209.

Kemper TL, Bauman ML (1993) The contribution of neuropathologic studies to the understanding of autism. Neurologic clinics 11:175-187.

Kew JN, Richards JG, Mutel V, Kemp JA (1998) Developmental changes in NMDA receptor glycine affinity and ifenprodil sensitivity reveal three distinct populations of NMDA receptors in individual rat cortical neurons. J Neurosci 18:1935-1943.

Kim DH, Sarbassov DD, Ali SM, King JE, Latek RR, Erdjument-Bromage H, Tempst P, Sabatini DM (2002) mTOR interacts with raptor to form a nutrient-sensitive complex that signals to the cell growth machinery. Cell 110:163-175.

Kim DH, Sarbassov DD, Ali SM, Latek RR, Guntur KV, Erdjument-Bromage H, Tempst P, Sabatini DM (2003) GbetaL, a positive regulator of the rapamycin-sensitive pathway required for the nutrient-sensitive interaction between raptor and mTOR. Molecular cell 11:895-904.

Kirson ED, Yaari Y (1996) Synaptic NMDA receptors in developing mouse hippocampal neurones: functional properties and sensitivity to ifenprodil. The Journal of physiology 497 (Pt 2):437-455.

Kumar V, Zhang MX, Swank MW, Kunz J, Wu GY (2005) Regulation of dendritic morphogenesis by Ras-PI3K-Akt-mTOR and Ras-MAPK signaling pathways. J Neurosci 25:11288-11299.

Kwon CH, Zhu X, Zhang J, Baker SJ (2003) mTor is required for hypertrophy of Pten-deficient neuronal soma in vivo. Proceedings of the National Academy of Sciences of the United States of America 100:12923-12928.

Kwon CH, Zhu X, Zhang J, Knoop LL, Tharp R, Smeyne RJ, Eberhart CG, Burger PC, Baker SJ (2001) Pten regulates neuronal soma size: a mouse model of Lhermitte-Duclos disease. Nature genetics 29:404-411.

Kwon CH, Luikart BW, Powell CM, Zhou J, Matheny SA, Zhang W, Li Y, Baker SJ, Parada LF (2006) Pten regulates neuronal arborization and social interaction in mice. Neuron 50:377-388.

Kyosseva SV (2004) Mitogen-activated protein kinase signaling. International review of neurobiology 59:201-220.

Lachyankar MB, Sultana N, Schonhoff CM, Mitra P, Poluha W, Lambert S, Quesenberry PJ, Litofsky NS, Recht LD, Nabi R, Miller SJ, Ohta S, Neel BG, Ross AH (2000) A role for nuclear PTEN in neuronal differentiation. J Neurosci 20:1404-1413.

Lainhart JE, Piven J, Wzorek M, Landa R, Santangelo SL, Coon H, Folstein SE (1997) Macrocephaly in children and adults with autism. Journal of the American Academy of Child and Adolescent Psychiatry 36:282-290.

Lainhart JE et al. (2006) Head circumference and height in autism: a study by the Collaborative Program of Excellence in Autism. American journal of medical genetics 140:2257-2274.

Lan Y, Wang Q, Ovitt CE, Jiang R (2007) A unique mouse strain expressing Cre recombinase for tissue-specific analysis of gene function in palate and kidney development. Genesis 45:618-624.

Larsen RS, Corlew RJ, Henson MA, Roberts AC, Mishina M, Watanabe M, Lipton SA, Nakanishi N, Perez-Otano I, Weinberg RJ, Philpot BD (2011) NR3A-containing NMDARs promote neurotransmitter release and spike timing-dependent plasticity. Nature neuroscience 14:338-344.

Lee HK, Kirkwood A (2011) AMPA receptor regulation during synaptic plasticity in hippocampus and neocortex. Seminars in cell & developmental biology 22:514-520.

Lee JO, Yang H, Georgescu MM, Di Cristofano A, Maehama T, Shi Y, Dixon JE, Pandolfi P, Pavletich NP (1999) Crystal structure of the PTEN tumor suppressor: implications for its phosphoinositide phosphatase activity and membrane association. Cell 99:323-334.

Lerma J, Morales M, Ibarz JM, Somohano F (1994) Rectification properties and Ca2+ permeability of glutamate receptor channels in hippocampal cells. The European journal of neuroscience 6:1080-1088.

Leslie NR, Downes CP (2004) PTEN function: how normal cells control it and tumour cells lose it. The Biochemical journal 382:1-11.

Li BG, Hasselgren PO, Fang CH (2005) Insulin-like growth factor-I inhibits dexamethasone-induced proteolysis in cultured L6 myotubes through PI3K/Akt/GSK-3beta and PI3K/Akt/mTOR-dependent mechanisms. The international journal of biochemistry & cell biology 37:2207-2216.

Li J, Yen C, Liaw D, Podsypanina K, Bose S, Wang SI, Puc J, Miliaresis C, Rodgers L, McCombie R, Bigner SH, Giovanella BC, Ittmann M, Tycko B, Hibshoosh H, Wigler MH, Parsons R (1997) PTEN, a putative protein tyrosine phosphatase gene mutated in human brain, breast, and prostate cancer. Science (New York, NY 275:1943-1947.

Lindsay Y, McCoull D, Davidson L, Leslie NR, Fairservice A, Gray A, Lucocq J, Downes CP (2006) Localization of agonist-sensitive PtdIns(3,4,5)P3 reveals a nuclear pool that is insensitive to PTEN expression. Journal of cell science 119:5160-5168.

Liu JL, Mao Z, LaFortune TA, Alonso MM, Gallick GE, Fueyo J, Yung WK (2007) Cell cycle-dependent nuclear export of phosphatase and tensin homologue tumor suppressor is regulated by the phosphoinositide-3-kinase signaling cascade. Cancer research 67:11054-11063.

Liu K, Lu Y, Lee JK, Samara R, Willenberg R, Sears-Kraxberger I, Tedeschi A, Park KK, Jin D, Cai B, Xu B, Connolly L, Steward O, Zheng B, He Z (2010) PTEN deletion enhances the regenerative ability of adult corticospinal neurons. Nature neuroscience 13:1075-1081.

Liu Y, Zhang J (2000) Recent development in NMDA receptors. Chinese medical journal 113:948-956.

Liu Y, Wang L, Long ZY, Wu YM, Wan Q, Jiang JX, Wang ZG (2013) Inhibiting PTEN protects hippocampal neurons against stretch injury by decreasing membrane translocation of AMPA receptor GluR2 subunit. PloS one 8:e65431.

Ljungberg MC, Sunnen CN, Lugo JN, Anderson AE, D'Arcangelo G (2009) Rapamycin suppresses seizures and neuronal hypertrophy in a mouse model of cortical dysplasia. Disease models & mechanisms 2:389-398.

Low CM, Wee KS (2010) New insights into the not-so-new NR3 subunits of N-methyl-D-aspartate receptor: localization, structure, and function. Molecular pharmacology 78:1-11.

Luikart BW, Schnell E, Washburn EK, Bensen AL, Tovar KR, Westbrook GL (2011) Pten knockdown in vivo increases excitatory drive onto dentate granule cells. J Neurosci 31:4345-4354.

Maccario H, Perera NM, Davidson L, Downes CP, Leslie NR (2007) PTEN is destabilized by phosphorylation on Thr366. The Biochemical journal 405:439-444.

MacDonald A (1998) A randomised, placebo-controlled trial of rapamune in primary renal allograft recipients. In: The Transplantation Society XVII World Congress. Montreal, Canada.

Maehama T, Dixon JE (1998) The tumor suppressor, PTEN/MMAC1, dephosphorylates the lipid second messenger, phosphatidylinositol 3,4,5-trisphosphate. The Journal of biological chemistry 273:13375-13378.

Maier D, Jones G, Li X, Schonthal AH, Gratzl O, Van Meir EG, Merlo A (1999) The PTEN lipid phosphatase domain is not required to inhibit invasion of glioma cells. Cancer research 59:5479-5482.

Malinow R, Malenka RC (2002) AMPA receptor trafficking and synaptic plasticity. Annual review of neuroscience 25:103-126.

Manning BD, Cantley LC (2007) AKT/PKB signaling: navigating downstream. Cell 129:1261-1274.

Maren S, Baudry M (1995) Properties and mechanisms of long-term synaptic plasticity in the mammalian brain: relationships to learning and memory. Neurobiology of learning and memory 63:1-18.

Marsh DJ et al. (1999) PTEN mutation spectrum and genotype-phenotype correlations in Bannayan-Riley-Ruvalcaba syndrome suggest a single entity with Cowden syndrome. Human molecular genetics 8:1461-1472.

Mathern GW, Pretorius JK, Kornblum HI, Mendoza D, Lozada A, Leite JP, Chimelli LM, Fried I, Sakamoto AC, Assirati JA, Levesque MF, Adelson PD, Peacock WJ (1997) Human

hippocampal AMPA and NMDA mRNA levels in temporal lobe epilepsy patients. Brain 120 (Pt 11):1937-1959.

McBain CJ, Mayer ML (1994) N-methyl-D-aspartic acid receptor structure and function. Physiological reviews 74:723-760.

McBride KL, Varga EA, Pastore MT, Prior TW, Manickam K, Atkin JF, Herman GE (2010) Confirmation study of PTEN mutations among individuals with autism or developmental delays/mental retardation and macrocephaly. Autism Res 3:137-141.

Mebratu Y, Tesfaigzi Y (2009) How ERK1/2 activation controls cell proliferation and cell death: Is subcellular localization the answer? Cell cycle (Georgetown, Tex 8:1168-1175.

Mehta MV, Gandal MJ, Siegel SJ (2011) mGluR5-antagonist mediated reversal of elevated stereotyped, repetitive behaviors in the VPA model of autism. PloS one 6:e26077.

Meikle L, Pollizzi K, Egnor A, Kramvis I, Lane H, Sahin M, Kwiatkowski DJ (2008) Response of a neuronal model of tuberous sclerosis to mammalian target of rapamycin (mTOR) inhibitors: effects on mTORC1 and Akt signaling lead to improved survival and function. J Neurosci 28:5422-5432.

Meikle L, Talos DM, Onda H, Pollizzi K, Rotenberg A, Sahin M, Jensen FE, Kwiatkowski DJ (2007) A mouse model of tuberous sclerosis: neuronal loss of Tsc1 causes dysplastic and ectopic neurons, reduced myelination, seizure activity, and limited survival. J Neurosci 27:5546-5558.

Meldrum BS (1994) The role of glutamate in epilepsy and other CNS disorders. Neurology 44:S14-23.

Meng Y, Zhang Y, Jia Z (2003) Synaptic transmission and plasticity in the absence of AMPA glutamate receptor GluR2 and GluR3. Neuron 39:163-176.

Mohamad O, Song M, Wei L, Yu SP (2013) Regulatory roles of the NMDA receptor GluN3A subunit in locomotion, pain perception and cognitive functions in adult mice. The Journal of physiology 591:149-168.

Monyer H, Burnashev N, Laurie DJ, Sakmann B, Seeburg PH (1994) Developmental and regional expression in the rat brain and functional properties of four NMDA receptors. Neuron 12:529-540.

Moult PR, Cross A, Santos SD, Carvalho AL, Lindsay Y, Connolly CN, Irving AJ, Leslie NR, Harvey J (2010) Leptin regulates AMPA receptor trafficking via PTEN inhibition. J Neurosci 30:4088-4101.

Nakazawa K, McHugh TJ, Wilson MA, Tonegawa S (2004) NMDA receptors, place cells and hippocampal spatial memory. Nature reviews 5:361-372.

Napoli E, Ross-Inta C, Wong S, Hung C, Fujisawa Y, Sakaguchi D, Angelastro J, Omanska-Klusek A, Schoenfeld R, Giulivi C (2012) Mitochondrial dysfunction in Pten haplo-insufficient mice with social deficits and repetitive behavior: interplay between Pten and p53. PloS one 7:e42504.

Nave BT, Ouwens M, Withers DJ, Alessi DR, Shepherd PR (1999) Mammalian target of rapamycin is a direct target for protein kinase B: identification of a convergence point for opposing effects of insulin and amino-acid deficiency on protein translation. The Biochemical journal 344 Pt 2:427-431.

Niederhofer H (2007) Glutamate antagonists seem to be slightly effective in psychopharmacologic treatment of autism. Journal of clinical psychopharmacology 27:317-318.

Nieuwenhuis MH, Kets CM, Murphy-Ryan M, Yntema HG, Evans DG, Colas C, Moller P, Hes FJ, Hodgson SV, Olderode-Berends MJ, Aretz S, Heinimann K, Gomez Garcia EB, Douglas F, Spigelman A, Timshel S, Lindor NM, Vasen HF (2013) Cancer risk and genotype-phenotype correlations in PTEN hamartoma tumor syndrome. Familial cancer.

Ning K, Pei L, Liao M, Liu B, Zhang Y, Jiang W, Mielke JG, Li L, Chen Y, El-Hayek YH, Fehlings MG, Zhang X, Liu F, Eubanks J, Wan Q (2004) Dual neuroprotective signaling mediated by downregulating two distinct phosphatase activities of PTEN. J Neurosci 24:4052-4060.

Nishi M, Hinds H, Lu HP, Kawata M, Hayashi Y (2001) Motoneuron-specific expression of NR3B, a novel NMDA-type glutamate receptor subunit that works in a dominant-negative manner. J Neurosci 21:RC185.

O'Brien RJ, Kamboj S, Ehlers MD, Rosen KR, Fischbach GD, Huganir RL (1998) Activity-dependent modulation of synaptic AMPA receptor accumulation. Neuron 21:1067-1078.

Pachernegg S, Strutz-Seebohm N, Hollmann M (2012) GluN3 subunit-containing NMDA receptors: not just one-trick ponies. Trends in neurosciences.

Pachernegg S S-SN, Hollmann M (2011) GluN3 subunit-containing NMDA receptors: not just one trick ponies. Trends Neurosci.

Parisi MA, Dinulos MB, Leppig KA, Sybert VP, Eng C, Hudgins L (2001) The spectrum and evolution of phenotypic findings in PTEN mutation positive cases of Bannayan-Riley-Ruvalcaba syndrome. Journal of medical genetics 38:52-58.

Pause A, Belsham GJ, Gingras AC, Donze O, Lin TA, Lawrence JC, Jr., Sonenberg N (1994) Insulin-dependent stimulation of protein synthesis by phosphorylation of a regulator of 5'-cap function. Nature 371:762-767.

Petralia RS, Wenthold RJ (1992) Light and electron immunocytochemical localization of AMPA-selective glutamate receptors in the rat brain. The Journal of comparative neurology 318:329-354.

Pfaffl MW (2001) A new mathematical model for relative quantification in real-time RT-PCR. Nucleic acids research 29:e45.

Pilarski R (2009) Cowden syndrome: a critical review of the clinical literature. Journal of genetic counseling 18:13-27.

Pilarski R, Stephens JA, Noss R, Fisher JL, Prior TW (2011) Predicting PTEN mutations: an evaluation of Cowden syndrome and Bannayan-Riley-Ruvalcaba syndrome clinical features. Journal of medical genetics 48:505-512.

Plyte SE, Hughes K, Nikolakaki E, Pulverer BJ, Woodgett JR (1992) Glycogen synthase kinase-3: functions in oncogenesis and development. Biochimica et biophysica acta 1114:147-162.

Podsypanina K, Ellenson LH, Nemes A, Gu J, Tamura M, Yamada KM, Cordon-Cardo C, Catoretti G, Fisher PE, Parsons R (1999) Mutation of Pten/Mmac1 in mice causes neoplasia in multiple organ systems. Proceedings of the National Academy of Sciences of the United States of America 96:1563-1568.

Radu A, Neubauer V, Akagi T, Hanafusa H, Georgescu MM (2003) PTEN induces cell cycle arrest by decreasing the level and nuclear localization of cyclin D1. Molecular and cellular biology 23:6139-6149.

Redfern RE, Daou MC, Li L, Munson M, Gericke A, Ross AH (2010) A mutant form of PTEN linked to autism. Protein Sci 19:1948-1956.

Rembach A, Turner BJ, Bruce S, Cheah IK, Scott RL, Lopes EC, Zagami CJ, Beart PM, Cheung NS, Langford SJ, Cheema SS (2004) Antisense peptide nucleic acid targeting GluR3 delays disease onset and progression in the SOD1 G93A mouse model of familial ALS. Journal of neuroscience research 77:573-582.

Richter JD, Sonenberg N (2005) Regulation of cap-dependent translation by eIF4E inhibitory proteins. Nature 433:477-480.

Rinaldi T, Kulangara K, Antoniello K, Markram H (2007) Elevated NMDA receptor levels and enhanced postsynaptic long-term potentiation induced by prenatal exposure to valproic acid. Proceedings of the National Academy of Sciences of the United States of America 104:13501-13506.

Roberts AC, Diez-Garcia J, Rodriguiz RM, Lopez IP, Lujan R, Martinez-Turrillas R, Pico E, Henson MA, Bernardo DR, Jarrett TM, Clendeninn DJ, Lopez-Mascaraque L, Feng G, Lo DC, Wesseling JF, Wetsel WC, Philpot BD, Perez-Otano I (2009) Downregulation of NR3A-

containing NMDARs is required for synapse maturation and memory consolidation. Neuron 63:342-356.

Roux PP, Blenis J (2004) ERK and p38 MAPK-activated protein kinases: a family of protein kinases with diverse biological functions. Microbiol Mol Biol Rev 68:320-344.

Saal LH et al. (2008) Recurrent gross mutations of the PTEN tumor suppressor gene in breast cancers with deficient DSB repair. Nature genetics 40:102-107.

Salmena L, Carracedo A, Pandolfi PP (2008) Tenets of PTEN tumor suppression. Cell 133:403-414.

Sarbassov DD, Guertin DA, Ali SM, Sabatini DM (2005) Phosphorylation and regulation of Akt/PKB by the rictor-mTOR complex. Science (New York, NY 307:1098-1101.

Sato T, Umetsu A, Tamanoi F (2008) Characterization of the Rheb-mTOR signaling pathway in mammalian cells: constitutive active mutants of Rheb and mTOR. Methods in enzymology 438:307-320.

Sauer B, Henderson N (1988) Site-specific DNA recombination in mammalian cells by the Cre recombinase of bacteriophage P1. Proceedings of the National Academy of Sciences of the United States of America 85:5166-5170.

Sheng M, Cummings J, Roldan LA, Jan YN, Jan LY (1994) Changing subunit composition of heteromeric NMDA receptors during development of rat cortex. Nature 368:144-147.

Shinohe A, Hashimoto K, Nakamura K, Tsujii M, Iwata Y, Tsuchiya KJ, Sekine Y, Suda S, Suzuki K, Sugihara G, Matsuzaki H, Minabe Y, Sugiyama T, Kawai M, Iyo M, Takei N, Mori N (2006) Increased serum levels of glutamate in adult patients with autism. Progress in neuro-psychopharmacology & biological psychiatry 30:1472-1477.

Shveygert M, Kaiser C, Bradrick SS, Gromeier M (2010) Regulation of eukaryotic initiation factor 4E (eIF4E) phosphorylation by mitogen-activated protein kinase occurs through modulation of Mnk1-eIF4G interaction. Molecular and cellular biology 30:5160-5167.

Siekierka JJ, Hung SH, Poe M, Lin CS, Sigal NH (1989) A cytosolic binding protein for the immunosuppressant FK506 has peptidyl-prolyl isomerase activity but is distinct from cyclophilin. Nature 341:755-757.

Silverman JL, Tolu SS, Barkan CL, Crawley JN (2010) Repetitive self-grooming behavior in the BTBR mouse model of autism is blocked by the mGluR5 antagonist MPEP. Neuropsychopharmacology 35:976-989.

Sommer B, Keinanen K, Verdoorn TA, Wisden W, Burnashev N, Herb A, Kohler M, Takagi T, Sakmann B, Seeburg PH (1990) Flip and flop: a cell-specific functional switch in glutamate-operated channels of the CNS. Science (New York, NY 249:1580-1585.

Sperow M, Berry RB, Bayazitov IT, Zhu G, Baker SJ, Zakharenko SS (2011) Phosphatase and tensin homologue (PTEN) regulates synaptic plasticity independently of its effect on neuronal morphology and migration. The Journal of physiology 590:777-792.

Spira ME, Hai A (2013) Multi-electrode array technologies for neuroscience and cardiology. Nature nanotechnology 8:83-94.

Stambolic V, Suzuki A, de la Pompa JL, Brothers GM, Mirtsos C, Sasaki T, Ruland J, Penninger JM, Siderovski DP, Mak TW (1998) Negative regulation of PKB/Akt-dependent cell survival by the tumor suppressor PTEN. Cell 95:29-39.

Steck PA, Pershouse MA, Jasser SA, Yung WK, Lin H, Ligon AH, Langford LA, Baumgard ML, Hattier T, Davis T, Frye C, Hu R, Swedlund B, Teng DH, Tavtigian SV (1997) Identification of a candidate tumour suppressor gene, MMAC1, at chromosome 10q23.3 that is mutated in multiple advanced cancers. Nature genetics 15:356-362.

Stocca G, Vicini S (1998) Increased contribution of NR2A subunit to synaptic NMDA receptors in developing rat cortical neurons. The Journal of physiology 507 (Pt 1):13-24.

Sucher NJ, Yu E, Chan SF, Miri M, Lee BJ, Xiao B, Worley PF, Jensen FE (2010) Association of the small GTPase Rheb with the NMDA receptor subunit NR3A. Neuro-Signals 18:203-209.

Sucher NJ, Akbarian S, Chi CL, Leclerc CL, Awobuluyi M, Deitcher DL, Wu MK, Yuan JP, Jones EG, Lipton SA (1995) Developmental and regional expression pattern of a novel NMDA receptor-like subunit (NMDAR-L) in the rodent brain. J Neurosci 15:6509-6520.

Sun H, Lesche R, Li DM, Liliental J, Zhang H, Gao J, Gavrilova N, Mueller B, Liu X, Wu H (1999) PTEN modulates cell cycle progression and cell survival by regulating phosphatidylinositol 3,4,5,-trisphosphate and Akt/protein kinase B signaling pathway. Proceedings of the National Academy of Sciences of the United States of America 96:6199-6204.

Sun L, Margolis FL, Shipley MT, Lidow MS (1998) Identification of a long variant of mRNA encoding the NR3 subunit of the NMDA receptor: its regional distribution and developmental expression in the rat brain. FEBS letters 441:392-396.

Sun SY, Rosenberg LM, Wang X, Zhou Z, Yue P, Fu H, Khuri FR (2005) Activation of Akt and eIF4E survival pathways by rapamycin-mediated mammalian target of rapamycin inhibition. Cancer research 65:7052-7058.

Tamura M, Gu J, Matsumoto K, Aota S, Parsons R, Yamada KM (1998) Inhibition of cell migration, spreading, and focal adhesions by tumor suppressor PTEN. Science (New York, NY 280:1614-1617.

Tavazoie SF, Alvarez VA, Ridenour DA, Kwiatkowski DJ, Sabatini BL (2005) Regulation of neuronal morphology and function by the tumor suppressors Tsc1 and Tsc2. Nature neuroscience 8:1727-1734.

Thiagarajan TC, Lindskog M, Tsien RW (2005) Adaptation to synaptic inactivity in hippocampal neurons. Neuron 47:725-737.

Torres J, Pulido R (2001) The tumor suppressor PTEN is phosphorylated by the protein kinase CK2 at its C terminus. Implications for PTEN stability to proteasome-mediated degradation. The Journal of biological chemistry 276:993-998.

Tovar KR, Westbrook GL (1999) The incorporation of NMDA receptors with a distinct subunit composition at nascent hippocampal synapses in vitro. J Neurosci 19:4180-4188.

Trotman LC, Wang X, Alimonti A, Chen Z, Teruya-Feldstein J, Yang H, Pavletich NP, Carver BS, Cordon-Cardo C, Erdjument-Bromage H, Tempst P, Chi SG, Kim HJ, Misteli T, Jiang X, Pandolfi PP (2007) Ubiquitination regulates PTEN nuclear import and tumor suppression. Cell 128:141-156.

Tsien JZ, Huerta PT, Tonegawa S (1996a) The essential role of hippocampal CA1 NMDA receptor-dependent synaptic plasticity in spatial memory. Cell 87:1327-1338.

Tsien JZ, Chen DF, Gerber D, Tom C, Mercer EH, Anderson DJ, Mayford M, Kandel ER, Tonegawa S (1996b) Subregion- and cell type-restricted gene knockout in mouse brain. Cell 87:1317-1326.

Turrigiano G (2008) Homeostatic Synaptic Plasticity. In: Structural and Functional Organization of the Synapse (Hell JW, Ehlers MD, eds), pp 535-552: Springer Science+Business Media LLC.

van Diepen MT, Eickholt BJ (2008) Function of PTEN during the formation and maintenance of neuronal circuits in the brain. Developmental neuroscience 30:59-64.

Varnai P, Bondeva T, Tamas P, Toth B, Buday L, Hunyady L, Balla T (2005) Selective cellular effects of overexpressed pleckstrin-homology domains that recognize PtdIns(3,4,5)P3 suggest their interaction with protein binding partners. Journal of cell science 118:4879-4888.

Vazquez F, Ramaswamy S, Nakamura N, Sellers WR (2000) Phosphorylation of the PTEN tail regulates protein stability and function. Molecular and cellular biology 20:5010-5018.

Vazquez F, Grossman SR, Takahashi Y, Rokas MV, Nakamura N, Sellers WR (2001) Phosphorylation of the PTEN tail acts as an inhibitory switch by preventing its recruitment into a protein complex. The Journal of biological chemistry 276:48627-48630.

Ventruti A, Kazdoba TM, Niu S, D'Arcangelo G (2011) Reelin deficiency causes specific defects in the molecular composition of the synapses in the adult brain. Neuroscience 189:32-42.

Vicini S, Wang JF, Li JH, Zhu WJ, Wang YH, Luo JH, Wolfe BB, Grayson DR (1998) Functional and pharmacological differences between recombinant N-methyl-D-aspartate receptors. Journal of neurophysiology 79:555-566.

Vlahos CJ, Matter WF, Hui KY, Brown RF (1994) A specific inhibitor of phosphatidylinositol 3-kinase, 2-(4-morpholinyl)-8-phenyl-4H-1-benzopyran-4-one (LY294002). The Journal of biological chemistry 269:5241-5248.

Waite KA, Eng C (2002) Protean PTEN: form and function. American journal of human genetics 70:829-844.

Wan X, Harkavy B, Shen N, Grohar P, Helman LJ (2007) Rapamycin induces feedback activation of Akt signaling through an IGF-1R-dependent mechanism. Oncogene 26:1932-1940.

Wang L, Harris TE, Roth RA, Lawrence JC, Jr. (2007) PRAS40 regulates mTORC1 kinase activity by functioning as a direct inhibitor of substrate binding. The Journal of biological chemistry 282:20036-20044.

Wang SJ, Gu W (2013) To be, or not to be: functional dilemma of p53 metabolic regulation. Current opinion in oncology.

Wee KS, Zhang Y, Khanna S, Low CM (2008) Immunolocalization of NMDA receptor subunit NR3B in selected structures in the rat forebrain, cerebellum, and lumbar spinal cord. The Journal of comparative neurology 509:118-135.

Welsh GI, Wilson C, Proud CG (1996) GSK3: a SHAGGY frog story. Trends in cell biology 6:274-279.

Weng LP, Smith WM, Brown JL, Eng C (2001) PTEN inhibits insulin-stimulated MEK/MAPK activation and cell growth by blocking IRS-1 phosphorylation and IRS-1/Grb-2/Sos complex formation in a breast cancer model. Human molecular genetics 10:605-616.

Weng QP, Kozlowski M, Belham C, Zhang A, Comb MJ, Avruch J (1998) Regulation of the p70 S6 kinase by phosphorylation in vivo. Analysis using site-specific anti-phosphopeptide antibodies. The Journal of biological chemistry 273:16621-16629.

Wenthold RJ, Petralia RS, Blahos J, II, Niedzielski AS (1996) Evidence for multiple AMPA receptor complexes in hippocampal CA1/CA2 neurons. J Neurosci 16:1982-1989.

Williams K, Russell SL, Shen YM, Molinoff PB (1993) Developmental switch in the expression of NMDA receptors occurs in vivo and in vitro. Neuron 10:267-278.

Winter JN, Jefferson LS, Kimball SR (2011) ERK and Akt signaling pathways function through parallel mechanisms to promote mTORC1 signaling. American journal of physiology 300:C1172-1180.

Yamauchi T (2005) Neuronal Ca2+/calmodulin-dependent protein kinase II--discovery, progress in a quarter of a century, and perspective: implication for learning and memory. Biological & pharmaceutical bulletin 28:1342-1354.

Yang Q, Guan KL (2007) Expanding mTOR signaling. Cell research 17:666-681.

Ye Q, Cai W, Zheng Y, Evers BM, She QB (2013) ERK and AKT signaling cooperate to translationally regulate survivin expression for metastatic progression of colorectal cancer. Oncogene.

Yizhar O, Fenno LE, Prigge M, Schneider F, Davidson TJ, O'Shea DJ, Sohal VS, Goshen I, Finkelstein J, Paz JT, Stehfest K, Fudim R, Ramakrishnan C, Huguenard JR, Hegemann P, Deisseroth K (2011) Neocortical excitation/inhibition balance in information processing and social dysfunction. Nature 477:171-178.

Yu SP, Yeh C, Strasser U, Tian M, Choi DW (1999) NMDA receptor-mediated K+ efflux and neuronal apoptosis. Science (New York, NY 284:336-339.

Yu Y, Yoon SO, Poulogiannis G, Yang Q, Ma XM, Villen J, Kubica N, Hoffman GR, Cantley LC, Gygi SP, Blenis J (2011) Phosphoproteomic analysis identifies Grb10 as an mTORC1 substrate that negatively regulates insulin signaling. Science (New York, NY 332:1322-1326.

Zaccara G, Giovannelli F, Cincotta M, Iudice A (2013) AMPA receptor inhibitors for the treatment of epilepsy: the role of perampanel. Expert review of neurotherapeutics 13:647-655.

Zeng LH, Rensing NR, Wong M (2009) The mammalian target of rapamycin signaling pathway mediates epileptogenesis in a model of temporal lobe epilepsy. J Neurosci 29:6964-6972.

Zeng LH, Xu L, Gutmann DH, Wong M (2008) Rapamycin prevents epilepsy in a mouse model of tuberous sclerosis complex. Annals of neurology 63:444-453.

Zhang YJ, Duan Y, Zheng XF (2011) Targeting the mTOR kinase domain: the second generation of mTOR inhibitors. Drug discovery today 16:325-331.

Zheng XF, Florentino D, Chen J, Crabtree GR, Schreiber SL (1995) TOR kinase domains are required for two distinct functions, only one of which is inhibited by rapamycin. Cell 82:121-130.

Zhou H, Huang S (2010) The complexes of mammalian target of rapamycin. Current protein & peptide science 11:409-424.

Zhou J, Parada LF (2012) PTEN signaling in autism spectrum disorders. Current opinion in neurobiology 22:873-879.

Zhou J, Blundell J, Ogawa S, Kwon CH, Zhang W, Sinton C, Powell CM, Parada LF (2009) Pharmacological inhibition of mTORC1 suppresses anatomical, cellular, and behavioral abnormalities in neural-specific Pten knock-out mice. J Neurosci 29:1773-1783.

Zhu JJ, Esteban JA, Hayashi Y, Malinow R (2000) Postnatal synaptic potentiation: delivery of GluR4-containing AMPA receptors by spontaneous activity. Nature neuroscience 3:1098-1106.

Zori RT, Marsh DJ, Graham GE, Marliss EB, Eng C (1998) Germline PTEN mutation in a family with Cowden syndrome and Bannayan-Riley-Ruvalcaba syndrome. Am J Med Genet 80:399-402.

Zukin RS, Bennett MV (1995) Alternatively spliced isoforms of the NMDARI receptor subunit. Trends in neurosciences 18:306-313.

Zukor K, Belin S, Wang C, Keelan N, Wang X, He Z (2013) Short Hairpin RNA against PTEN Enhances Regenerative Growth of Corticospinal Tract Axons after Spinal Cord Injury. J Neurosci 33:15350-15361.